Uloga RNA helikaze DDX5 u signalnom putu NF-kB

Postić, Sandra

Master's thesis / Diplomski rad

2018

Download date / Datum preuzimanja: **2025-03-12**

Repository / Repozitorij:

Repository of the Faculty of Science - University of Zagreb

University of Zagreb

Faculty of Science

Department of Biology

Sandra Postić

The role of DDX5 RNA helicase in NF-κB signaling

Graduation thesis

Zagreb, 2018.

Sveučilište u Zagrebu

Prirodoslovno-matematički fakultet

Biološki odsjek   Diplomski rad

Uloga RNA helikaze DDX5 u signalnom putu NF-κB

Sandra Postić

Rooseveltov trg 6, 10000 Zagreb

DEAD-kutija RNA helikaza DDX5 uključena je u brojne stanične procese kroz metabolizam RNA ili kao koregulator raznih transkripcijskih faktora. U ovom radu istražen je utjecaj proteina DDX5 u signalnom putu NF-κB i staničnom ciklusu. Kako bismo dobili stanice HeLa bez ekspresije DDX5 ili s delecijom C-terminalnog kraja DDX5 proteina koji sadrži proteinsku domenu Pfam za koju se smatra da je odgovorna za aktivaciju puta NFκB, korištena je metoda delecije pomoću plazmida CRISPR/Cas9. Delecija gena DDX5 bila je letalna za stanice. Stanice HeLa s delecijom dijela sekvence DDX5, HeLa DDX5ΔPfam bile su vijabilne, ali su također pokazivale smanjenu stopu umnožavanja. Usporedno su metodom unosa antisens RNA za DDX5 uzgojene stanice HeLa i primarne stanice HUVEC sa utišanom ekspresijom DDX5, te se istražio utjecaj ove promjene na NF-κB aktivaciju i stanični ciklus.

(stranice 88, slika 43, tablica 28, literaturnih navoda 54, jezik izvornika: engleski)

Rad je pohranjen u Središnjoj biološkoj knjižnici.

Ključne riječi: proliferacija, stanični ciklus, CRISPR/Cas9, HUVEC, shRNA

Voditelj: Dr. sc. Rainer de Martin, red. prof.

Suvoditelj: Dr. sc. Maja Matulić izv. prof.

Ocjenjivači: Dr. sc. Maja Matulić, izv. prof., Dr. sc. Sven Jelaska, izv. prof. i Dr. sc. Tomislav Ivanković, doc.

Zamjena: Dr. sc. Jasna Hrenović, red. prof.

Rad prihvaćen:

BASIC DOCUMENTATION CARD

University of Zagreb

Faculty of Science

Division of Biology   Graduation Thesis

The role of DDX5 RNA helicase in NF-κB signaling

Sandra Postić

Rooseveltov trg 6, 10000 Zagreb

The DEAD-box RNA helicase DDX5 is included in all sort of cellular processes through its ability to metabolize RNA or as a co-regulator of different transcription factors. In this study, the function of the DDX5 protein was investigated in the context of NF-κB signaling and proliferation. The CRISPR/Cas9 genome editing method was employed to generate DDX5-gene knockout, as well as C-terminal deleted DDX5 HeLa cells, the latter comprising a pfam-protein domain assumed to be responsible for the activation of NF-κB. While complete DDX5 knockout cells were not able to proliferate, DDX5ΔPfam HeLa cells were viable, but exhibited a reduced cell growth rate. Complementary to the CRISPR/Cas9 gene editing, short-hairpin mediated RNA interference (shRNA) was employed to establish DDX5 knock- down in HeLa, as well as primary HUVEC cells and its impact on NF-κB activation and cell cycle was investigated.

Acknowledgments

Content:

1. Introduction

1.1. Cell cycle

The cell cycle is a highly regulated process made up of DNA synthesis (S phase) and mitosis (M phase), separated by gap phases (G1 and G2). In resting cells, Cyclin-Dependent Kinase (CDK) activities are low and the retinoblastoma protein (Rb) is not phosphorylated, and it binds and inhibits the E2F transcription factor. The cell cycle can be activated through mitogenic stimuli which lead to extracellular signal regulated kinase (ERK)- dependent activation of transcription factors c-Myc and Ets-1, subsequently regulating transcription of the Cyclin D1. Cyclin D1 binds CDK4 and CDK6, which now initiate phosphorylation of Rb. Phosphorylated Rb releases E2F transcription factor. E2F initiates transcription of genes involved in G1/S transition including Cyclin E. Up-regulation of Cyclin E initiates CDK2/Cyclin E activity, leading to hyper-phosphorylation of Rb and release of additional E2F in a positive feedback loop. At the beginning of the S-phase, Cyclin A levels increase and Cyclin A/CDK2 constitute the dominant CDK activity through the S-phase. DNA replication is initiated when the origin recognition complex (ORC) binds to the DNA and stays bound to the origin of replication throughout the whole cycle, up to G1. Near the end of the S-phase, Cyclin B levels increase, giving rise to the Cyclin B/CDK1 activity that direct cells into mitosis. The anaphase-promoting complex (APC) triggers exit from mitosis and is responsible for resetting the cell cycle at the end of mitosis via the degradation of Cyclin A, Cyclin B, and many other substrates (Figure 1) [1].

Cell cycle progression is also controlled by the inhibitors of CDKs, including p21 regulated by p53 and p27. Degradation of these proteins promotes the S-phase.

The p53 tumor suppressor protein plays a central role in the decision of a cell cycle arrest or apoptosis after different stresses such as DNA damage and hypoxia. All cells have low levels of p53 expressed due to MDM2-mediated ubiquitination followed by proteasomal degradation. MDM2 also regulates p53 activity by facilitating nuclear export. After DNA damage, p53 is phosphorylated at several sites in its transactivation domain, including serines 15 and 20. The DNA-damage sensing kinases ATM and ATR phosphorylate the p53 at serine 15, thereby inhibiting the interaction of p53 with MDM2, resulting in p53 stabilization. The ATM also phosphorylates MDM2 and reduces its capability to promote nucleo-cytoplasmic shuttling and degradation of p53. p53 is thought to be essential for the G1 arrest in response to DNA damage. The key transcriptional target of the p53 is the p21 Cdk inhibitor which inhibits Cyclin E/Cdk2 activity. The p21 also binds to the Cyclin D/CDK4 complex and prevents it from phosphorylating Rb, thereby suppressing the Rb/E2F pathway and G1/S transition. However, p21-deficient cells are apparently normal in the initiation of the G1 arrest, although the maintenance of G1 arrest appears to be impaired, suggesting an alternative target should exist downstream of p53. Also, the G1 arrest can be induced by CHK2 (Checkpoint kinase 2) independent of ATM and p53. CHK2 activity induces phosphorylation of Cdc25A, thereby decreasing its abundance and activity and additionally

reducing Cyclin D1 quantities, thus leading to decreased levels of the Cyclin D1/CDK4 complex. This results in the redistribution of p21 to the Cyclin E/CDK2 and the inhibition of the Cyclin E/CDK2 [2].
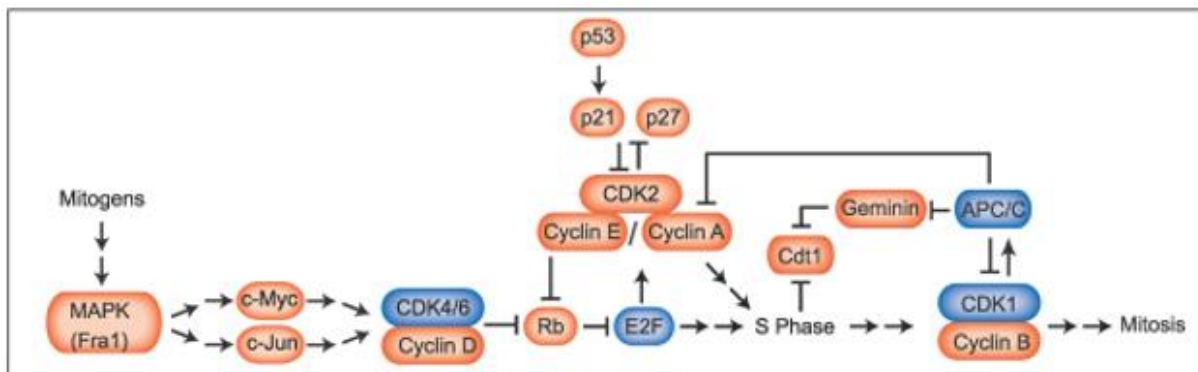
Figure 1: Schematic representation of the cell cycle signaling network [3].

1.2. Nuclear Factor kappa B pathway

There are hundreds of genes which utilize Nuclear Factor kappa B NF-κB through variations of DNA sequence found in their enhancers or promoters, with a consensus sequence of 5'-GGGRNWYYCC-3' (N being any base, R purine, W adenine/thymidine, Y pyrimidine) called Kb. That site binds dimers of five proteins made of the Rel transcription factor family: p50, p52, p65 (Rel A), Rel B and c-Rel, which share N-terminal homology. The Rel homology domain (RHD) is 300 amino acids long and has three different functions: sequence-specific DNA binding, dimerization and inhibitory protein binding. Following the RHD is a nuclear localization sequence (NLS). The Rel family proteins fall into two classes. First, the p50 and p52 arise from precursor proteins p105 (NFKB1) and p100 (NFKB2), respectively. From those precursor proteins a C-terminal region containing ankyrin repeats (AnkR) is posttranslationally cleaved off. The second group, p-65 (Rel A), Rel B and c-Rel are synthesized as mature proteins with transcription transactivation domains (TADs). Two classic dimers are p50:p65 and p52:Rel B, although other combinations including homo- and heterodimers with distinct functions exist. TAD-containing heterodimers are transcriptional activators, whereas p50 or p52 homodimers are repressors, unless bound to secondary proteins. The inhibitors, IκBα, IκBβ, IκBε, BCL-3, IκB, IκBNS, and the C-terminal portions of the precursor proteins p105 (IκBγ) and p100 (IκBδ), all contain five to seven tandem ankyrin repeats (AnkRs). AnkRs are 33 amino acid ankyrin-like protein-protein association domains that extend as helices capable of binding to NF-κB, covering the NLS. The C-terminal AnkR-containing IκB-like regions of p100 and p105 undergo limited proteolysis to make p52 and p50 which transit to the nucleus. For the p50, this occurs constitutively, but the p52 is generated only after specific signaling events. The canonical p50:p65 heterodimer is regulated by IκBα [4].

NF-κB activation starts with post-transcriptional modifications of IκB inhibitors. This occurs by a canonical and non-canonical pathway. In the canonical pathway, a kinase complex called IκB kinase (IKK) specifically phosphorylates the IκB proteins, leading to their degradation. This causes NF-κB dimers shuttling between the nucleus and cytosol to stay nuclear and induce gene expression. The cytosolic IKK holoenzyme contains a regulatory subunit "NF-κB essential modifier" (NEMO), and two kinase subunits IKK1 and IKK2 [4]. The IKK holoenzyme is activated through the phosphorylation of key serine in the T loops of IKK1 and IKK2, either by IKK kinase or by oligomerization-induced autophosphorylation. Regulatory ubiquitination of upstream scaffold proteins and NEMO is thought to mediate IKK activation through the recruitment of IKK kinases or oligomerization of IKK. Once activated, the IKK phosphorylates the IκB proteins in the conserved destruction box, which leads to their proteasomal degradation. Because IKK activation represents a bottleneck in NF-κB signaling, the IKK complex is the most thoroughly studied point of cross-regulation with non-NF-κB pathways [5]. NEMO is a non-catalytic subunit that tethers IKK1 and IKK2 into a regulatory holocomplex and it is required for ubiquitination reactions that begin protein oligomerization and signaling. The TNF receptor (TNFR) induces an IKK induction process. Tumor necrosis factor (TNF) stimulation of the TNFR recruits the RIP-1, TRADD, TRAF2, cIAP, TAB, and TAK1 proteins into a megacomplex with the linear ubiquitin assembly complex (LUBAC) stabilized by linear and K63-linked polyubiquitin chains. In that point, the IKK is incorporated, causing ubiquitination of NEMO and phosphorylation of IKK that induce its kinase activity. The composition of the megacomplex depends on specific ubiquitin modifications. This determines whether TNFR engagement causes NF-κB induction and survival or an alternative fate in which recruitment of RIP kinases 1 and 3 induce cell death instead of NF-κB. Fast and irreversible demolition of IκB proteins in the proteasome is triggered by phosphorylation and ubiquitination. In the canonical pathway, the IKK2 phosphorylates the IκBα on serines 32 and 36, or IκBβ on serines 19 and 23. Phosphorylated IκBs are then polyubiquitinated and degraded in proteasome. In the non-canonical pathway a dimer of IKK1 is utilized to phosphorylate p100 on serines 176 and 180, causing proteosomal processing to p52. p100 is mainly complexed with RelB with its AnkR domain to retain initial p52 and RelB in the cytoplasm. Phosphorylation of the p100 AnkR domain requires the NF-κB-inducing kinase (NIK). NIK is unstable because a TRAF complex controls its ubiquitination and proteosomal turnover. Receptors induce the non-canonical pathway by removing the TRAF complex, and stabilizing NIK, so now it can phosphorylate IKK1. IKK1 specifically phosphorylates the cytoplasmic p100:RelB complex on serines 866 and 870 and leads to ubiquitination and proteolysis of the C-terminal AnkR domain and nuclear ingress of p52:RelB. On the other hand, IκBα and IκBε can go into the nucleus and recapture DNA-bound NF-κB and stop the transcription. NF-κB induces the IκBα gene expression, establishing negative feedback. There are continuous discoveries of an increasing diversity of activators, signaling components, and responding genes for the NF-κB system [4], some of which are shown in Figure 2. The canonical and non-canonical NF-κB pathway are shown in Figure 3.
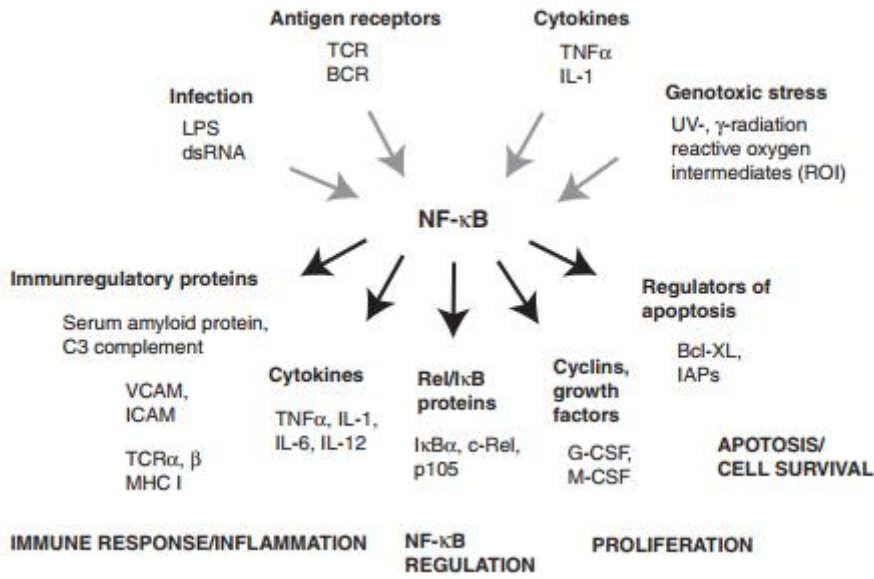
Figure 2: Schematic overview of NF-κB stimuli and target genes. NF-κB is a central mediator of immune and inflammatory responses, and is involved in stress responses and regulation of cell proliferation and apoptosis [6].
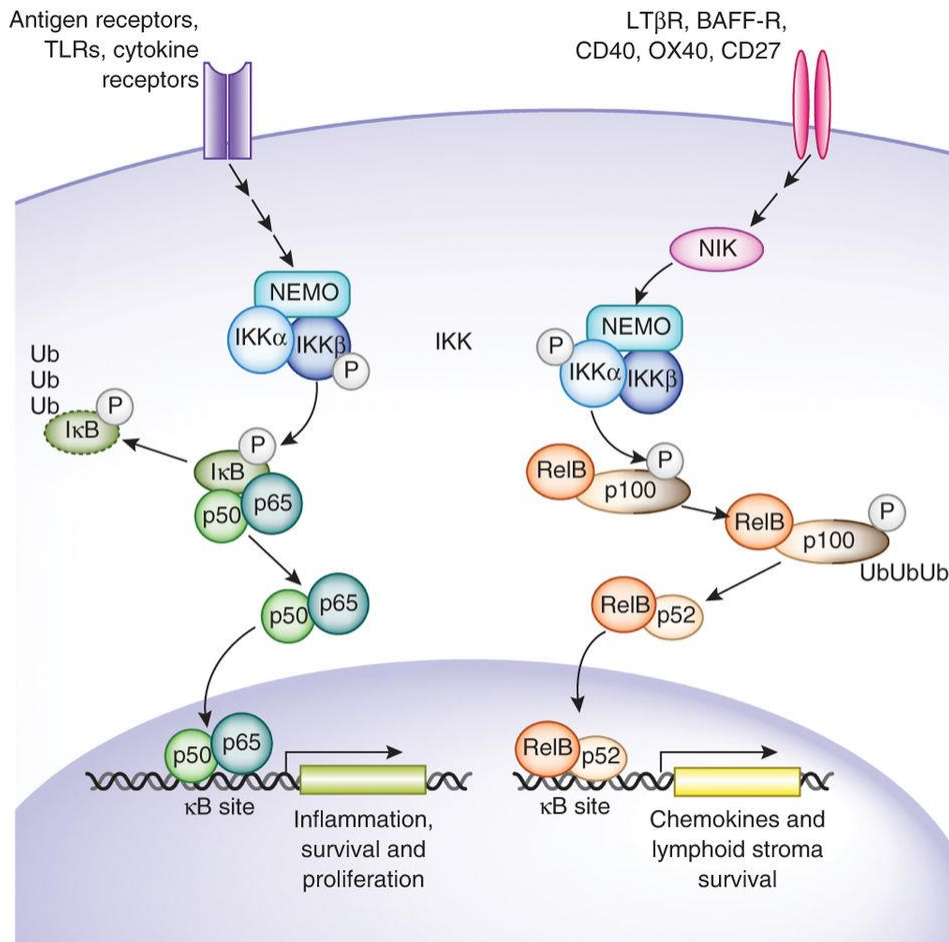
Figure 3: The canonical (left) and non-canonical (right) NF-κB signaling pathway. The canonical NF-κB pathway is TAK1-dependent in activating the IKK complex composed of the substrates IKKα, IKKβ and NEMO. Upon receptor stimulation, rapid assembly of an intracellular receptor complex occurs, containing the adaptor proteins, E3 ubiquitin ligases as well as the protein kinases mediating signaling downstream to the TGF-ß activated kinase 1, TAK1. Proximity of the IKK complex to the activated TAK1 in turn activates IKK. Activation of IKK represents a crucial step which is required to phosphorylate IκBs, targeting them for ubiquity-dependent degradation, thereby enabling nuclear translocation of former bound NF-κB dimers. The non-canonical pathway is induced by certain TNF family cytokines, such as lymphotoxin-ß, CD40L or TNF-like weak inducer of apoptosis. Under resting conditions, the NIK is constitutively degraded following ubiquitination by a complex involving TRAF2/3 and cIAP1/2. Upon stimulation, the latter complex is recruited to the receptor and ubiquitination now targets TRAF3 of the complex, resulting in the stabilization of NIK, enabling phosphorylation of IKKα, which in turn marks p100 for cleavage to p52. The pathway predominantly mediates then the persistent activation of p52/RelB complexes translocating to the nucleus [3].

1.3. The DEAD-box RNA helicase DDX5 (p68)

The RNA helicase DDX5 belongs to the DEAD box family of proteins with a characteristic Asp-Glu-Ala-Asp (DEAD in single letter code) motif [7]. The DDX5 protein has RNA helicase activity, as it was firstly discovered through a monoclonal antibody against SV40 large T, a protein with both DNA and RNA helicase activity [8, 9]. The RNA binding activity of DDX5 is independent of ATP or Mg^{2+} and is resistant to high salt levels. The protein also has two short repeats of the pfam (P68HR) domain at its C-terminus [10] (Figure 6).

DDX5-structure

DEAD-Box		Helicase	Pf I	Pf II
N-pos:	353-894	1079-1307	1493-1589	1651-1749
AS:	118-289	360-436	498-532	551-583
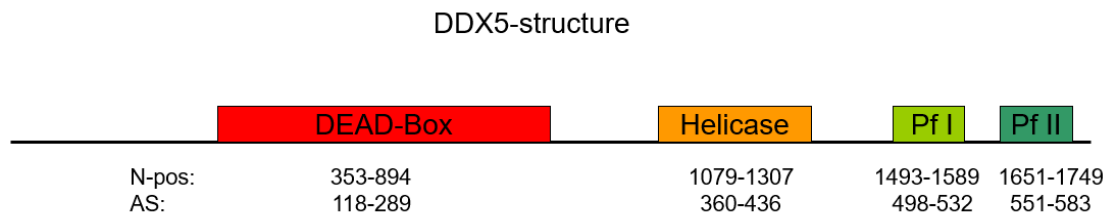
Figure 6: Schematic representation of DDX5-protein domain structure. N-pos: nucleotide position from the 5-prime end. AS: amino acid.

The DDX5 helicase is essential in human splicing *in vitro* and it plays a role in unwinding the transient U1:5' splice site duplex [11]. It also has a role in the pre-mRNA splicing [12] as well as in pre-miRNA processing through the large Dorsha complex [13]. Through transcriptional and splicing regulation, DDX5 controls estrogen- and androgen-signaling pathways [14]. It has been proposed that DDX5 is recruited to the promoter by transcriptional factors and serves as a bridge between transcriptional factors and other transcriptional regulators (such as CBP, Histone deacetylases). The DDX5 is upregulated during reprogramming of the cell and it serves as a barrier, which can change the epigenetic environment and, through such interactions, regulate cell fate transitions. The DDX5 helicase influences transcription and translation of genes through rearrangements of chromatin and miRNA processing, respectively [15].

The DDX5 protein is involved in the regulation of skeletal myogenesis through its interaction with MyoD, a protein that acts as a transcriptional activator and promotes transcription of muscle-specific target genes and plays a role in muscle differentiation [16]. DDX5 interacts with the MyoD and is recruited to the chromatin only when the MyoD binds and activates its targets. It seems that it regulates the formation of a competent transcriptional complex as it has a role in chromatin recruitment of the TATA binding protein, Polymerase II, the brahma-related gene-1 and the catalytic subunit of the ATPase chromatin remodelling complex (SWI/SNF) [17]. The DDX5 contributes to the initiation of a differentiation-specific transcriptional program and elicits the biogenesis of specific miRNAs, triggering a feedback control loop that contributes to the switching of splicing programs during differentiation in epithelial cells and in myoblasts through interactions with SMADs, which act as transcriptional modulators [18]. It was also shown that the DDX5 interacts with and co-

activates the Runx2, inessential transcription factor for osteoblast differentiation. It was, suggested that DDX5 inhibits osteoblast differentiation, but it was also shown that Runx2 itself suppresses the DDX5 expression [19].

The DDX5 has a role in cell proliferation through activation of the mTOR/S6K1 complex, a key downstream effector of phosphatidylinositol-4,5,-bisphosphate 3-kinase(PI3K)/Rac-serine/threonine kinase (AKT) and 5′-AMP-activated protein kinase (AMPK) pathways [20]. Downregulation of the DDX5 activates the mTOR signaling pathway downstream of AKT. The DDX5 depletion decreases cell growth and activates the mTOR/MDM2 cell survival mechanisms, which results in the inhibition of the pro-apoptotic factor p53. DDX5 depletion has been shown to activate cap-dependent translation and inhibit IRES-mediated translation of the transcription factor c-Myc [21].

DDX5 plays an important role in the p53 response to DNA damage, it is crucial for p21 expression but not for the expression of proapoptotic genes [22]. DDX5 shows clear cell cycle-related localization in the nucleus and it is important in the proliferation process downstream of Rb and E2F through elevating DNA-replication-factor expression, resulting in enhanced cell proliferation [8]. Here, amplification or overexpression of DDX5 leads to increased transcription via a new mechanism that is downstream of the Rb regulation. The DDX5 DNA replication promoting activity is cell context dependent and it is shown only in cells with overexpressed and/or amplified DDX5 [23].

It has been observed that the DDX5 is phosphorylated at multiple sites including serine/threonine and tyrosine [24]. Cellular DDX5 in HeLa cells is phosphorylated at tyrosine residues. It was shown that phosphorylation at tyrosine or threonine responds differently to TNF treatments in HeLa cells. The DDX5 might be a downstream target for multiple protein kinases in the cell signaling pathways. Dephosphorylation in the tyrosine residue is triggered by TNF, TRAIL and STI-571. It was reported that both the TNF and TRAIL induced cell signals inhibit cell proliferation and trigger apoptosis through activation of the protein tyrosine phosphatase SHP-1 (Src homology phosphatase-1). It was shown that tyrosyl-phosphorylated DDX5 can be dephosphorylated by SHP-1 in HeLa cells *in vitro* and it is likely that SHP-1, activated by TNF and/or TRAIL, is responsible DDX5 dephosphorylation [24]. Phosphorylation of the DDX5 RNA helicase at Tyr593 mediates the effects of the PDGF (Platelet-derived growth factor) in promoting cell proliferation, such as activation of Cyclin D1 and c-Myc genes. Phosphorylation of p68 at Tyr593 by c-Abl (non-receptor tyrosine-protein kinase) mediates the effects of the PDGF in promoting the EMT (epithelial–mesenchymal transition). The Phospho-DDX5 promotes β-catenin nuclear translocation by blocking cytoplasmic β-catenin phosphorylation and, in a complex with nuclear β-catenin, it activates the EMT. Because of those interactions, Cyclin D1 and c-Myc genes are up-regulated, leading to cell proliferation [25]. Some additional post-translational modification of the DDX5 and their influence on function are shown in Figure 7.
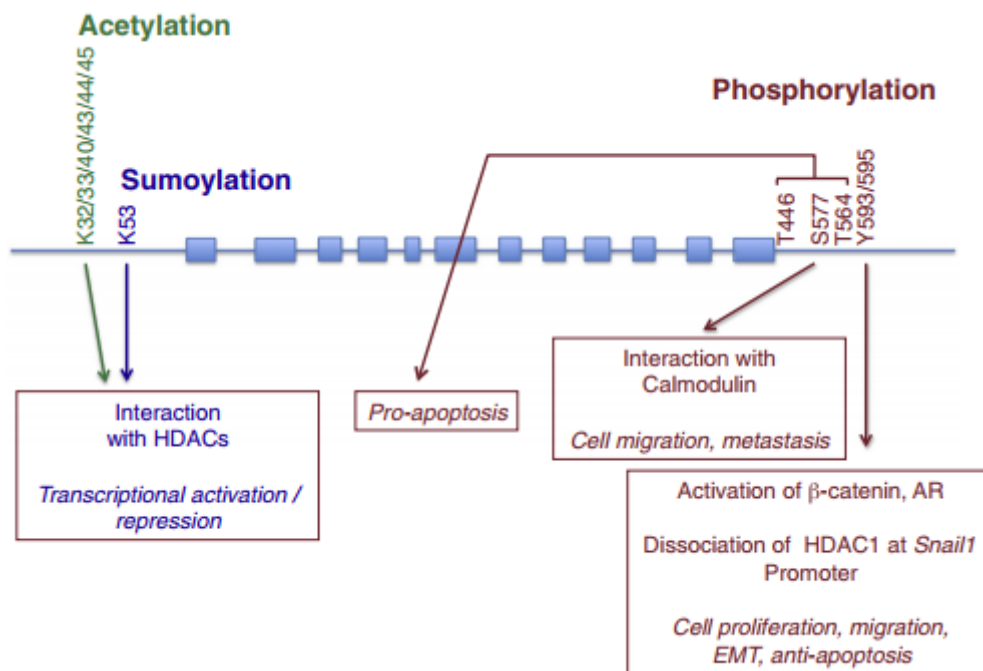
Figure 7: Scheme illustrating the reported post-translational modifications of the DDX5 and their effects on the DDX5 interactions and functions. Adopted from Fuller-Pace [26].

In glioma cells it has been shown that the DDX5 RNA helicase binds the p50 (NF-κB) protein and that the N-terminal part of the DDX5 protein is necessary for this function. The DDX5 can induce a p50 release from the IκBα and an accumulation of p50 in the nucleus for activation of transcription activity. The DDX5 and p50 promote proliferation in glioma cells [27].

1.4. Gene editing using the CRISPR/Cas9 method

Clustered regularly interspaced short palindromic repeats (CRISPR)/CRISPR-associated (Cas) systems constitute a microbial adaptive immune system that uses RNA-guided nucleases to cleave foreign genetic elements [28]. The CRISPR system II includes the CRISPR associated *Cas9* gene, the crRNA array, which comprises the guide RNAs and the required auxiliary trans-activating crRNA (tracr) and facilitates the processing of the crRNA array into discrete units [29]. The crRNA array is a distinctive array of repetitive elements interspaced by a short variable sequence derived from exogenous DNA targets known as protospacers. In the DNA, each protospacer is associated with a protospacer adjacent motif (PAM) which can vary depending on the CRISPR system [30]. The RNA guided nuclease function in mammalian cells requires heterologous expression of human codon optimized Cas9 and RNA components which can be fused together into one chimeric single-guide RNA (sgRNA). Cas9 can be re-

directed to any target of interest in immediate proximity of PAM sequence by altering the 20 nucleotides within the sgRNA [31] (Figure 4). In the system widely used, Cas9 is derived from *Streptococcus pyogene* and*,* the PAM sequence is NGG, N being any nucleotide.
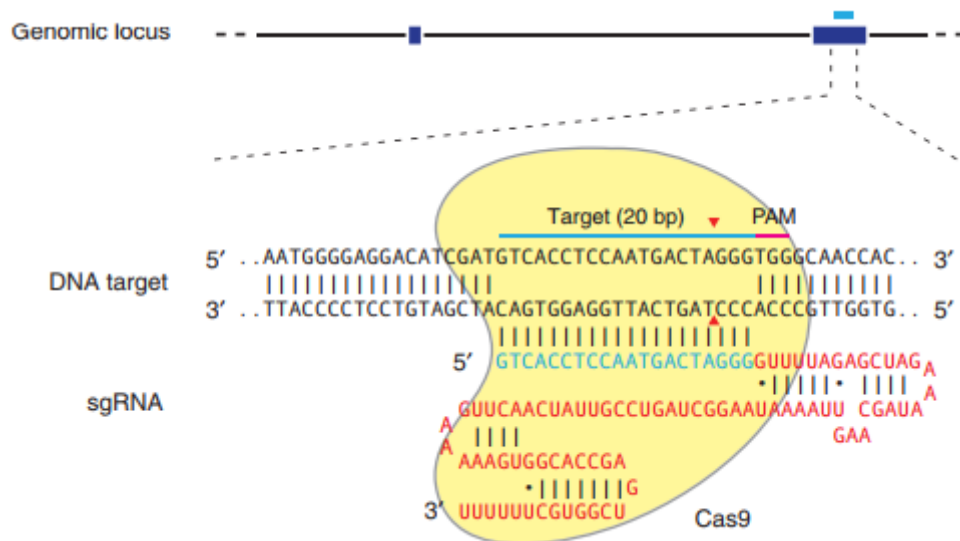
Figure 4: Schematic representation of the RNA-guided Cas9 nuclease. The Cas9 nuclease (in yellow) targets genomic DNA through sgRNA (blue) and a scaffold (red). The guide pairs up with the DNA target (blue line) directly upstream of a requisite NGG adjacent motif (PAM, pink). Cas9 mediates a double-strained break (DSB) approximately 3 bp upstream of the PAM [31].

The development of the CRISPR/Cas9 method enabled direct editing or modulating of the function of the DNA sequence in their endogenous context in virtually any organism of choice. The Cas9 is easy to target and it has high efficiency as a site-specific nuclease. Targeting the DNA and making the double-strand breaks can greatly stimulate genome editing through homologues-recombination events, or, in the absence of an exogenous homology repair template that localizes the double-strand break, can induce insertions or deletion mutations (indels) via the error prone nonhomologous end-joining (NHEJ) repair pathway [32]. In our experiments the NHEJ repair pathway was employed to get a premature STOP codon through a frame shift mutation (Figure 5).
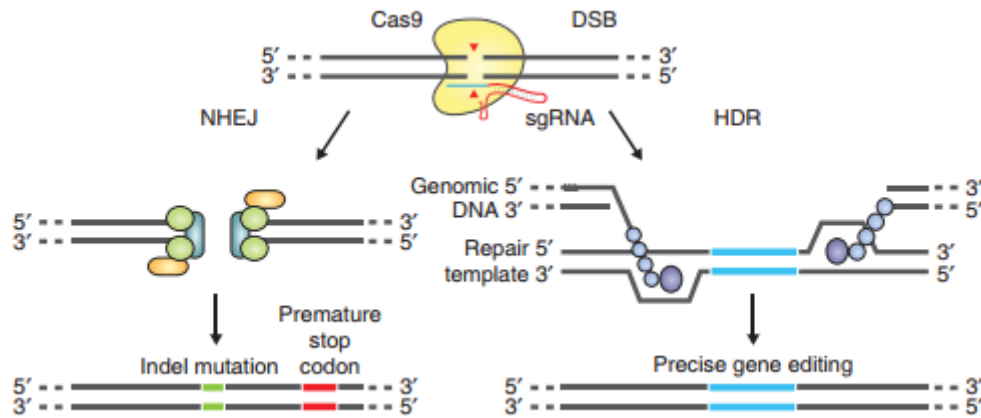
Figure 5: DSB repair promotes gene editing and it can be repaired in two ways. In error-prone NHEJ the ends of a DSB are processed by endogenous DNA repair machinery and re-joined, resulting in random indel (insertions and deletions) mutations at the site junction. Indel mutations occurring within the coding region of a gene can result in frameshifts and the creation of a premature stop codon, resulting in gene knockout. If a repair template in the form of a plasmid is provided, it can be supplied to leverage the homologues recombination pathway [31].

2. Aims and Objectives

This thesis aims to assess the function of DDX5 RNA helicase on NF-κB signaling pathway and to develop the tools to do so. This was accomplished by employing CRISPR/Cas9 mediated editing of DDX5 locus and establishing knockout in HeLa cells. To complement this approach, mRNA-interference studies (small hairpin RNA) were performed, generating a DDX5 knockdown in HeLa and primary HUVEC cells. Functional analyses were performed in reflection of downregulated DDX5 or DDX5ΔPfam HeLa cells on cell cycle and NF-κB signaling pathway.

3. Materials and methods

3.1. Cell culture: Cultivation of HEK293 and HeLa cells

Human embryonic kidney (HEK) 293 cells (ATCC-CRL 1573) and human cervix carcinoma cells (HeLa Ohio; ECACC 84121901) were maintained in complete DMEM (high-glucose Dulbecco´s Modified Eagles Medium (DMEM) (GE Healthcare HyClone; SH3002201) supplemented with 10% fetal bovine serum (FBS; Sigma-Aldrich), 2 mM L-glutamine (PAA), penicillin (100 U/ml) and streptomycin (100 U/ml; PAA) in a 5% CO_2 humidified atmosphere at 37°C. The cells were sub-cultured in a 1 to 5 ratio after trypsinization (Sigma-Aldrich).

3.2. Transient transfection by the calcium phosphate method

HEK293 or HeLa cells were transiently transfected using calcium phosphate [33]. In brief, cells were seeded in 6-, 12- or 24-well plates (Thermo Scientific) the day before transfection to obtain 70-80% confluent cells. The cells were transfected with 4 µg of plasmid DNA per a 9 cm^2 cell culture vessel (1 well of a 6-well plate). DNA amounts for transfections in other vessel formats were scaled down accordingly. The DNA was mixed with a dilution of 2 M $CaCl_2$ (9 µl) and H_2O (58 µl) to which and equal volume (71 µl) of 2xHeBS buffer (280 mM NaCl, 1.5 mM Na2HPO4, 50 mM Hepes, pH 7.05) was added followed by 10 sec vortexing. The mixture was then incubated for 2 min at room temperature and added dropwise to the cells. 6 h post-transfection medium was aspirated and replaced by complete DMEM. To control for transfection efficiency, 100 ng of the pmaxGFP expression plasmid (Amax, Lot No. DNC-00040-42; Netherlands) was included in the 4 µg DNA mix and cells were imaged using the JuLI™ Smart Fluorescent Cell Analyzer (Ruskinn; USA) 24 hours post-transfection.

3.3. Transfection by cationic polymer/lipid transfection

Alternatively, HeLa cells were transfected using TurboFect Transfection reagent (ThermoScientific) according to the manufacturer´s instructions or using polyethyleneimine (PEI) [34].

In brief, transfection was performed on 70-80% confluent cells which were seeded the previous day in a FBS and antibiotic (P/S)-free DMEM. The cells were transfected with 2 µg of DNA mixed with 200 µl of FBS-P/S- free DMEM and 6 µl of TurboFect Transfection reagent. That solution was used for transfecting a 9 cm^2 cell culture vessel, all the other vessels were scaled down accordingly. The solution was mixed well by pipetting and incubated for 15 min at room temperature. After the incubation period the solution was added dropwise to the cells. 6 h post-transfection medium was aspirated and replaced by DMEM-complete. For PEI-transfections, 2 µg plasmid-DNA were resuspended in 125 µl 1xHeBS and mixed with 125 µl 1xHeBS containing 3 µl PEI. After 20 min incubation at room temperature, the solution was added dropwise to the cells as described above. Transfection efficiency was controlled by co-transfection of pmaxGFP as described for the calcium phosphate method above.

3.4. DNA agarose-gel electrophoresis

Analysis of DNA (plasmids and genomic) was done by agarose-gel electrophoresis and percentage of agarose in the TAE Buffer (Tris-acetate-EDTA) was chosen according to the expected product size (DNA size in bp) and ranged from 0.5% to 2.5%. Gels were run in TAE for 1 h at 120 V. To visualize the DNA, the gel was pre-dyed with 4 µl of peqGreen (peqlab) per 100 ml of agarose solution. The gel was visualized by BIO-VISION-3026 system (peqLab). The 1 Kb Plus DNA ladder or low-range DNA-ladder (Thermo Fisher Scientific) was run on each gel to determine DNA-size.

3.5. CRISPR/Cas9 editing

3.5.1. Establishing a stable CRISPR/Cas9 mediated DDX5 knockout in HeLa cells

HeLa cells were transfected by the calcium phosphate method as described above. The method's strategy was to transfect two plasmids into the cells; one plasmid as a vector for single guide delivery (0.5 µg) and one expressing Cas9 protein (0.5 µg). For single guide delivery the HCP plasmid (GeneCopoeia, map shown in Supplement materials; Figure 41) was used, and Cas9 expression was achieved through co-transfection of the plasmid PX459 (Feng Zhang lab, map shown in Supplement materials; Figure 42) expressing *S. pyogenes* Cas9 (SpCas9-2A-Puro and single guide RNA) [31]. There were three different sgRNA constructs purchased from GeneCopoeia, targeting the first or the second exon of the *DDX5* gene. As HCP plasmids carry the resistance to hygromycin and PX459 has resistance to puromycin, double selection for both plasmids was performed 24 h after transfection, through adding to the supplemented DMEM medium 4 µg/ml puromycin and 400 µg/ml hygromycin. The cells were on the selection for 48 h when they were left to recover for seven days in DMEM supplemented for cultivation. The next step was picking the individual colonies by aspirating them into a 200 µL- pipet tip while viewing them under the JuLI™ Smart Fluorescent Cell Analyzer. Single cell clone colonies were seeded in a 24 well plate.

3.5.2. Cloning the sequence for sgRNA expression into an all-in-one plasmid vector PX459

On the basis of previous findings in the lab, implicating C-terminal Pfam domains in NF-κB signaling, sgRNAs were designed to introduce an in-frame STOP-codon mutation before Pfam domains and thus creating a C-terminal deleted DDX5.

sgRNA-sequences were designed based on the presence of a PAM-sequence adjacent to Pfam domains (CCDS11659.1, NM_001320595.1, nucleotide positions between 1414 to 1464) and off-target candidates were predicted using the Zhang-lab algorithm (http://crispr.mit.edu/). Oligonucleotides for sgRNA expression with overhangs for the cloning site (CACC and AAAC, respectively) were required from MicroSynth (sequence shown in Table 1). They were annealed in a thermal cycler (PCR System 2700, ThermoScientific)

starting from a temperature of 95° C going down 5° C each 5 min. Reaction conditions are shown in Table 1.

Table 1: Reaction setup for annealing oligos.

Reagent	Volume (µl)
Sense Oligo (100 µM): **CACC** GGTCGTTCCAGGGGTAGAGG	1
Antisense Oligo (100 µM): **AAAC** CCTCTACCCCTGGAACGACC	1
T4 DNA Ligase Buffer (ThermoScientific)	1
Nuclease free H_2O	Fill up to 10

The plasmid vector PX459 was digested with a BpiI restriction enzyme (ThermoScientific) overnight at 37° C, according to the conditions shown in Table 2. The digestion was analyzed by agarose-gel electrophoresis. The right size band was cut out of the gel and DNA was extracted from it.

Table 2: Reaction setup for PX459 BpiI digestion.

Reagent	Volume (µl)
Vector PX459 2 µg	2
Buffer G (ThermoScientific)	2
BpiI (ThermoScientific)	1
DTT (10 mM) (Invitrogen)	2
Nuclease free H_2O	Fill up to 20

Gel extraction was done with GFX™ PCR DNA and a Gel Band Purification Kit (GE Healthcare; components shown in Supplemental materials; Table 27) according to the manufacture's recommendation. The cutout band was weighed and 10 µl of Capture Buffer 3 were added

per each 10 mg of the gel slice. To dissolve the agarose, the mixture was put in a heating block on 60° C (Bioer, HB202). Once all the gel was dissolved, the color of the mixture was checked to insure that it had the right pH and if it was yellow it could be presided. The mixture was transferred onto an assembled GFX MicroSpin column and collection tube, and incubated for 1 min at room temperature; followed by centrifugation for 1 min at 4° C at the speed of 16,000 xg. The flow-through was discarded as the DNA bound to the column. Next, the column was washed with Wash buffer type 1, the centrifugation was repeated, and the flow-through discarded. To dry the column, it was centrifuged again, but this time empty with an open cap. To elute the DNA, 15 µl of Elution buffer type 6 was added and incubated for 3 min at room temperature, and then followed by centrifugation. The concentration of eluted DNA was measured on the Nanodrop (ThermoScientific™ NanoDrop 2000C).

Once the annealed oligos and the digested vector were acquired, they needed to be ligated. The ligation was performed according to the conditions written in Table 3. The reaction was incubated overnight in a thermal cycler (PCR System 2700, ThermoScientific) at 16° C.

Table 3: Reaction setup for the ligation of digested plasmid vector PX459 and the annealed oligos.

Reagent	Volume (µl)
50 ng digested vector	X
Annealed Oligos	1
T4 DNA Ligase Buffer (ThermoScientific)	0.5
T4 DNA Ligase	0.5
H_2O	Fill up to 5 µl

The ligation mix was used for transformation of chemically competent *E. coli*, strain DH5-α (Invitrogen). 5 µl of the ligation mix was added to 50 µl of chemically competent bacteria and incubated on ice for 20 min. After the incubation, the bacteria were heat shocked, on a heating block (Bioer, HB202) at 42° C for 60 sec. Subsequently, the cells were placed back on ice for recovery and plated on Luria Broth agar plates containing the appropriate antibiotic, Ampicillin (50 mg/ml) in a 1/500 dilution. Control bacteria with no transformed plasmid were also plated on a plate with Ampicillin as a control of antibiotic efficiency (expected not to have colonies).

Once colonies of bacteria were obtained, the single colonies were inoculated into a preculture of 4 ml liquid Luria Broth medium with a 1/1000 dilution of Ampicillin and incubated with shaking (150 rpm) at 37° C for around 6 h. From 1 ml of that culture, an overnight culture of 100 ml was inoculated. From that single clone liquid culture, plasmid purification followed, using the QIAGEN Plasmid Midi Kit according to the manufacturer's instructions (components shown in Supplemental materials; Table 26). The method is based on alkaline lysis, which are followed by plasmid DNA binding to a patented resin [35]. In brief, the bacterial cells were pelleted by centrifugation at 6 000 xg for 15 min at 4°C (Du Pont Instruments, Sorvall RC-5B). The supernatant was discarded and the cell pellet resuspended in a 4 ml Resuspension Buffer. After transferring the cell suspension to a 50 ml tube, a 4 ml Lysis Buffer containing RNaseA was added and thoroughly mixed by inverting the tube several times. After 5 min of incubation at room temperature, 4 ml of pre-chilled Neutralization Buffer was added and mixed thoroughly by vigorously shaking. The mixture was incubated on ice for approximately 20 min before plasmid DNA was cleared from precipitated cell debris, proteins and genomic DNA by centrifugation at 10 000 xg for 30 min at 4° C. In the meantime, Qiagen tips (columns) were equilibrated by applying a 4 ml Equilibration Buffer. The column was allowed to empty by gravity flow. The supernatant was additionally filtered through folded filters (Whatman), and added to the Qiagen column. The Qiagen column was then washed twice with approximately 10 ml of Wash Buffer. Finally, DNA was eluted with a 5 ml Elution Buffer into 30 ml round bottom glass tubes, precipitated by adding 3.5 ml isopropanol (Acros Organics), mixed and afterwards centrifuged at 15 000 xg for 30 min at 4° C. The supernatant was carefully decanted and the DNA pellet washed with 70% ethanol (EtOH) (Sigma-Aldrich). After a final centrifugation step, the DNA pellet was dissolved in 200 µl of endotoxin free TE buffer for 2 h at 37° C while shaking. The DNA concentration was determined by UV spectrophotometry using NanoDrop2000c (ThermoScientific, USA), as well as by agarose-gel electrophoresis. The concentration was adjusted to 1 µg/µl. Based on the absorbance ratios, an average DNA quality of A260/A280: 1.8 and A260/A230: 2.1 was obtained.

To check if the oligos have been inserted into the vector, a double digestion of 1 µg of plasmid, now called SG1, with BpiI (ThermoScientific) and EcoRV (New England BioLabs_inc.) was performed. Setup for the reaction is shown in Table 4. The reaction mix was incubated at 37° C overnight. The digestion mix was analyzed by 0.5% agarose-gel electrophoresis.

Table 4: Reaction setup for double digestion of SG1 plasmid.

Reagent	Volume (µl)
SG1 plasmid 1 µg	1
Buffer G (ThermoScientific)	1
BpiI (ThermoScientific)	1
EcoRV (New England BioLabs$_{inc}$)	1
H$_2$O	Fill up to 10

In addition to the digestion, the plasmid SG1 was sequenced at MicroSynth with sequencing primer PX459_hu6 fwd (sequence shown in Supplemental materials; Table 15).

3.5.3. Establishing a stable CRISPR/Cas9 mediated DDX5ΔPfam mutation in HeLa cells

HeLa cells (passage 13) were transfected with the calcium phosphate method using 0.5 µg of SG1 plasmid along with 0.1 µg of pmaxGFP as described above. 24 h post-transfection, medium was supplemented with puromycin (4 µg/ml final concentration), further incubated for 48 h and subsequently handled as described in 3.5.1. Individual clones were subcultured in triplicates in a 24 well plate, from which one was used for Western blot analysis, one for genomic DNA isolation followed by sequencing, and one for freezing, towing and further cultivation. The work flow of both CRISPR/Cas9 mediated knockouts approaches are shown in Figure 8.
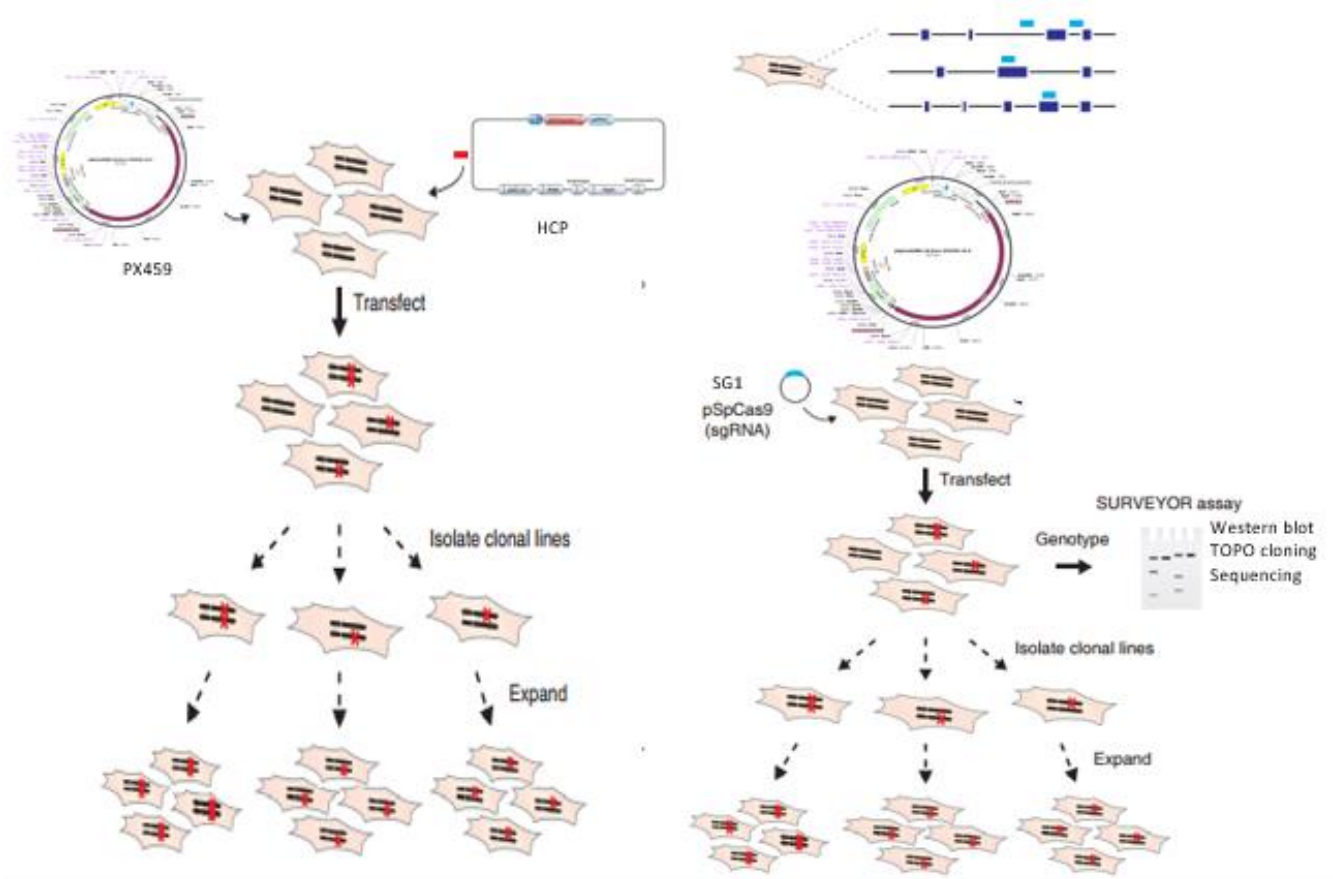
Figure 8: Work flow of CRISPR/Cas9 mediated editing. Left: Work flow of the experiment: "3.5.1. Establishing a stable CRISPR/Cas9 mediated DDX5 knockout in HeLa cells". Right: Work flow of experiment: "3.5.3. Establishing a stable CRISPR/Cas9 mediated DDX5ΔPfam mutation in HeLa cells" [31].

3.6. Analysis of the DDX5ΔPfam HeLa cells

3.6.1. Analysis of the DDX5ΔPfam HeLa cells by Western blot analysis

In order to determine if the CRISPR/Cas9 generated cells produce the C-terminal part of the DDX5 protein, the cells were harvested from a 24 well plate, washed once in PBS, resuspended in a 2x Laemmli sample buffer previously supplemented with 10% v/v β-mercaptoethanol (Sigma-Aldrich), and boiled for 10 min at 95° C and proteins of the whole cell lysate were separated on a 10% SDS polyacrylamide gel (PAGE). Buffer components for the buffers used for SDS PAGE and Western blotting are listed in the Supplemental material (Table 18-23). 10% PAGE was performed under the conditions written in Table 5 and Table 6. The gel was run in the beginning at a constant voltage of 80 V for 30 min and afterword's at an increased voltage of 120 V for the required time.

Table 5: Composition of 10% separation gel for SDS PAGE. *Solution A: Tris, Sodium Dodecylsulfat Hydrochlorid acid H2O (in details Supplemental materials, Table 18).

Reagent	Volume
dH$_2$O	4.1 ml
Solution A* (pH 8.8)	2.5 ml
Rothiphorese Gel 30 (37,5:1) (Roth)	3.4 ml
Ammoniumpersulfat (10% w/v in H2O) (Sigma-Aldrich)	50 µl
TEMED (Sigma-Aldrich)	10 µl

Table 6: Composition of stacking gel for SDS PAGE. *Solution Ast: Tris, Phenol red, Sodium Dodecylsulfat, Hydrochlorid acid, H2O (in details Supplemental materials, Table 19).

Reagent	Volume
dH$_2$O	3.1 ml
Solution Ast*(pH 6.8)	1.25 ml
Rothiphorese Gel 30 (37,5:1) (Roth)	0.65 ml
Ammoniumpersulfat	50 µl
TEMED (Sigma-Aldrich)	10 µl

In semidry Western blotting, the proteins were transferred from the gel onto a 0.45 µm nitrocellulose membrane (GE Healthcare - Amersham™Protran™) using the PerfectBlue Semi-Dry-Electroblotter (Peqlab). The proteins were transferred by applying electric current of 1 mA/cm^2 of gel for a duration of 2 h. Membrane and Whatman® 3MM chromatography filter papers (Whatman™) were pre-equilibrated in the blotting buffer (Towbin buffer 25 mM Tris, 192 mM glycine, 20% MeOH, pH 8.3). The gel sandwich was assembled from plus to

minus electrode in the following order: three pieces of Whatman paper, nitrocellulose membrane, gel and again three pieces of Whatman paper. After the blotting, a quick Ponceau S (Sigma-Aldrich) staining of the membrane was performed in order to confirm the protein transfer. The membrane was washed in Tris Buffered Saline (50 mM Tris-HCl, 150 mM NaCl, pH 7.4, supplemented with 0.1% v/v Tween®20 (Sigma-Aldrich) (TBS-T), followed by blocking in 5% w/v nonfat dry milk in TBS-T for 1 h at room temperature. The membrane was then incubated overnight at 4° C with a mouse monoclonal antibody, specific for epitope mapping between amino acids 547-579 near the C-terminus of human origin DDX5 (Santa Cruz Biotehnology, sc-365164) in a 1/5,000 dilution in TBS-T, or in a goat polyclonal antibody β-actin (Santa Cruz Biotehnology, sc-1616) in a 1/2,000 dilution in TBS-T. The next day, after washing the excess primary antibodies, the membrane was incubated in a secondary antibody complementing the primary, i.e. the anti-mouse IgG HRP Linked Whole Ab (1/5000 dilution; GE Healthcare, NA931v) or the anti-goat IgG HRP antibodies (1/5000 dilution; Sigma-Aldrich, A5420), for 1 h at room temperature, again followed by washing steps in TBS-T [36]. Membrane were developed and imaged using the AlphaImager™System (ProteinSimple) and later edited in Adobe Photoshop Version 8.0.

3.6.2. Isolation of genomic DNA (gDNA) from HeLa cells and DDX5ΔPfam HeLa cells

HeLa cells from a 24-well plate were harvested by trypsinization and centrifugation at 300 xg for 5 min and resuspended in a 100 μl 1xTE buffer (Tris pH 7.5, 10 mM/EDTA, 1 mM). Genomic DNA isolation was done according to Lanctot [37]. In brief, an equal volume of lysis buffer (components shown in Supplemental materials; Table 14) was added along with 2 μl of RNase (ThermoScientific, 10 mg/ml) to the suspension and incubated for 10 min at 37° C inside a heating block (Bioer, HB202). The proteins were then digested employing 20 μl of Proteinase K (Sigma-Aldrich, 1 mg/ml) overnight at 52° C inside a heating block (Bioer, HB202). In the morning the reaction was left to cool down to room temperature and 200 μl of Phenol:Chloroform:Isoamyl Alcohol 25:24:1 solution (Sigma-Aldrich) was added. The Eppendorf tube containing the mixture was sealed with parafilm and mixed by inverting for 5 min or until it became whitish. Separating the phases was done by centrifugation at 11,000 xg, at 4° C for 5 min, and 160 μl of aqueous phase was collected. To the aqueous phase the same volume of chloroform was added and again mixed by inversion, followed by the centrifugation step. This time 140 μl of aqueous phase was collected. To precipitate the DNA, 14 μl or 10% 3 M NaOAC (pH 5.2) was added along with 2-times the volume of absolute EtOH (EMSURE). For better precipitation it was left at -80° C for at least 15 min. Next, it was centrifuged at 200 xg for 2 min, washed in 70% EtOH and dissolved in a 0.1 xTE buffer.

3.6.3. Polymerase chain reaction (PCR) of the region including the CRISPR/Cas9 target site

The primers were designed using an online tool: Primer3 v. 0.4.0. (DDX5 check fwd and DDX5 check rev, sequence shown in Supplemental materials; Table 15). Predicted product size was 564 bp.

DreamTaq Green DNA polymerase (ThermoScientific) was used for the chain reaction according to the manufacturer's instructions. The reaction setup, as well as the program run in thermal cycler (PCR System 2700, ThermoScientific) are shown in the Table 7.

Table 7: Conditions of performed PCR.

Reagent	Volume μl		
10xDreamTaq Green Buffer (ThermoScientific)	5		
Primer 1788 fwd	5		
Primer 1787 rev	5		
dNTP 10 mM each (Fermentas)	1		
DreamTaq Polymerase	0.24		
H$_2$O (nuclease free)	Up to 50		
Template gDNA (50 ng)/Plasmid DDX5-flag 1 μg	1		
Step	Temperature (°C)	Time	Number of cycles
Initial denaturation	95	3 min	1
Denaturation	95	30 sec	25x
Annealing	55	30 sec	
Extension	72	30 sec	
Final extension	72	7 min	1
	4	∞	

The reaction was analyzed by 1% agarose-gel electrophoresis. As a positive control an N-terminal flag-tagged DDX5 pcDNA3 (Rainer de Martin´s lab) plasmid was used as a template, but due to the lack of introns, it generated a shorter product of 342 bp. The correct size

bands were cut-out and extracted using GFX™ PCR DNA and the Gel Band Purification Kit as written. 14-26 ng of DNA was sequenced by MicroSynth.

3.6.4. Surveyor assay

The Surveyor assay provides a simple, accurate and cost-effective means to scan DNA fragments for unmatched sensitivity and specificity. It is based on the T7 Endonuclease I's (New England BioLabs$_{inc.}$) ability to recognize and cleave mismatches in heteroduplex DNA [38].

For the Surveyor assay the same primers and the same PCR setup was used as written above. The PCR product was extracted from the gel using GFX™ PCR DNA and the Gel Band Purification Kit as written to get rid of primer-dimers. Next, the hybridization step was performed by mixing 200 ng of reference DNA (PCR product amplified from gDNA isolated form wild type HeLa cells) and 200 ng of our mutant DNA (PCR product amplified from gDNA isolated from CRISPR/Cas9 mediated clones). The volume was adjusted with nuclease free H$_2$O to 20 µl, put in a glass with boiling water and left to cool down to room temperature. The next step was the T7 Endonuclease I digestion (the reaction conditions are shown in Table 8). The digestion was done for 15 min at 37° C as the endonuclease is also a 5' exonuclease and that characteristic can affect the assay if left for longer incubation time. As the control reactions, 400 ng of nonhybridized PCR product of HeLa control cells, as well as of each clone was digested. The reaction was stopped after 15 min, by addition of 2.25 µl of 0.25 M EDTA. The fragment analysis was performed on 2.5% agarose-gel (Figure 9).

Table 8: Reaction setup for T7 Endonuclease I digestion.

Reagent	Volume µl
10xNEBuffer 2 (New England BioLabs$_{inc.}$)	3
Hybridization mix	20
T7 Endonuclease I (New England BioLabs$_{inc}$)	1
Nuclease free H$_2$O	Up to 30
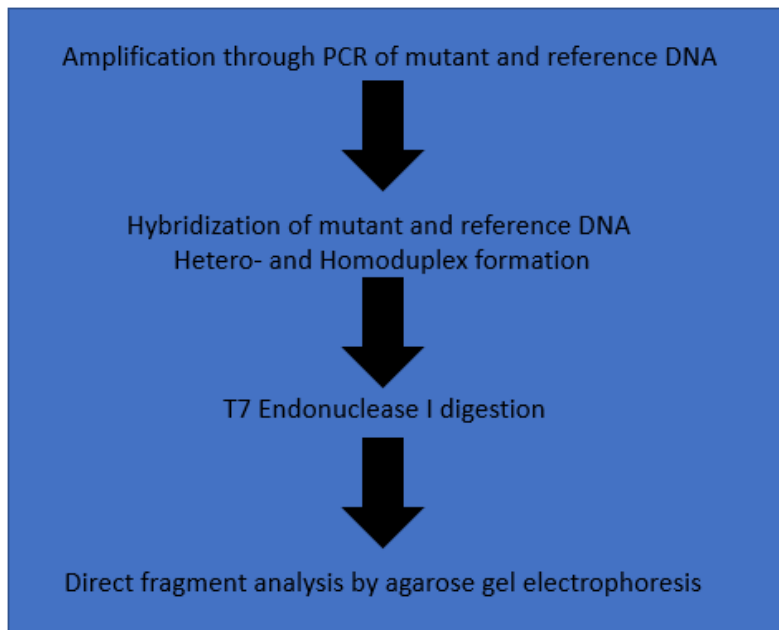
Figure 9: Schematic overview of Surveyor assay work flow to analyses CRISPR/Cas9 induced mismatches.

The estimation of cleavage intensity of fragment analysis gel was performed by employing ImageJ-win64.exe and measuring the integrated density of the same size area for each band. For each line, the fraction of cleaved PCR product was calculated (f_{cut}) by using the following formula:

$$f_{cut}=(B+C)/(A+B+C)$$

where A is the integrated density of the undegraded PCR product, and B and C are the integrated density of each cleavage product. Now the INDEL (% of insertion and deletion of nucleotides) occurrence can be calculated with the following formula, based on the binomial probability of duplex formation:

$$INDEL\ (\%) = 100\ x\ (1-\sqrt{(1-f cut)}\ )$$

[31].

3.6.5. TOPO TA cloning of the PCR product

TOPO TA cloning was done with TOPO® TA Cloning® Kit pCR™2.1-TOPO® (Invitrogen; plasmid map shown in Supplemental materials; Figure 43). The method is based on the use of DNA Topoisomerase I covalently bound to 3' deoxythymidine of the linearized vector which complements the 3' deoxyadenosine (A) that overhangs the PCR product. The PCR product was generated by the same PCR as for the sequencing. The DNA was extracted from the gel with GFX™ PCR DNA and the Gel Band Purification Kit as written before but in the elution step only 6 µl of Elution buffer type 6 were used to get a higher concentration of the DNA.

The TOPO TA cloning reaction was set up according to the manufacturer's instructions as written in Table 9, and it was mixed by pipetting and incubated at room temperature for 30 min.

Table 9: Reaction setup for TOPO TA cloning.

Regent	Volume (µl)
PCR product	4
Salt Solution (Invitrogen)	1
Nuclease free H_2O	Up to 6
TOPO Vector (Invitrogen)	1

The whole reaction mix was transformed into chemically competent *E. coli* strain DH5α as described above.

The TOPO vector insertion site interrupts the *LacZ α* gene coding for β-galactosidase which is best recognized for its reaction with X-gal (5-bromo-4-chloro-3-indoyl-β-d-galactopyranoside), a soluble colorless compound consisting of galactose linked to a substituted indole. The β-Galactose has high specificity for the galactose part of its substrates but low specificity for the remainder. Thus, it hydrolyzes X-gal, releasing the substituted indole that spontaneously dimerizes to give an insoluble, intensely blue product. On the growth medium containing X-gal, colonies of *E.coli* that have an active β-galactosidase become blue because of this reaction [39]. The selection plates containing 100 µg/ml of ampicillin (selection for the uptake of the plasmid) were prepared by spreading 40 µl of X-Gal (40 mg/ml in DMSO, Sigma-Aldrich) and 40 µl of 100 mM IPTG (Isopropyl β-D-thiogalactoside, dissolved in water, Sigma-Aldrich) on them. The prepared plates were incubated at 37° C until plating the bacteria. 50 µl of bacteria transformation was plated on to the plates and incubated over night at 37° C.

White single colonies were inoculated into 4 ml of culture and grown for 8 h at 37° C while shaking, for plasmid purification by Monarch® Plasmid Miniprep Kit (New England BioLabs_inc; components shown in Supplemental materials; Table 25) according to the manufacturer's instructions. All the centrifugation steps were done at 16,000 xg. Bacteria suspension was pelleted by centrifugation for 30 sec. The pellet was resuspended in 200 µl of Plasmid Resuspension Buffer (New England BioLabs_inc). To lyse the cells, the same volume of Plasmid Lysis Buffer (New England BioLabs_inc) was added and mixed by inversion, and it was left to

incubate for 1 min. The next step was to neutralize the lysate by adding 400 µl of Plasmid Neutralization Buffer (New England BioLabs_{inc}). It was mixed again by inversion and incubated for 2 min. To clarify the lysate, it was centrifuged for 5 min. The supernatant was transferred to the spin column and centrifuged for 1 min, and the flow-through was discarded. The column was washed twice; once with 200 µl of Plasmid Wash Buffer 1 (New England BioLabs_{inc}), and second time with Plasmid Wash Buffer 2 (New England BioLabs_{inc}). In order to dry the column, it was centrifuged empty for 1 min. To elute the DNA, 30 µl of DNA Elution Buffer was put on the membrane inside the column and incubated for 1 min, followed by centrifugation for 1 min. The plasmid concentration was measured on the Nanodrop (ThermoScientific™ NanoDrop 2000C).

In order to confirm the insert, digestion with EcoRI (New England BioLabs_{inc}) was performed under the conditions written in Table 10. The reaction was incubated overnight at 37° C and analyzed by 1% agarose-gel electrophoresis. The plasmids containing the insert were sequenced by MicroSynth with M13r primer (sequence shown in the Supplemental materials; Table 15).

Table 10: Conditions of EcoRI digestion.

Reagent	Volume (µl)
Plasmid 1 µg	1
10X NEBuffer™ EcoRI (New England BioLabs_{inc})	1
EcoRI (New England BioLabs_{inc})	1
Nuclease free H$_2$O	Up to 7

3.6.6. Freezing and thawing of HeLa cells

In order to freeze the cells, they were harvested and resuspended in the DMEM medium (GE Healthcare HyClone), supplemented with 20% fetal bovine serum (FBS) (Sigma-Aldrich), 2mM L-glutamine (PAA), penicillin (100 U/ml), streptomycin (100 U/ml) (PAA) and 10% DMSO, and then transferred to the Nunc® CryoTubes® 1.8 ml (Sigma-Aldrich). The Nunc® CryoTubes® were put into Mr. Frosty™ Freezing Container (ThermoScientific) filled with isopropanol (Acros Organics) at 4° C and transferred to -80° C from where they were put into liquid nitrogen the following day.

The thawing was done on ice by addition of a cold medium. The cells were centrifuged at 300 xg for 5 min, the supernatant was removed and the cells were resuspended in pre-warmed DMEM supplemented for cultivation, after which the cells were seeded in a T75 dish.

3.6.7. Analysis of the top three off-targets predicted for the sgRNA targeting of the last DDX5 exon

In order to find the off-target sites, Feng-Zhangs algorithm was used (http://crispr.mit.edu/). The top three off-targets were taken into consideration and the primers surrounding them were designed using an online tool: Primer3 v. 0.4.0. (T1 fwd, T1 rev, T2 fwd, T2 rev, T3 fwd, T3 rev, sequence shown in Supplemental materials; Table 15). The PCR reaction was performed under the same conditions as before. The PCR product was analyzed by 1% agarose-gel electrophoresis. The right-size band was cut-out, and the DNA extracted with GFX™ PCR DNA and the Gel Band Purification Kit as written before. The DNA was sequenced by MicroSynth from both ends (Results shown in Supplemental materials).

3.7. Functional analysis

3.7.1. Influence of DDX5ΔPfam on cell growth rate and cell cycle in DDX5ΔPfam HeLa cells

3.7.1.1. Trypan blue cell counting

The cells were maintained for at least 2 passages in a subconfluent state before being seeded in a 12-well plate as 200,000 cells/well in the DMEM medium containing 10% FBS. The cells were counted at three time points, after 12 h, 24 h and 32 h in triplicates. They were trypsinized in 200 µl trypsin (Sigma-Aldrich) and to stop the trypsinization, 800 µl of medium was added. The cells were dyed in Trypan blue (Sigma-Aldrich) 1:1, mixed well by pipetting and 10 µl was applied to the hemocytometer (Neubauer chamber). All four sets of 16 corner squares inside the hemocytometer were counted. The microscopy was done with an Eclipse TS100 Nikon microscope with a 10x magnification ocular (Nikon), and a 4x magnification objective (Nikon). The average cell number out of the 4 sets of 16 corner squares was multiplied by 10,000 (10^4) and by 2 because of the Trypan Blue dilution to get the number of cells per ml. The same procedure was done for the three wells of wild type HeLa, as well as for the DDX5ΔPfam clone F, clone G and clone I at each time point.

3.7.1.3. Cell cycle analysis

The approach to analyze the cell cycle status is to measure cellular DNA content at a single time point. This reveals a snapshot of cell cycle status among three distinct groups: G_0/G1 (2n), S (2n-4n) and G2/M (4n) phase [40].

The cells for the assay were seeded on the previous day, 600,000 cells per well in a 6 well plate. The following day, 5 hours prior to harvesting, the cells were stimulated with TNF

(R&D Systemes, 10 µg/ml stock solution in PBS+0.1% BSA) in a 1/1000 dilution yielding 10 ng/ml TNF or Etoposide (Sigma-Aldrich, 50 mM stock solution in DMSO) in a 1/500 dilution resulting in 100 µM final concentrations. The cells were harvested 24 h after the seeding. They were washed once in PBS to get rid of the medium and fixed and permeabilized in 70% EtOH for 30 min with vortexing every 5 min. After the fixation/permeabilization, the cells were centrifuged for 10 min at 300 xg, washed three times and resuspended well in a prepared RNaseA/AAD7 mix (Table 11). They were left to incubate in the dark for 1 h at room temperature. Because the used dye stains all the nucleic acids, RNase A is added to the mix to degrade the RNA. In the end 100 µl of PBS were added to the mix and the cells were analyzed by flow cytometry (FACSCalibur).

Table 11: RNaseA/AAD7 mix components. PBS: Phosphate-buffered saline. 7-AAD, SXTOX AADvanced: 7-Aminoactinomycin D.

Reagent	Volume (µl)
PBS	98.9
7-AAD, SYTOX™ AADvanced™	0.1
RNaseA (10 mg/ml)	1

3.7.2. Luciferase reporter gene assay in HEK293 cells, HeLa cells and DDX5ΔPfam HeLa cells

Luciferase reporter gene assays are commonly used to study the impact of proteins or reagents on transcriptional activity. Here, the impact of DDX5 and DDX5-Pfam domains with regards to their potency in inducing firefly luciferase (luc) synthesis driven by a synthetic, multimerized NF-κB-p65-transcription factor binding site (5xTGGGGGACTTTTCCGC, 5xNF-κB-luc, Stratagene) promoter element was investigated. In detail, reporter gene assays were performed in 24-well plates. The cells were seeded one day before the transfection, with the aim to have 70-80% confluence on the next day. For the NF-κB-luc reporter in HEK293 cells, the following master mix was prepared: 0.5 µg 5xNF-κB-luc, 0.5 µg UBT-ß-gal (Rainer de Martin´s lab) and 1.5 µg empty-vector, pcDNA3 plasmid. Then N-terminal flag-tagged DDX5 or a truncation mutant lacking Pfam domains expression plasmids (all in pcDNA3, Rainer de Martin´s lab) was added to the transfection mix in quantities of 0.5 µg (filed up to 1 µg with empty vector pcDNA3) or 1 µg. Additionally, HA-p65- in pcDNA3 (0.25 µg), HA-IKK1- (0.5 µg) or myc-IKK2 (0.5 µg) expression plasmids (all in pcDNA3, Manolis Pasparakis lab and Johannes Schmid lab, respectively) were co-transfected to establish low levels of NF-κB activation. 48 h post-transfection, the medium was aspirated and the plates were put to -80° C for at least 20 min, in order to facilitate proper cell lysis later. For reporter gene assays in

wild type and CRISPR/Cas9 edited HeLa cells, transient transfections were done with Turbofect as described above and amounts of DNA were adjusted accordingly (0.25 µg 5xNF-кB-luc, 0.25 µg pmaxGFP, in the absence or presence of 0.1 µg of HA-p65).

After thawing the plates at room temperature, 75 µl of 1 x passive lysis buffer (5 x Passive Lysis Buffer; Promega) was added. Cell lysis was performed for 15 min at room temperature while shaking the plates on a rocking platform (VWR). The cell lysate was collected by tilting the plate 45°; 15 µl of the cell lysate were transferred into a white 96-well plate for the luciferase assay and another 15 µl were transferred into a translucent 96-well plate for the ß-galactosidase assay. A detailed composition of reagents used for the following buffers and reagents is provided in the Supplemental materials (Table 16 and 17).

The luciferase activity was measured by adding a 100 µl reaction mix to each well. The plate was then put into the luminometer, which was previously set up to inject 40 µl of the injection mix to each well. The luminescence was read at an integration time of 10,000 ms. In the meantime, 90 µl of the CPRG substrate was added to the cell lysates, which were transferred into the translucent 96-well plate. The ß-galactosidase assay was incubated at 37° C until a significant change in color from yellow to orange/red was observed. Absorbance was measured at 595 nm. The obtained luciferase values were divided by the absorbance values of the ß-galactosidase assay, in order to acquire relative light units (RLUs). The average of the RLU values was used to calculate the fold induction relative to the negative control, namely untreated cells.

Transfection was normalized in one of two ways. One is by co-transfecting ubiquitin-driven ß-galactosidase (UBT-ß-gal), where the enzymatic activity of expressed ß-galactosidase was analyzed using chlorophenol red galactopyranosid substrate (1 mM CPRG – 12.15 mg dissolved in 20 ml PBS supplemented with 0.1% BSA) (Roche). The CPRG substrate turns from yellow to red in the presence of ß-galactosidase, depending on the level of enzyme activity. Color change and hence enzyme activity was measured at 595 nm (wallacVICTOR[2], 1420 multilabel counter). The second way is by co-transfecting pmaxGFP (Amax, Lot No. DNC-00040-42; Netherlands) and measuring the GFP expression at 480 nm (wallacVICTOR[2], 1420 multilabel counter).

To confirm the expression of Flag-DDX5 plasmid and the respective deletion mutant, Western blot analysis of cell lysates was performed with using anti-Flag M2-antibodies (1/2000; Sigma-Aldrich, Lot No. 080M6034) and analysis was done as described above.

3.7.3. Real time quantitive PCR analysis of HeLa and primary HUVEC DDX5 knockdown cells and DDX5ΔPfam HeLa cells

3.7.3.1. Total RNA isolation

With the purpose to evaluate HeLa and primary HUVEC (Human Umbilical Vein Endothelial Cells) cell responses to a DDX5 knockdown (cells obtained from Ulrike Resch, used a lentivirus delivery of shRNA to generate a knockdown; sequences are shown in the Supplemental materials) or a DDX5ΔPfam HeLa cells in relation to the TNF, the etoposide or the CD40L stimulation on the mRNA level, the total RNA was isolated using the PeqGold Total RNA Isolation Kit (Peqlab). The cells were cultured in 12-well or 24-well plates and treated with TNF, etoposide or CD40L (100 ng/ml, Enzo Life Sciences). Total RNA isolation was performed according to the manufacturer´s instructions. The cells were lysed with 400 µl of Lysis buffer at room temperature for 5 min while shaking. The cell lysate was afterwards transferred to a DNA-removing column placed into a 1.5 ml Eppendorf tube. Following a centrifugation step at 12,000 xg for 1 min, 400 µl of 70% ethanol (EtOH) was added to the flow-through in order to precipitate the RNA. The mixture was then transferred to RNA-binding columns, placed into a 2 ml Eppendorf tube. A centrifugation step at 10,000 x g for 1 min served to bind RNA to the column membrane, while cell debris and proteins were collected in the flow-through. The obtained RNA was washed once with 500 µl of Wash Buffer I and once with 600 µl of Wash Buffer II by centrifugation at 10,000 xg for 30 sec. After the washing steps, in order to completely remove the remaining wash buffer residues, the columns were centrifuged dry for 2 min at 10,000 xg. Following centrifugation, the columns were placed into fresh 1.5 ml Eppendorf tubes, in which RNA was eluted by adding 30 µl of DEPC treated water (Ambion). After 3 min of incubation at room temperature, RNA was eluted by a final centrifugation step at 5,000 xg for 1 min. Isolated RNA was immediately placed on ice and the RNA concentration was quantified with NanoDrop2000c.

3.7.3.2. Reverse Transcription

For obtaining cDNA, reverse transcription was performed using 500 ng of isolated RNA. RNA was mixed with DEPC-treated water to the final volume of 13.5 µl RNA/H_2O solution, transferred into PCR single cap tubes (Biozym Scientific). A master mix was prepared with 2 µl of 10 x-RT Buffer, 2 µl of 50 mM magnesium chloride (MgCl2), 1 µl of 50 µM random hexamers (Qiagen, Lot No. 79236), 1 µl of 25 mM dNTPs (Fermentas, Lot No. R0181) and 0.5 µl of MulV reverse transcriptase (ThermoScientific). The final reaction volume for each sample was 20 µl. RT-PCR was run using a thermal cycler (PCR System 2700, ThermoScientific) applying the following reaction protocol: 25° C for 5 min, 42° C for 60 min and 95° C for 5 min. After finishing the PCR reaction, cDNA was cooled down to 4° C. In the next step, cDNA, serving as template for RT-qPCR, was diluted with DEPC-treated water with a 1:3 ratio.

3.7.3.3. Real-time quantitative PCR

Amplification of diverse target genes was monitored using DNA binding dye SYBR Green I. A pre-formulated qPCR master mix containing buffers, dNTPs, DNA polymerase and SYBR Green I dye, the SsoAdvanced™Universal SYBR® Green Supermix (Bio-Rad) was utilized. Real-time quantitative PCR (RT-qPCR) was performed with the following reaction setup: 2 µl of 1:3 diluted cDNA, 5 µl SYBR Green I master mix, 0.5 µl forward primer (20 µM), 0.5 µl reverse primer (20 µM) and 2 µl nuclease free H_2O. RT-qPCR was further performed using the StepOnePlus Real-Time PCR System (AppliedBiosystems) as cycling instrument. A summary of the used cycling protocol is listed in Table 12. The real-time quantitative PCR primers used are shown in the Supplemental materials (Table 15). All the targets cycled with Real-time qPCR were normalized to β-2-microglobulin housekeeping gene (B2MG; Δct value). Secondly treated cells were normalized to the respective control (ΔΔct values). The calculated ΔΔct values were used to calculate fold induction (fold induction= $2^{-\Delta\Delta ct}$). All the primers used for RT-qPCR are shown in Supplemental materials (Table 15).

Table 12: Cycling program used for Real time quantitative PCR (RT-qPCR).

Step	Temperature (°C)	Time	Number of cycles
Initial denaturation	95	10 min	
Denaturation	95	15 sec	40x
Annealing/Extension	60	1 min	

3.7.4. Protein preparation from the kept flow through of the Total RNA isolation

Up to 2 ml of cold acetone (Sigma-Aldrich) was added to the flow-through and put on -20° C for at least 30 min to precipitate the proteins. It was centrifuged for 10 min at 4° C at 16,000 x g. Because a large amount of salt precipitated with the proteins, they were washed two times in 1 ml 70% EtOH and left on a heating block (Bioer, HB202) at 37° C for 10 min, while being shaken, followed by a centrifugation step, this time at 24° C. The proteins were resuspended in a 2 xLaemmli sample buffer previously supplemented with 10% v/v β-mercaptoethanol and used for Western blot analysis as written before.

3.7.5. IκBα kinetics analysis

IκBα kinetics analysis was performed in HeLa DDX5 knockdown cells and in DDX5ΔPfam HeLa cells to elucidate the NF-κB activity as the IκBα is a negative feedback loop mechanism in NF-κB pathway. Cells were stimulated with TNF (in concentration as written before) for 15 min, 30 min, 60 min and 120 min or 5 min, 25 min and 45 min in knockdown and knockout cells, respectively. They were lysed in 2 xLaemmli sample buffer previously supplemented with 10% v/v β-mercaptoethanol (Sigma-Aldrich) and whole cell lysate was analyzed by Western blot analysis as written with the mouse IκBα antibody (CellSignaling, #9242). The Western blot results were quantified by ImageJ-win64.exe by measuring the integrated density of the same size area for each band. The retrieved results were compared with the measured integrated density of Ponceau S (Sigma-Aldrich) staining of the respectable blot and compared in the relation to the wild type (to unspecific shRNA treated cells in the case of knockdown cells) and in relation to the untreated cells.

4. Results

4.1. Establishing a stable CRISPR/Cas9 mediated knockout cells

The aim of this experiment was to create a stable cell line lacking the expression of the DDX5 protein. Therefore, we targeted the first or the second exon of the *DDX5* gene using a two-component strategy, providing Cas9- and sgRNA expression plasmids (schematic representation of sgRNA target sites is given in Figure 10 and sequences are depicted in Supplemental materials).

Figure 10: Schematic representation of sgRNA targeting *DDX5*

To control for proper transfection of HeLa cells, GFP expression was monitored by microscopy and a representative picture is shown in Figure 11A. Based on GFP-positivity, the double-selection strategy to select for cells that express both Cas9 and sgRNA was employed as described in 3.5.1. The antibiotic selection was also checked by microscopy to make sure the selection is effective and that the cells are dying (Figure 11B). As shown in Figure 11 C and D, HeLa cells surviving 48 h of puromycin/hygromycin selection still expressed GFP and it is assumed that they have taken up the other two plasmids as well.
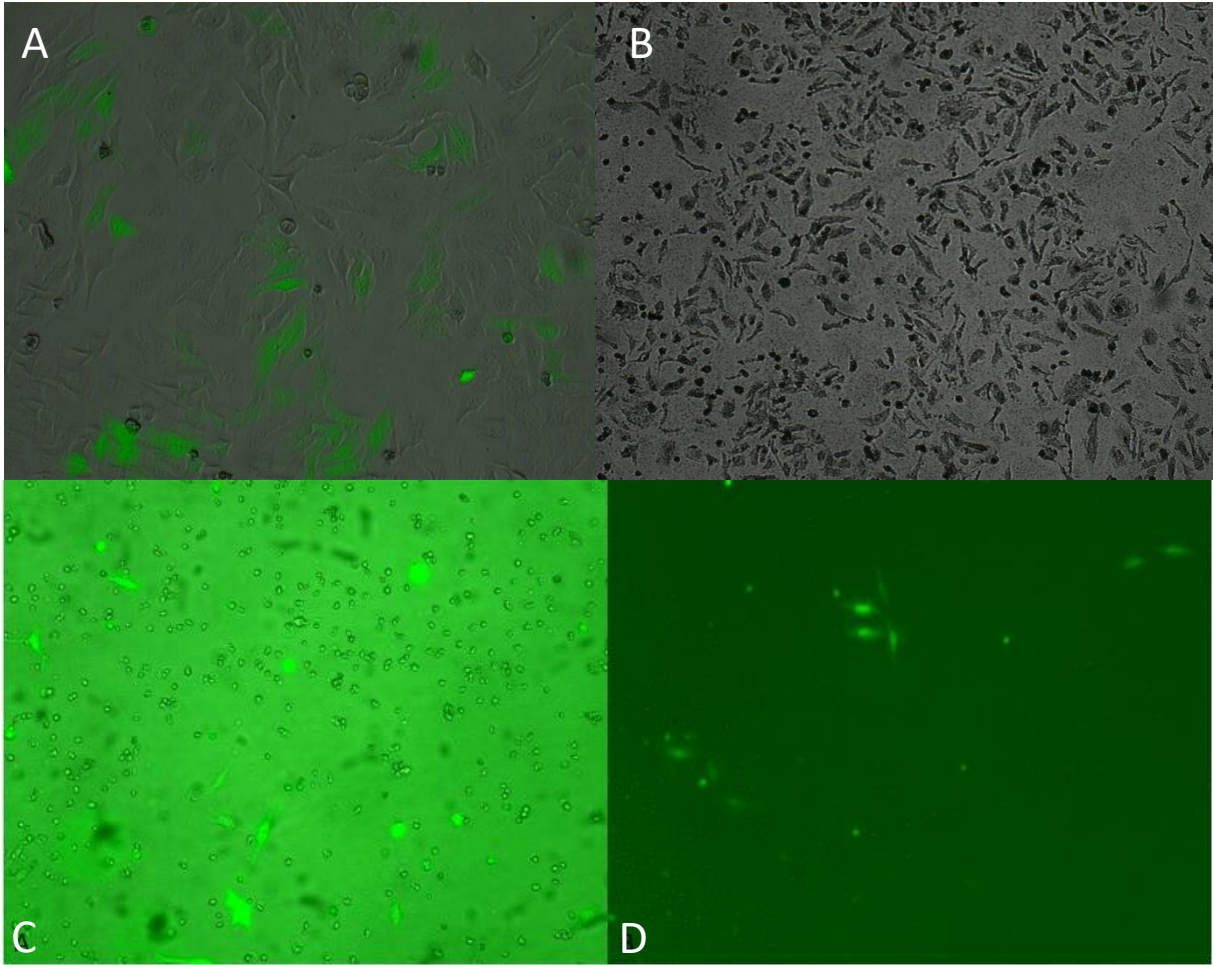
Figure 11: A) HeLa cells transfected with Cas9 (PX459 plasmid), sgRNA expression plasmid (HCP) and GFP expressing plasmid (pmaxGFP) 24 hours post-calcium phosphate transfection. B) HeLa cells 24 h after puromycin/hygromycin selection. C and D) HeLa cells surviving puromycin/hygromycin double-selection after 48 hours, transfected with HCP sgB (C) and sgC (D), respectively. Representative images were acquired with the JuLI™ Smart Fluorescence Cell Imager at 40 x magnification; settings were 20% bright field and 80% GFP, overlay was done in A, C and D.

Targeting cells with sgB and sgC sgRNA´s gave one colony each after selection, hence we supposed that mutation had occurred generating a premature stop codon in frame. But since cells did not proliferate, further characterization at the protein level through Western blot or isolation of genomic DNA was unfeasible. We have frozen one-half colony each for later confirmation, while in the other half we tried to rescue the cells by introducing the DDX5 expression plasmid. The flag-DDX5-pcDNA3 expression plasmid was transfected by the calcium phosphate method into the cells in order to yield a larger amount of cells and confirm the knockout (Figure 12). Unfortunately, the rescue experiment did not succeed. If the DDX5 knockout is true, we can say that the DDX5 knockout cells do not proliferate.
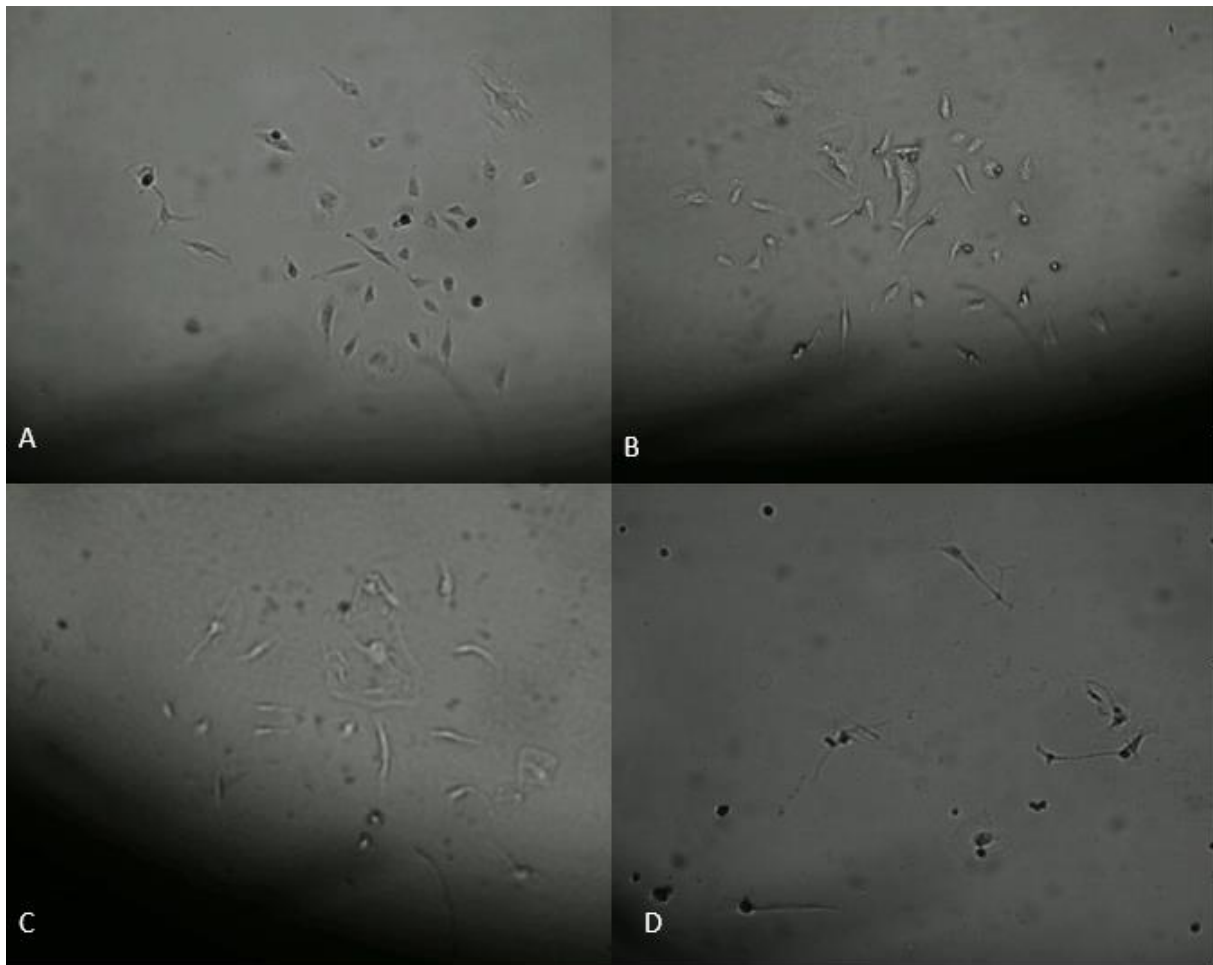
Figure 12: DDX5 knockout HeLa cells. A) DDX5 knockout HeLa cells generated through targeting with sgRNA construct sgB 17 days after puromycin/hygromycin treatment. B) DDX5 knockout HeLa cells generated through targeting with sgRNA construct sgB 21 days after puromycin/hygromycin treatment. C) DDX5 knockout HeLa cells generated through targeting with sgRNA construct sgC; Start of the "Rescue experiment" 25 days after puromycin/hygromycin treatment. D) Last image of the cells taken before they died, 39 days after the puromycin/hygromycin treatment. The images were taken with the JuLI™ Smart Fluorescence Cell Imager, representative bright field pictures were taken at 40x magnification.

The DDX5 knockout cells also displayed different morphology in comparison with the wild type HeLa cells. They were elongated, flattened and more branched in comparison to the wild type HeLa which usually have epitheloid appearance. From this experiment we concluded that a full DDX5 knockout leads to cessation of proliferation and subsequently to cell death, and proceeded with another approach.

4.2. Targeting the C-terminal part of DDX5

As knocking out DDX5 gene in HeLa cells appeared to be lethal, we decided to construct CRISPR/Cas9 plasmids enabling partial deletion of the DDX5 gene by targeting Pfam domain.

The first step was to construct a CRISPR/Cas9 plasmid with targeting sgRNA. The annealed oligos were inserted (sequence for sgRNA is given in Supplemental materials) into the PX459, Cas9 expressing vector. In order to do so, the plasmid vector was digested with BpiI restriction enzyme and the results of the agarose-gel analysis are shown in Figure 13.
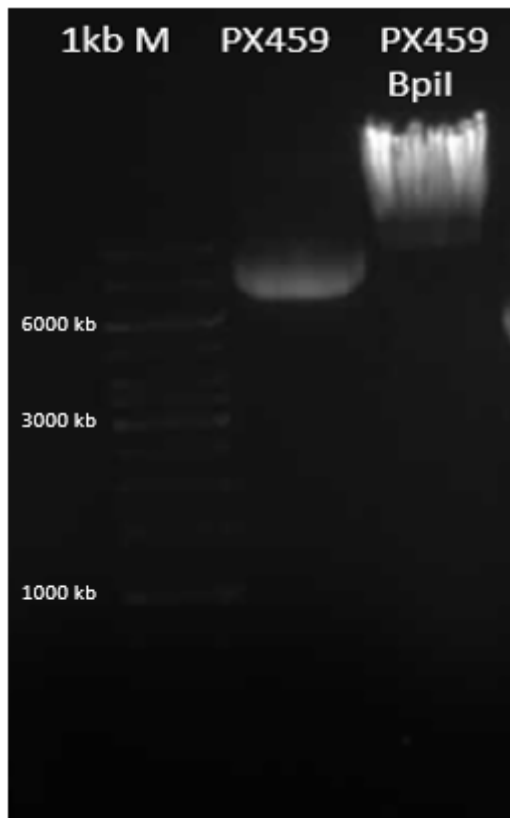
Figure 13: Overnight digestion of the PX459 plasmid with the BpiI restriction enzyme. Electrophoresis conditions were 0.5% agarose-gel, 1 h, 120 V. PX459: circular plasmid PX459, PX459 BpiI: plasmid PX459 digested with BpiI restriction enzyme. 1kb M: 1 kb Plus DNA ladder.

The digestion of PX459 plasmid with BpiI restriction enzyme was successful and it was proceeded with ligation of annealed oligos into the linearized plasmid. Ligation reaction was transformed into bacteria. From the two obtained colonies plasmids were isolated and digested with BpiI (BpiI cutting site should be destroyed if the plasmid contains the insert) plus EcoRV restriction enzyme (to linearize the plasmid for easier analysis). The digestion was analyzed by agarose-gel electrophoresis (Figure 14).
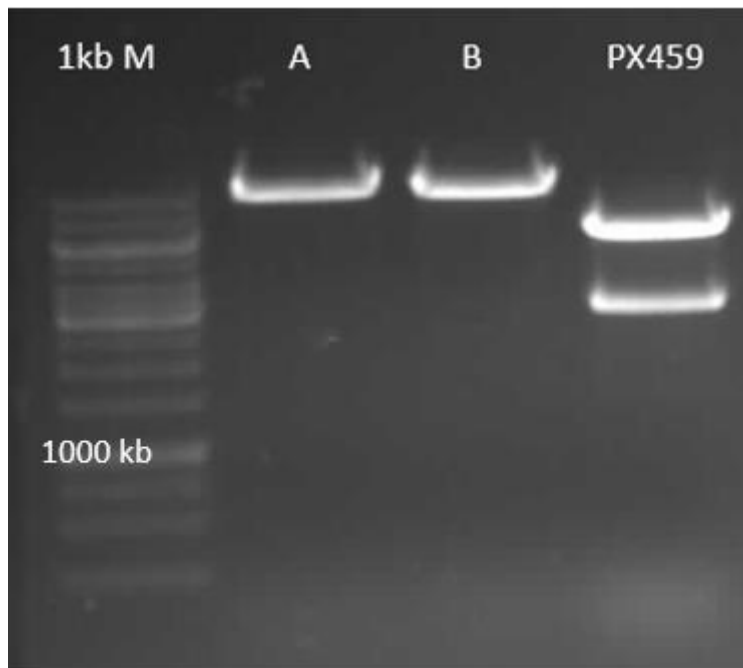
Figure 14: Restriction analysis of PX459, using BpiI plus EcoRV. Electrophoresis conditions were: 0.5% agarose-gel, 45 min, 120 V. A: Digested plasmid obtained from the first bacteria colony. B: Digested plasmid obtained from the second bacteria colony. PX459: Digested PX459 plasmid. 1kb M: 1 kb Plus DNA ladder.

Isolated plasmids from two obtained colonies of bacteria (A and B; Figure 15) gave only one band in the restriction analysis after the double digestion with BpiI and EcoRV indicating that the insert is ligated. This result was confirmed by sequencing (results shown in the Supplemental materials). In the downstream experiments plasmid from lane A (Figure 15) was used, which will be called SG1 plasmid from now on.

4.3. Establishing a stable CRISPR/Cas9 mediated DDX5ΔPfam HeLa cells

The aim of this experiment was to create a stable cell line expressing a DDX5 mutant lacking the Pfam domains. Therefore, we targeted the last exon of the *DDX5* gene. After plasmid construction and analysis, we transfected HeLa cells and selected clones for SG1 plasmid with puromycin (4 μg/ml) for 48 h to obtain colonies. In this experiment we were able to obtain viable colonies, from which the knockout DNA analysis was performed. Viable colonies from A-I are shown in Figure 15.
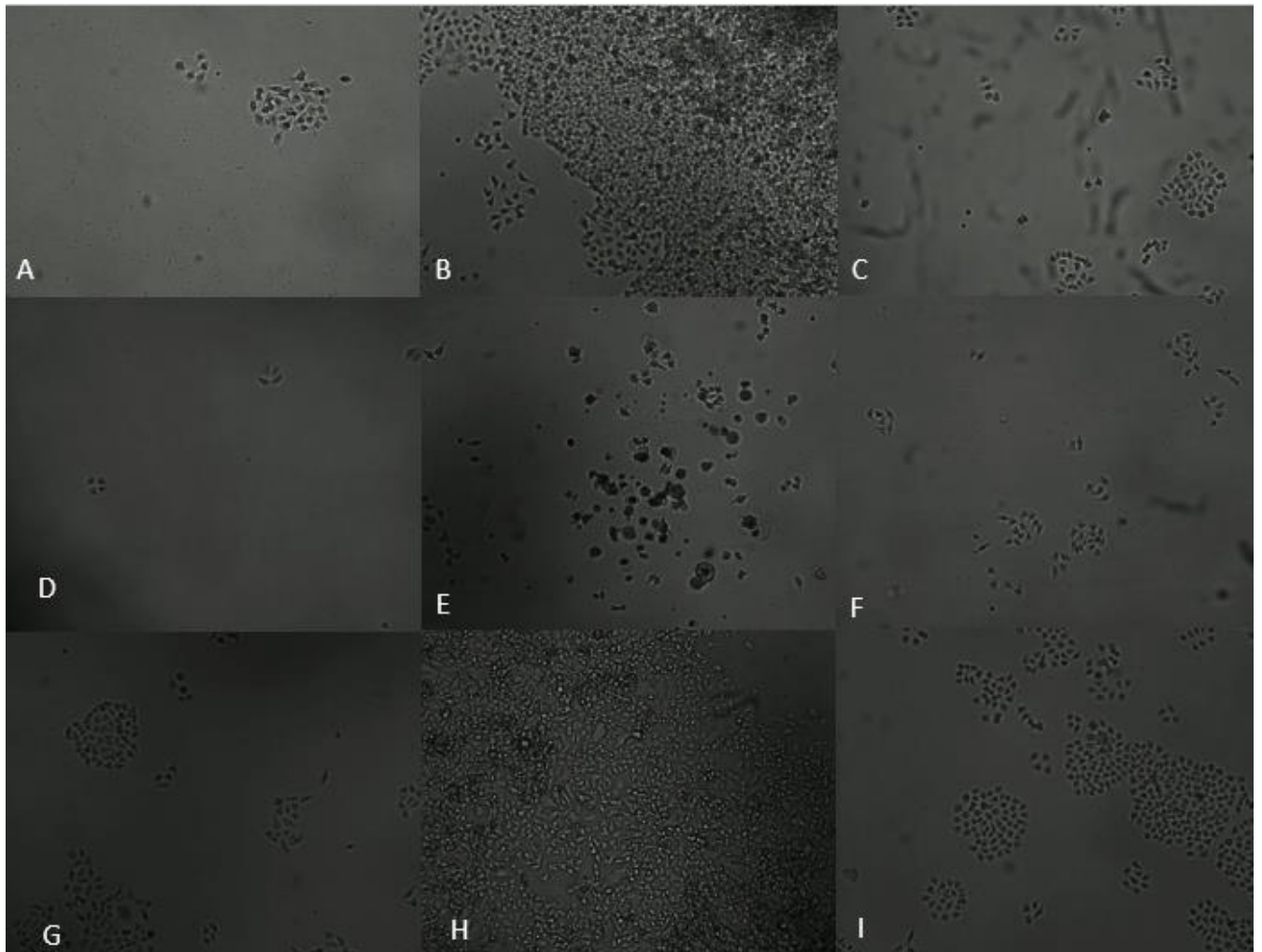
Figure 15: CRISPR/Cas9 edited HeLa colonies in the second passage after transfection. A-I shows representative bright field pictures of different single cells colonies of CRISPR/Cas9 edited HeLa cells. The images were taken with the JuLI™ Smart Fluorescence Cell Imager at 40x magnification.

4.4. Analysis of the DDX5Pfam domain deletion in HeLa cells

4.4.1. Analysis of the DDX5Pfam domain deletion in HeLa cells by Western blot analysis

The Western blot analysis was performed with a primary antibody against C-terminal part of the DDX5 protein containing the targeted Pfam domain and the lack of a protein on the Western blot indicated successful CRISPR/Cas9 editing. The Western blot analysis of DDX5 expression is shown in Figure 16.
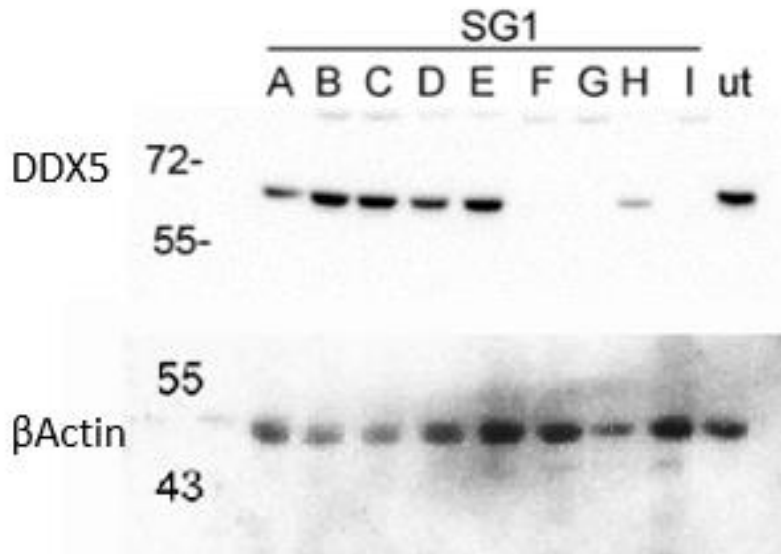
Figure 16: Western blot analysis for DDX5 protein expression in CRISPR/Cas9 edited clones. Protein lysates were prepared from CRISPR/Cas9 edited HeLa colonies (SG1 clones A-I recovered after transfection with CRISPR/Cas9-SG1 all-in-one plasmid targeting Pfam domain. Upper panel: a band is visible at 68 kDa in all lanes except F, G and I. Lower panel: presence of β-actin serving as a protein loading control visible in all lines. SG1 A-I: Proteins isolated from different colonies of HeLa cells transfected. ut: Wild type HeLa cells.

4.4.2. Analysis of Pfam domain deletion in HeLa cells on genomic DNA level

We analyzed the genomic DNA of cells obtained by from CRISPR/Cas9 edited cells which in Western blot analysis showed lack of Pfam domain (Figure 17) by PCR amplification of the targeted region. The amplification product of the PCR was analyzed by agarose-gel electrophoresis for which the results are presented in Figure 17.
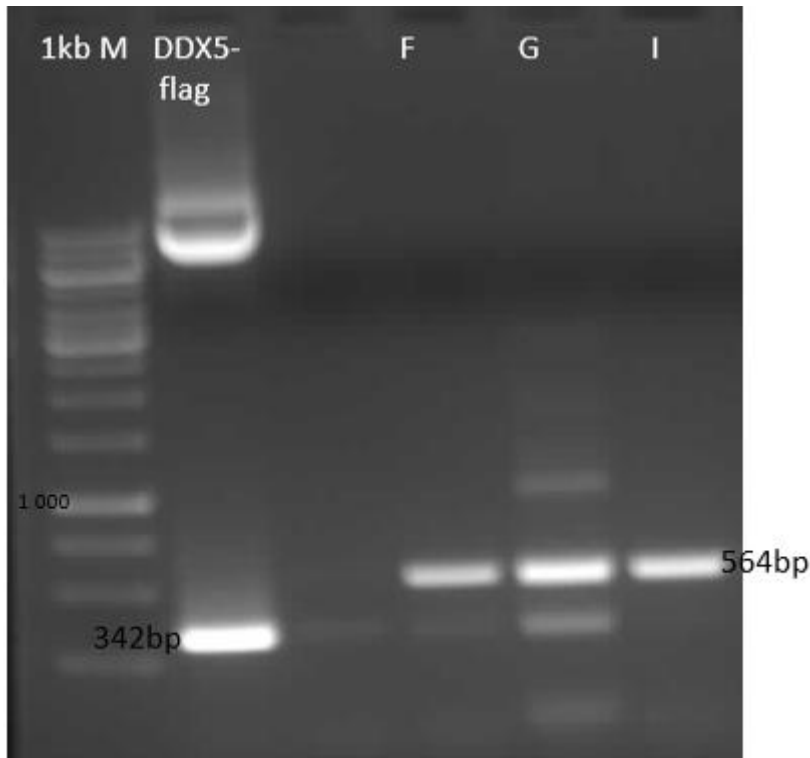
Figure 17: PCR product analysis of CRISPR/Cas9 targeted region in DNA isolated from colonies obtained by CPRISPR/Cas9 presumed DDX5ΔPfam HeLa cells. DDX5-flag: PCR product generated from N-terminal flag-tagged DDX5-pcDNA3 expression plasmid template. F: PCR product of CRISPR/Cas9 targeted region in DNA isolated from colony F; G: PCR product of CRISPR/Cas9 targeted region in DNA isolated from colony G. I: PCR product of CRISPR/Cas9 targeted region in DNA isolated from colony I. 1kb M: 1 kb plus DNA ladder. Electrophoresis conditions were: 1% agarose-gel, 1 h, 120 V.

On Fig. 17 it could be seen, in the first lane (DDX5-flag), the large band of 6000 bp presenting the plasmid N-terminal flag-tagged DDX5 pcDNA3 expression plasmid, which was the template for this PCR reaction and was put in the large excess. The smaller band at 342 bp was the expected size of the PCR product, generated from a plasmid which contained the coding *DDX5* sequence without the introns. PCR product of CRISPR/Cas9 targeted region in DNA isolated from colonies F, G and I gave the most intense band of 564 pb which was the expected size of the CRISPR/Cas9 target site including the exons from the gDNA.

The wild type gene was sequenced from all three colonies (colonies F, G and I). Sequencing results from the PCR products showed a clear sequence up to the presumed point of targeting, and thereafter showed double peaks, suggesting heterozygosity (Figure 18).
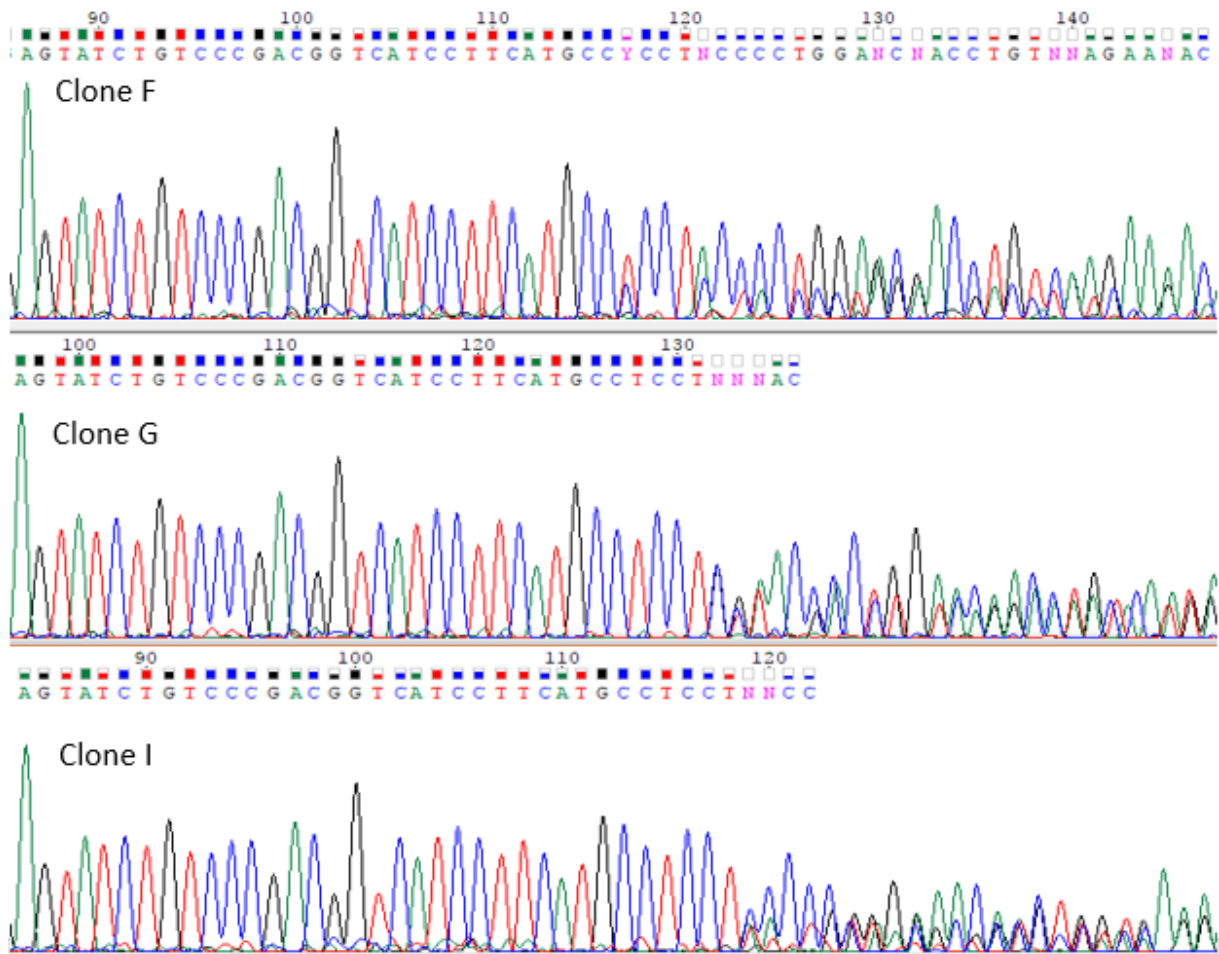
Figure 18: Sequencing chromatograms from PCR products isolated from amplified CRISPR/Cas9 targeted region of DDX5, obtained from clones F, G and I, after HeLa cell's transfection with SG1 plasmid.

4.4.3. Surveyor assay

In addition to the above analysis, a Surveyor assay was performed [38]. The Surveyor assay provides a simple, accurate and cost-effective means to scan DNA fragments for unmatched sensitivity and specificity. It is based on the T7 Endonuclease I's ability to recognize and cleave mismatches in heteroduplex DNA and is commonly used in CRISPR/Cas9 mediated gene targeting [31].

PCR was performed for the amplification of the CRISPR/Cas9 target site on the DNA isolated from the wild type HeLa cells as well as on the DNA isolated from the three colonies (F, G and I). The amplified CRISPR/Cas9 target site (564 bp) from the wild type HeLa cells was hybridized to each of the three colonies (formation of heteroduplexes). Followed by the T7 endonuclease I digestion of each reference PCR product, unhybridized PCR product from HeLa wild type as well as each of the colonies (F, G and I) and hybridized DNA-s. The direct fragment analysis was performed by agarose-gel electrophoresis (Figure 19).
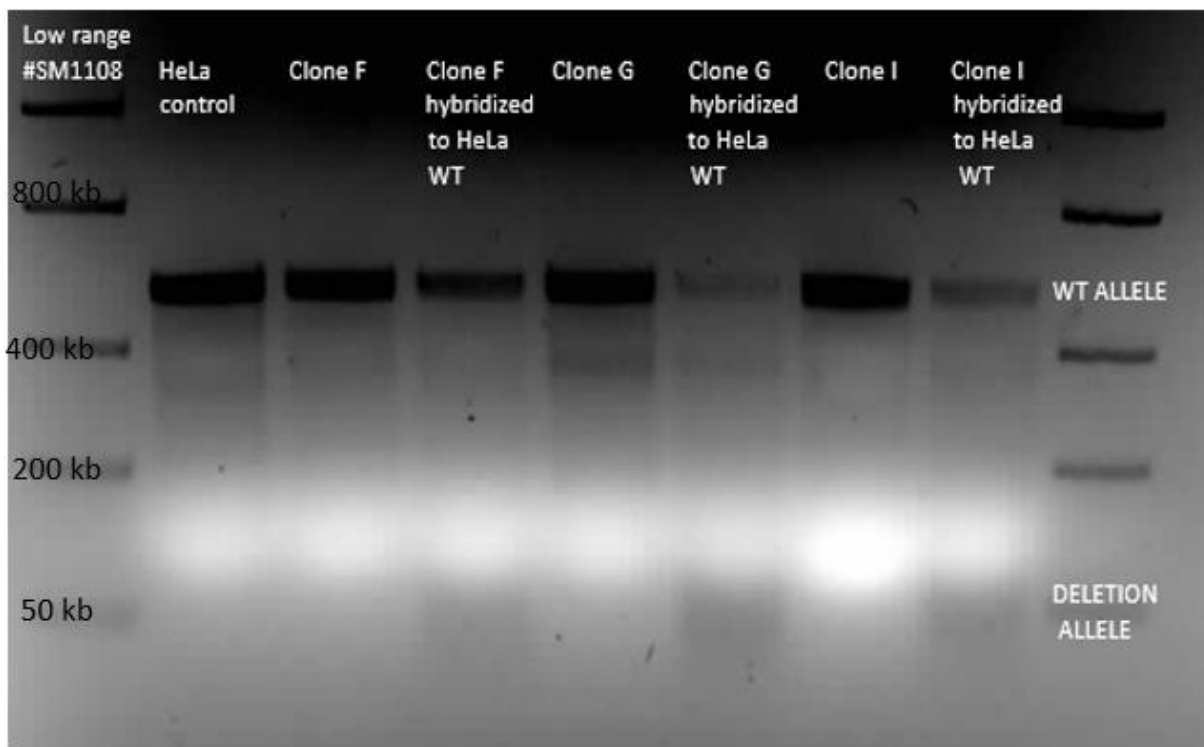
Figure 19: Direct fragment analysis through Surveyor assay. Description of analyzed samples from left to right: HeLa control: PCR product of CRISPR/Cas9 target region in DNA from wild type HeLa cells treated with T7 Endonuclease I. Clone F: PCR product of CRISPR/Cas9 target region in DNA from colony F treated with T7 Endonuclease I. Clone F hybridized to HeLa WT: PCR product of CRISPR/Cas9 target region in DNA from wild type HeLa cells hybridized to the PCR product of CRISPR/Cas9 target region in DNA from colony F treated with T7 Endonuclease I. Clone G: PCR product of CRISPR/Cas9 target region in DNA from colony G treated with T7 Endonuclease I. Clone G hybridized to HeLa WT: PCR product of CRISPR/Cas9 target region in DNA from wild type HeLa cells hybridized to the PCR product of CRISPR/Cas9 target region in DNA from colony G treated with T7 Endonuclease. Clone I: PCR product of CRISPR/Cas9 target region in DNA from colony I treated with T7 Endonuclease I; Clone I hybridized to HeLa WT: PCR product of CRISPR/Cas9 target region in DNA from wild type HeLa cells hybridized to the PCR product of CRISPR/Cas9 target region in DNA from colony I treated with T7 Endonuclease I. Electrophoresis conditions: 2.5% gel, 1 h, 120V.

On Figure 19 it could be seen that in lanes where no hybridization had been performed, only one band could be seen. In the lanes where the hybridization had been performed there was an additional band at 50 bp, meaning that the Endonuclease 7I found a mismatch.

From the direct fragment analysis of cleaved PCR product, values were calculated using the formula:

$$f_{cut}=(B+C)/(A+B+C)$$

where A was the integrated density of the undegraded PCR product, and B and C were the integrated density of each cleavage product. Now the INDEL (insertion or deletion of bases) occurrence can be calculated with the following formula, based on the binomial probability of duplex formation:

$$\text{INDEL (\%)} = 100 \times (1 - \sqrt{(1 - f\text{cut})})$$

(Table 13) [31].

Table 13: Indel (%) calculated from Surveyor assay. F, G, I: colonies F, G and I. WT: wild type HeLa cells.

clone	F	G	I	WT
INDEL (%)	70,06365	73,40032	71,02685	0

INDEL values calculated for all colonies were higher than 70% indicating high probability of insertions and deletions. F, G, I: mutated HeLa colonies. WT: wild type HeLa cells

4.4.4. TOPO TA cloning of the PCR product of the CRISPR/Cas9 targeted region

Sequences obtained by PCR amplification of the CRISPR/Cas9 target region from the colonies F, G and I were cloned in TOPO plasmid, in order to analyze them by sequencing as independent alleles. The TOPO plasmid was then transformed into bacteria producing three white colonies with the PCR product obtained from colony G, three from I and four from F. The white color of the colonies indicated that the PCR product was inserted inside the vector and disrupted the lacZα gene (blue/white screening). To confirm the insertion of the PCR products, the TOPO vector was digested with the EcoRI restriction enzyme and analyzed by agarose-gel electrophoresis (Figure 20).
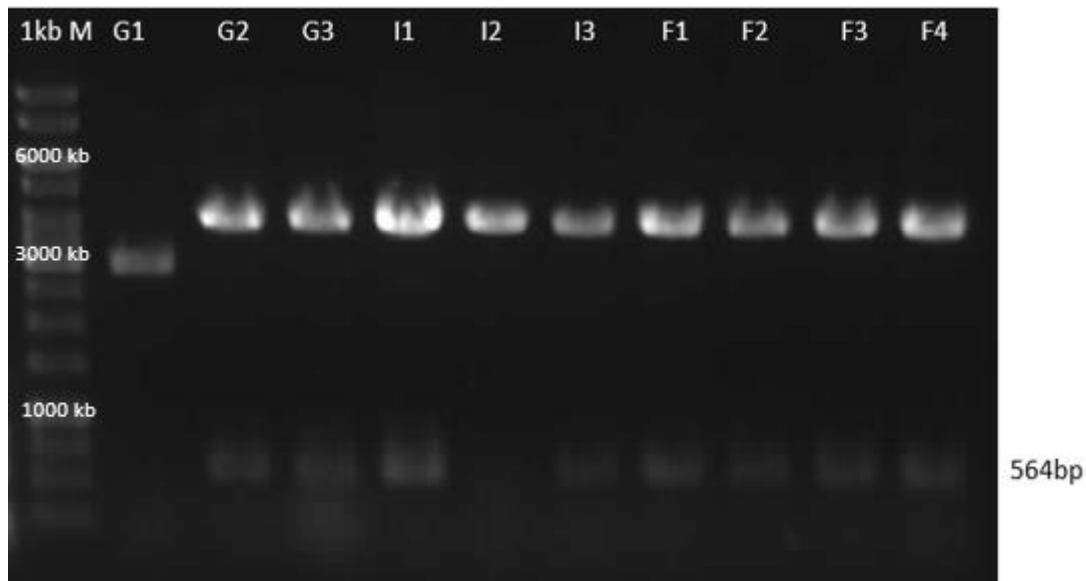
Figure 20: Overnight digestion with EcoRI of the TOPO vector ligated to PCR fragment obtained from CRISPR/Cas9 targeted DDX5 sequences in HeLa cells, to demonstrate a presumably incorporated PCR amplicon. Lanes G1-G3 show the digestion of TOPO plasmids with a presumably incorporated PCR product of CRISPR/Cas9 target region from colony G. Lanes I1-I3: digestion of TOPO plasmids with a presumably incorporated PCR product of CRISPR/Cas9 target region from colony I. Lanes F1-F4: digestion of TOPO plasmids with a presumably incorporated PCR product of CRISPR/Cas9 target region from colony F. 1kb M: 1 kb Plus DNA ladder. Electrophoresis conditions: 1% agarose-gel, 1 h, 120 V.

From the TOPO plasmid digestion with EcoRI it was concluded that all isolated TOPO plasmids except those analyzed in lanes G1 and I2 had taken up the PCR product of CRISPR/Cas9 target region amplified from the colonies F, G and I. In all lanes on Fig. 20, except G1 and I2, a band of 564 bp was visible, corresponding to the PCR product size of the CRISPR/Cas9 target region.

From all the lanes, except G1 and I2 the respected TOPO plasmids were sequenced with M13r primer. The sequencing results showed a mutation which put an out-of-frame stop codon into frame (Figure 21) (sequences shown in the Supplemental materials).

```
Wt   1802  GGTCGTTCCAGGGGTAGAGGAGGCATGAAGGATGACCGTCGGGACAGATACTC
     481   G   R   S   R   G   R   G   G   M   K   D   D   R   R   D   R   Y ...
```

```
G2   1802  GGTCGTTCCAGGGGTAGGAGGAGGCATGAAGGATGACCGTCGGGACAGATACTC
     481   G   R   S   R   G   R   R   R   H   E   G   *
G3   1802  GGTCGTTCCAGG--------AGGCATGAAGGATGACCGTCGGGACAGATACTC
     481   G   R   S   R           R   H   E   G   *
```

```
I1   1802  GGTCGTTCCAGGGGTA-AGGAGGCATGAAGGATGACCGTCGGGACAGATACTC
     481   G   R   S   R   G   K   E   A   *
I2   1802  GGTCGTTCCAGGGGTAG--GAGGCATGAAGGATGACCGTCGGGACAGATACTC
     481   G   R   S   R   G   R   R   H   E   G   *
```

```
F1   1802  GGTCGTTCCAGGGGTAGGAGGAGGCATGAAGGATGACCGTCGGGACAGATACTC
     481   G   R   S   R   G   R   R   R   H   E   G   *
F2   1802  GGTCGTTCCAGGGGTAG-GG-GGCATGAAGGATGACCGTCGGGACAGATACTC
     481   G   R   S   R   G   R   G   H   E   G   *
```

Figure 21: Sequence alignment of different CRISPR/Cas9 edited HeLa colonies (F, G and I) to a DDX5 consensus sequence. The differences are shown in red and the new in-frame stop codon is marked with a star (*). Wt: consensus DDX5 sequence. G2: sequencing result from TOPO plasmid G2. G3: sequencing result from TOPO plasmid G3. I1: sequencing result from TOPO plasmid I1. I2: sequencing result from TOPO plasmid I2. F1: sequencing result from TOPO plasmid F1. F2: sequencing result from TOPO plasmid F2.

Together with the supporting evidence obtained by Western blot analysis, the sequencing results, as well as the Surveyor assay, we have concluded that we do in fact have a CRISPR/Cas9 mediated DDX5ΔPfam HeLa cells in all three colonies: F, G and I. From now on we called them DDX5ΔPfam HeLa cells F, G and I, respectively.

4.4.5. Checking predicted off-target sites

The analysis of potential off-target Cas9-endonuclease activities is needed to confirm sgRNA and thus gene-specific genotype-phenotype relationships [41]. Thus, PCR-amplification of predicted sgRNA-off-target sites was performed and PCRs with primers surrounding predicted sgRNA-off-target sites in the genomic DNA from DDX5ΔPfam HeLa cells F, G and I (primers are shown in a primer list as T1 fwd, T1 rev, T2 fwd, T2 rev, T3 fwd, T3 rev, in Supplemental materials; Table 16) were analyzed by agarose-gel electrophoresis (Figure 22).
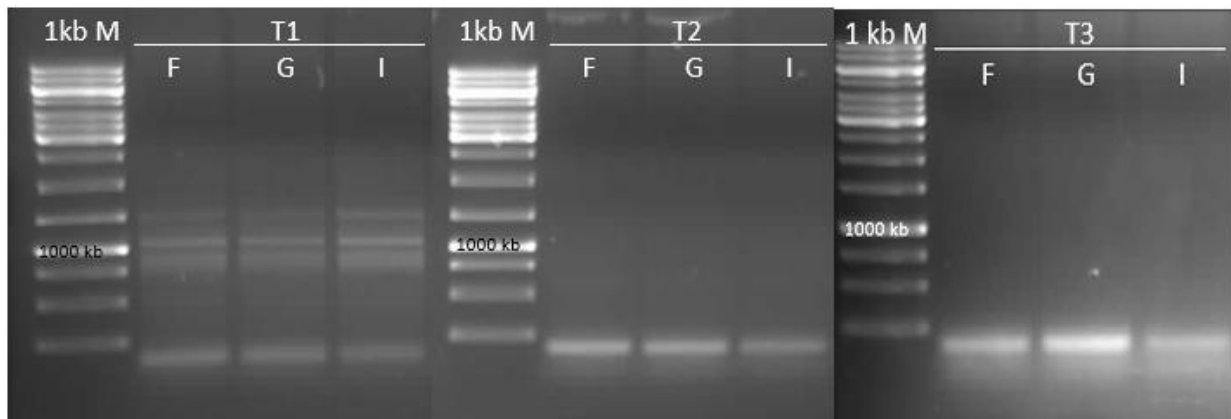
Figure 22: PCR product of predicted off-target sites obtained from genomic DNA of DDX5ΔPfam HeLa cells, clones F, G and I. T1: Amplification of site off-target 1 from DDX5ΔPfam HeLa cells F (F), DDX5ΔPfam HeLa cells G (G) and DDX5ΔPfam HeLa cells I (I). T2: Amplification of site off-target 2 from DDX5ΔPfam HeLa cells F (F), DDX5ΔPfam HeLa cells G (G) and DDX5ΔPfam HeLa cells I (I). T3: Amplification of site off-target 3 from DDX5ΔPfam HeLa cells F (F), DDX5ΔPfam HeLa cells G (G) and DDX5ΔPfam HeLa cells I (I). 1kb M: 1 kb plus DNA ladder. Electrophoresis conditions: 1% gel, 1h, 120V.

The analysis of PCR product surrounding site of off-target 1 from all the DDX5ΔPfam HeLa clones F, G and I, showed, beside some unspecific bands, the correct size band of 159 bp, which was extracted and send for sequencing (Fig. 22). From the analysis of PCR product surrounding site of off-target 2 from all the DDX5ΔPfam HeLa cells F, G and I the correct size band was amplified the correct size band of 186 bp and sequenced. From the analysis of PCR product surrounding site of off-target 3 from all the DDX5ΔPfam HeLa cells F, G and I the correct size band was amplified the correct size band of 187 bp and sequenced. From the sequencing results it was concluded that there were no off-target effects (sequences and the explanation shown in Supplemental materials).

4.5. Functional analysis

4.5.1. Trypan blue cell counting

For cell proliferation analysis, the cells were counted and seeded at the same number in a number of dishes needed for experiment. The proliferation rate estimations were based on counting the cells at three time points after the seeding, so after 12 h, 24 h and 32 h. The number of different DDX5ΔPfam HeLa cells F, G and I were compared to the wild type HeLa cells at respected time points and p-values were calculated using unpaired Student´s T-Test From the graph (Figure 23), it was visible that the DDX5ΔPfam HeLa cells F, G and I grew at a slower rate compared to the wild type HeLa cells.
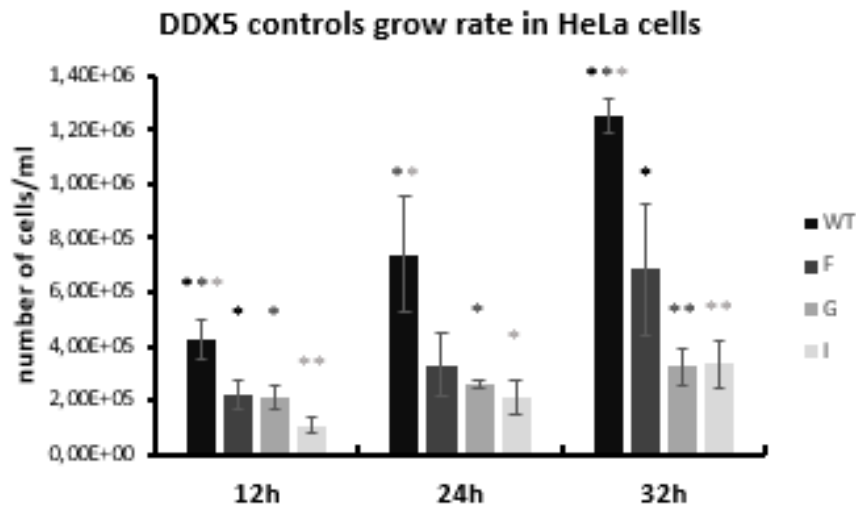
Figure 23: DDX5ΔPfam HeLa cells grow at a slower rate compared to the wild type HeLa cells. Cells were stained by Trypan blue and counted under a microscope. Asterisks indicate levels of significance versus wild type HeLa cells * Significance <0,05, ** significance <0,01. Calculated by Student´s T-TEST, 2 tailed, unpaired, two-sample equal variance. WT: wild type HeLa cells. F: DDX5ΔPfam HeLa cells F. G: DDX5ΔPfam HeLa cells G. I: DDX5ΔPfam HeLa cells I.

4.5.2. Cell cycle analysis

Cell cycle analysis was done by flow cytometry on wild type HeLa cells as well as on the DDX5ΔPfam HeLa cells F, G and I.

The percentage of cells in phases G1, S and G2/M was estimated by cell cycle histogram analysis and as can be seen in Figure 24, there was less percentage of DDX5ΔPfam HeLa cells F, G and I in the S-phase in contrast to the wild type HeLa cells.
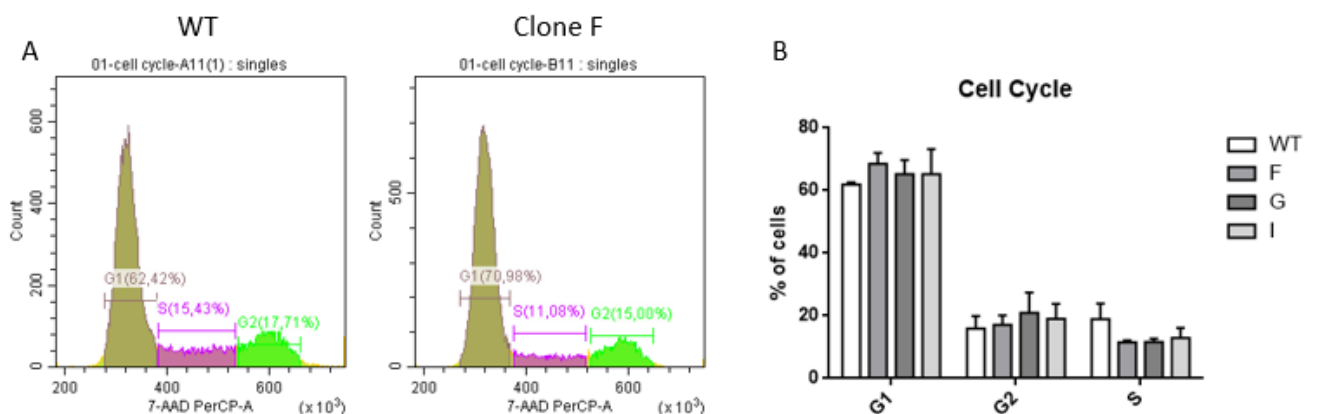
Figure 24: Cell cycle analysis by flow cytometry. A) Cell cycle histograms of wild type HeLa cells and DDX5ΔPfam HeLa cells F representative. B) Graph of all the analyzed HeLa cell

subtypes. WT: wild type HeLa cells. F, G, I: DDX5ΔPfam HeLa cells F, G and I. G1: G1-phase of a cell cycle. G2: G2/M-phase of a cell cycle. S: S-phase of a cell cycle.

In order to see possible differences in cell response, wild type and DDX5ΔPfam HeLa cells F, G and I were treated with TNF and etoposide. TNF causes activation of the NF-κB pathway, and etoposide causes DNA damage through provoking double-strand breaks. Upon the TNF and etoposide treatment there was also a visible difference in the distribution of cells in the cell cycle phases. While the G1- and G2/M-phases follow the same pattern in the DDX5ΔPfam HeLa cells and the wild type HeLa cells, there was no visible reduction in the S-phase cell number upon stimulation in the DDX5ΔPfam HeLa cells. On the contrary, a reduction in the S-phase cell number was observed in the wild type HeLa cells. Upon the stimulation with TNF or etoposide there was a decrease of cell number in G1-phase and their increase in G2/M-phase in all cell strains in regard to the untreated control (Figure 25).
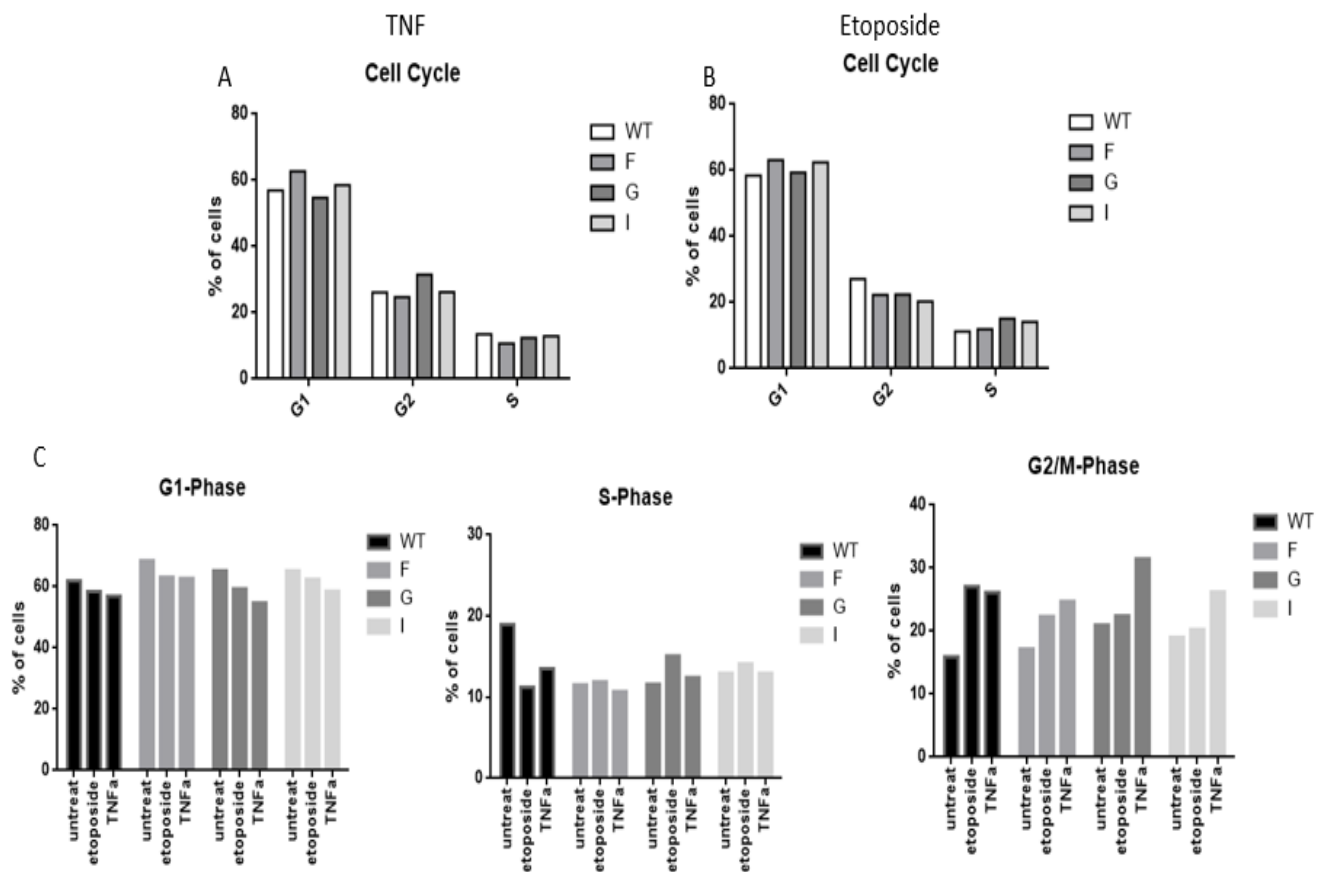
Figure 25: Cell cycle analysis of wild type HeLa cells and DDX5ΔPfam HeLa cells, after stimulation with TNF or etoposide. A) Cells were treated with TNF (10 ng/ml) for 5 h when harvested and analyzed by flow cytometry. B) Cells were treated with etoposide 100 µM for 5 h when harvested and analyzed by flow cytometry. C) Individual cell cycle phases upon the different treatment (untreated, etoposide, TNF). WT: wild type HeLa cells; F, G, I: DDX5ΔPfam HeLa cells. Representative experiment of cell cycle analysis upon TNF or etoposide stimulation.

4.5.3. Luciferase reporter gene assay in HEK293 cells, HeLa cells and DDX5ΔPfam HeLa cells

In order to see the influence of wild type DDX5, as well as DDX5ΔPfam under the conditions of overexpression on NF-κB activation, Luciferase reporter gene assay was performed. Since in this experiment wild type cells were used, HEK293 cells were employed because of their ability to easily uptake plasmid DNA transfected by calcium phosphate method.

The HEK293 cells were transfected with the N-terminal flag-tagged DDX5 pcDNA3 expression plasmid or B1-pfam in pcDNA3 (expression plasmid of DDX5ΔPfam), along with 5x-NF-κB-luc reporter and UBT-ß-gal plasmids. The induction of NF-κB-luc activity was noted only in the cells overexpressing wild type DDX5, but not in those overexpressing DDX5ΔPfam. To analyze whether DDX5 or its mutant would further augment already pre-elevated NF-κB activity, the two versions of DDX5 expression plasmids were co-transfected with a HA-p65- in pcDNA3 expression vector. Upon 1 µg of transfected plasmid DNA wild type DDX5, but not upon mutant DDX5 transfection, augmentation of NFκB activity was observed (Figure 26).
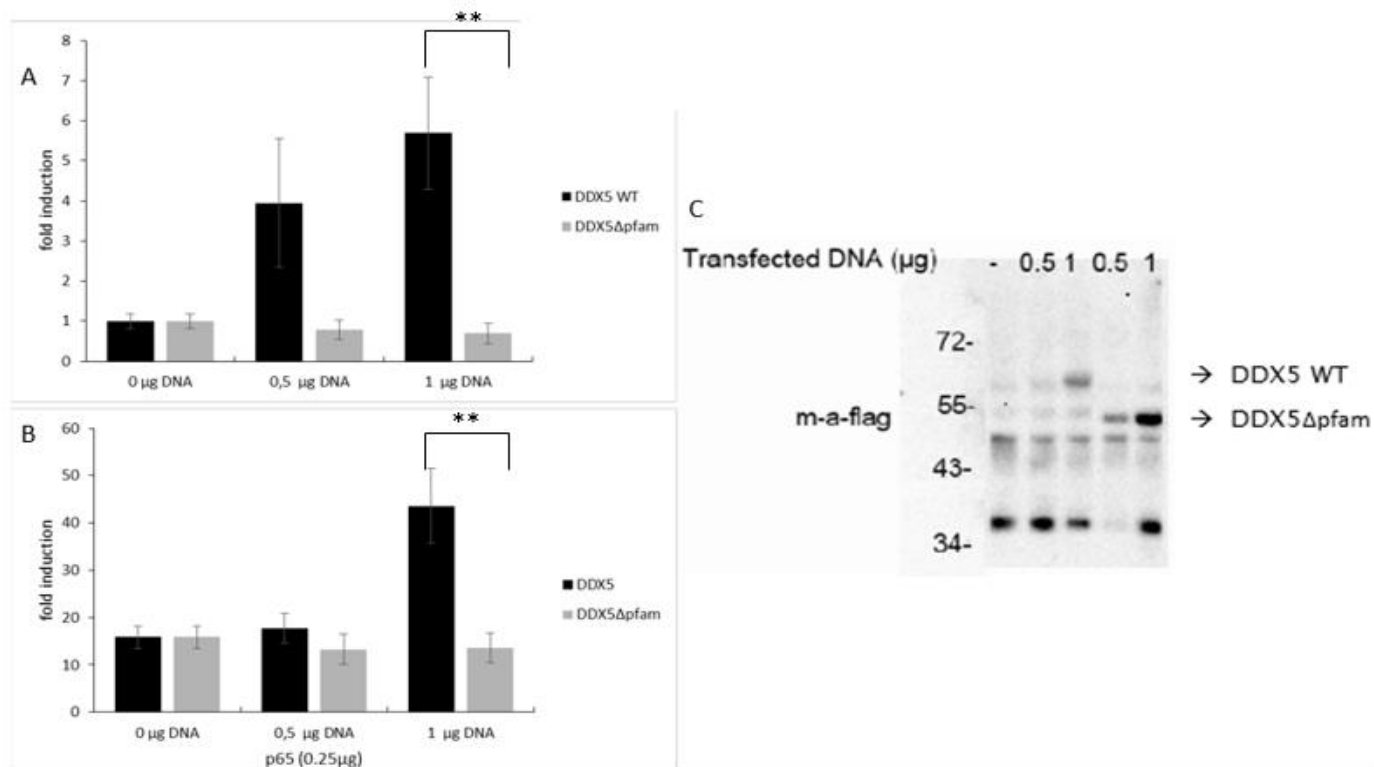
Figure 26: Reporter gene analysis in HEK293 cells transfected with the DDX5 expression plasmid or B1-pfam (DDX5ΔPfam expression plasmid). A) Luciferase activity in HEK293 cells transfected by 5x-NF-κB-luc reporter plasmid, UBT-ß-gal and N-terminal flag-tagged DDX5 pcDNA3 (DDX5 expression plasmid) or B1-pfam (DDX5ΔPfam expression plasmid). B) Luciferase activity in HEK293 cells transfected with 5x-NF-κB-luc reporter plasmid, UBT-ß-gal, HA-p65- in pcDNA3 and N-terminal flag-tagged DDX5 pcDNA3 (DDX5 expression plasmid) or B1-pfam (DDX5ΔPfam expression plasmid). C) Western blot analysis of expression of exogenous DDX5 and exogenous DDX5ΔPfam expression plasmid probed with anti-flag antibody. DDX5: cells co-transfected with DDX5 wild type expression plasmid (N-terminal

flag-tagged DDX5 pcDNA3). DDX5Δpfam: cells co-transfected with DDX5ΔPfam expression plasmid (B1-pfam). Asterisks indicate levels of significance versus wild type HeLa cells *: $p < 0.05$; **: $p < 0.01$ calculated by student T.TEST, 2 tailed, unpaired, Two-sample equal variance.

It is visible from the graph (Figure 26 A and B) that the wild type DDX5 activates NF-κB but not the DDX5 mutant lacking its Pfam domain (DDX5Δpfam). In case of co-transfected p65 there were higher levels of induction of NF-κB when wild type DDX5 is present than when the DDX5 lacking Pfam domain was present. Figure 26C presents Western blot analysis of exogenous DDX5 and DDX5Δpfam showing that the transfected plasmids really do express proteins of different sizes, corresponding to the wild type DDX5 and truncated DDX5 missing the Pfam domain.

To test further the influence of DDX5 in the NF-κB-pathway, myc-IKK2 expression plasmid or HA-IKK1 in pcDNA3 was co-transfected with a N-terminal flag-tagged DDX5 pcDNA3, 5x-NF-κB-luc reporter plasmid and UBT-ß-gal. Reporter gene assay demonstrated that in the case of IKK2 expression, no further induction was noticeable in the cells with DDX5 overexpression. On the other hand, when IKK1 was expressed, DDX5 overexpression stimulated the NF-κB activity (Figure 27). This could suggest that DDX5 is a part of the non-canonical, IKK1-dependent pathway.
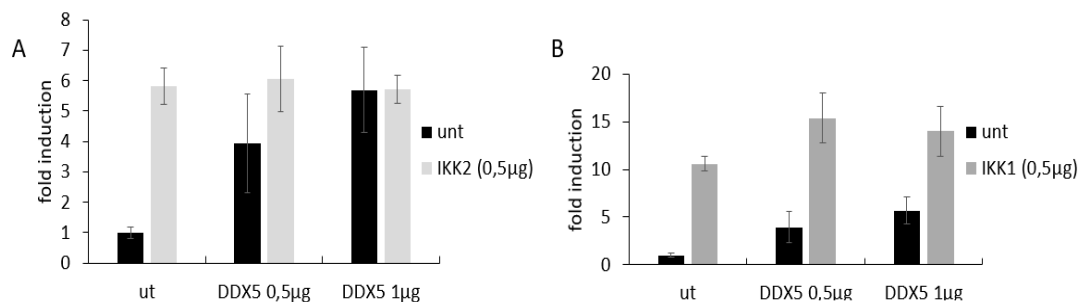
Figure 27: DDX5 can augment IKK1- but not IKK2-induced NF-κB activity. A) myc-IKK2 was co-transfected with different amounts of DDX5 expression plasmid plus a 5xNF-κB-luc reporter plasmid and UBT-ß-gal into HEK293 cells, and NF-kB activity was measured by reporter gene analysis. B) HA-IKK1 in pcDNA3 was co-transfected with different amounts of DDX5 expression plasmid plus a 5xNF-κB-luc reporter plasmid and UBT-ß-gal into HEK293 cells, and NF-κB activity was measured by reporter gene analysis. unt: untreated HEK293 cells. IKK2: HEK293 cells co-transfected with myc-IKK2 along with the other plasmids noted before; IKK1: HEK293 cells co-transfected with HA-IKK1 along with the other plasmids noted before.

Next, I assayed basal and p65-inuced NF-κB activity in wild type HeLa cells and DDX5ΔPfam HeLa cells F, G and I. The 5xNF-κB reporter plasmid plus a vector for constitutive EGFP (pmaxGFP) expression were co-transfected into DDX5ΔPfam HeLa cells F, G and I, and wild type HeLa cells; NF-κB activity was measured by luciferase assay. As shown in Figure 28, NF-

κB activity tended to be lower in the DDX5ΔPfam HeLa cells in comparison with wild type cells, in cells activated by co-transfection of HA-p65- in pcDNA3 (Figure 28).
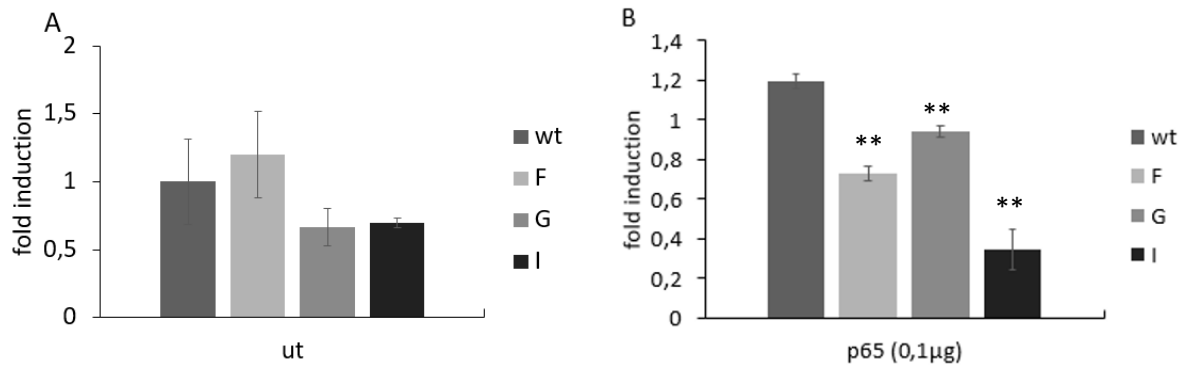
Figure 28: Reporter gene assay in wild type HeLa cells and DDX5ΔPfam HeLa cells. A) DDX5ΔPfam HeLa cells and wild type HeLa cells were co-transfected with 5xNF-κB reporter plasmid and pmaxGFP plasmid; NF-κB activity was measured by reporter gene analysis. B) DDX5ΔPfam HeLa cells and wild type HeLa cells were co-transfected with 5xNF-κB reporter plasmid, pmaxGFP plasmid and HA-p65- in pcDNA3; NF-κB activity was measured by reporter gene analysis. Asterisks indicate levels of significance versus wt cells (*: p<0.05; **: p<0.01) calculated by student T.TEST, 2 tailed, unpaired, Two-sample equal variance. wt: wild type HeLa cells; F, G, I: DDX5ΔPfam HeLa cells F, G and I. ut: cells co-transfected with 5xNF- κB reporter plasmid and pmaxGFP plasmid. p65 (0,1 μg): cells co-transfected with 5xNF- κB reporter plasmid, pmaxGFP plasmid and p65 expression plasmid 0.1 μg.

4.5.4. RT-qPCR and associated Western blot analysis of HeLa and primary HUVEC DDX5 knockdown cells and DDX5ΔPfam HeLa cells

In a complementary approach we have knocked down DDX5 in HeLa cells using lentiviral vectors expressing four different shRNAs (A-D). These cells were obtained after selection for stable integration based on a puromycin-casette. In addition, the internal-ribosomal-entry-site (IRES) driven GFP-expression was used to enrich transduced cells early after transduction by Fluorescence activated cell sorting (FACS). Cells were kindly provided by U. Resch. Cells were analyzed for DDX5 mRNA and protein levels which were different in different cell pools (Figure 29A). Cells were also analyzed on IL8 expression in basal conditions and after 1 h TNF stimulation (Figure 29B and C).
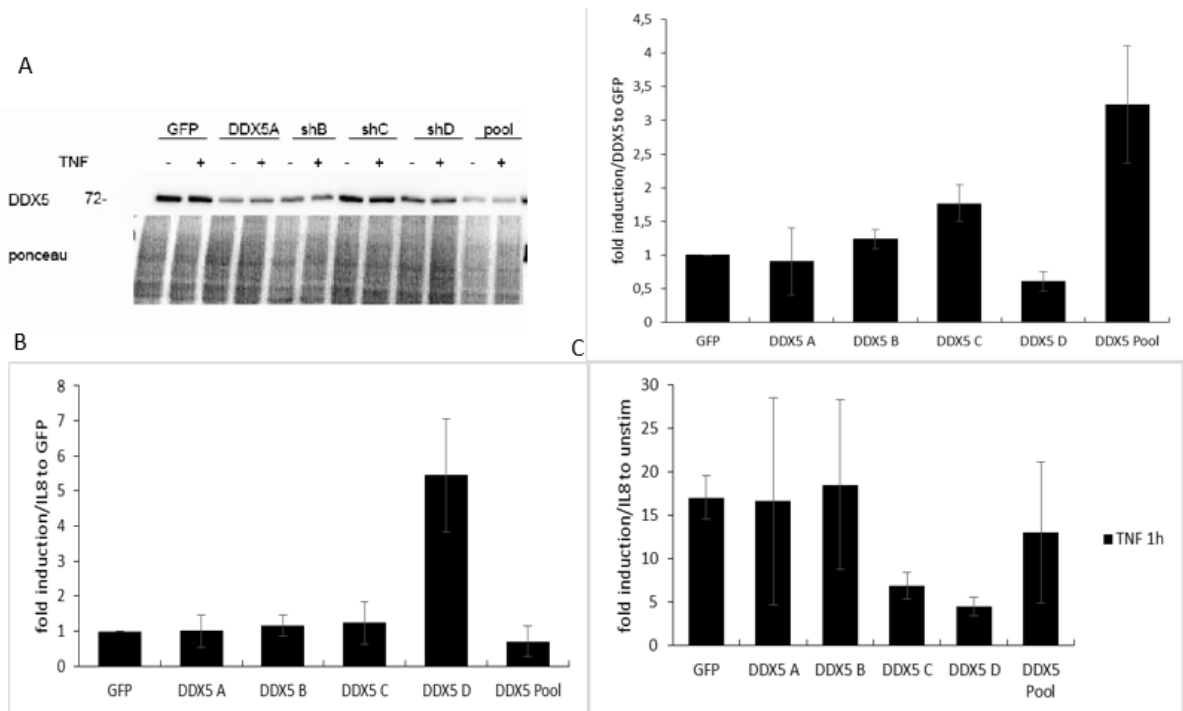
Figure 29: Analysis of mRNA and protein levels of DDX5 as well as mRNA basal and induction levels of IL8 from the experiment performed in HeLa cells stably expressing different shRNA targeting DDX5. A) Left panel: Western blot analysis of isolated proteins from HeLa cells treated with different shRNAs, PonceauS staining is shown as loading control. Right panel: RT-qPCR of basal DDX5 mRNA expression levels. Expression levels were first normalized to ß-2-microglobulin (B2MG) housekeeping gene and secondly to scrambled shRNA control in HeLa cells treated with different shRNA. B) RT-qPCR of IL8, first normalized to the B2MG housekeeping gene and secondly to scrambled shRNA control in HeLa cells treated with different shRNA. C) RT-qPCR of 1 h TNF (10 ng/ml) stimulated HeLa cells treated with different shRNAs, IL8 is first normalized to the B2MG housekeeping gene and secondly to the unstimulated corresponding cells. GFP: HeLa cells treated with the scrambled shRNA. DDX5A: HeLa cells treated with the lentiviral particle DDX5A (also called shA). shB: HeLa cells treated with lentiviral particle shB. shC: HeLa cells treated with lentiviral particle shC. shD: HeLa cells treated with lentiviral particle shD. pool: mix of HeLa cells treated with all four lentiviral particles for knocking down DDX5.

RT-qPCR performed on HeLa cells treated with one of four different constructs of lentiviral particles and the respecting Western blot analysis showed that the most effective in knocking down DDX5 protein and mRNA levels was lentiviral particle shD. With that in mind, it is visible that mRNA basal levels of NF-κB dependent gene IL8 were higher in the lentiviral particle shD treated HeLa cells when compared to the lentiviral particle carrying scrambled shRNA treated control. Upon the TNF stimulation, induction levels of IL8 mRNA were lower in shD treated HeLa cells in comparison to the scrambled shRNA treated cells.

In addition, the knockdown experiments were also done in HUVEC cells. The RT-qPCR and Western blot analysis shown in Figure 30 confirmed the knockdown DDX5 mRNA and protein levels.
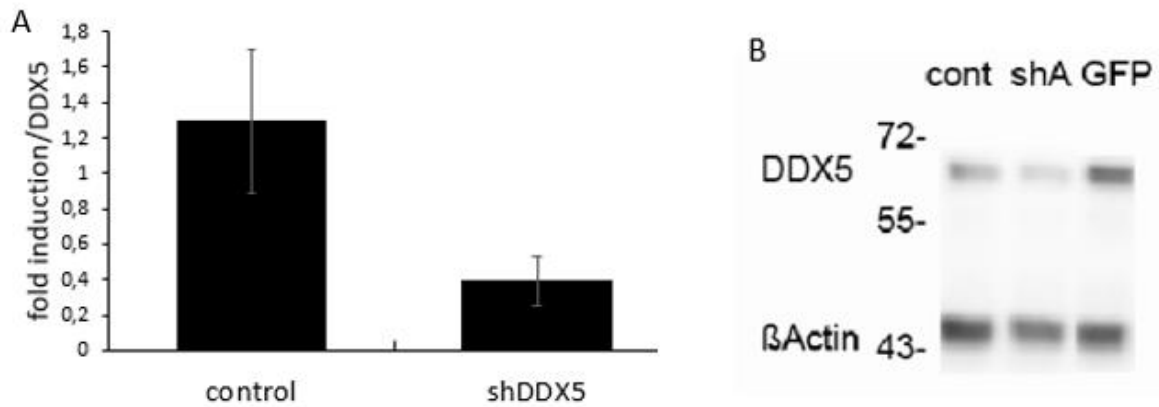
Figure 30: Analysis of DDX5 expression on protein and RNA level in HUVEC cells stably expressing different shRNA targeting DDX5 (shDDX5). A) Cells were transfected with lentiviral particle shDDX5 (also called shA) or scrambled shRNA, and mRNA levels of DDX5 were analyzed by RT-qPCR, DDX5 mRNA levels were first normalized to the B2MG housekeeping gene and secondly to scrambled shRNA treated cells. B: Western blot analysis of whole cell lysate isolated proteins were probed with antibodies against DDX5 and β actin control. Control: untreated HUVEC cells. shDDX5/shA: HUVEC cells treated with lentiviral particle shDDX5 (also called shA). GFP: HUVEC cells treated with scrambled shRNA.

Next, I assayed basal and TNF stimulated mRNA levels of two NF-κB-dependent genes (IκBα and A20) using RT-qPCR analysis on the shRNA treated HUVEC cells, as well as on untreated control. There was a weak effect of DDX5 knockdown on the basal levels of both genes, but no effect upon the TNF stimulation induced levels. NF-κB family members IκBα and A20 had similar basal levels in knockdown DDX5 primary HUVEC cells in comparison with wild type cells (Figure 31).
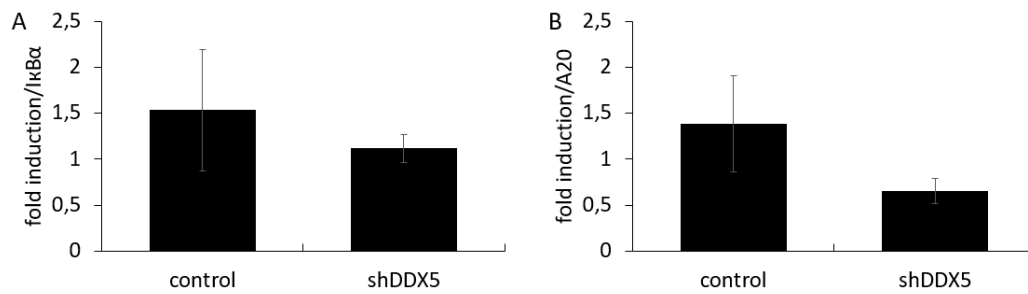
Figure 31: Analysis of basal mRNA levels of NF-κB family members IκBα and A20 in HUVEC cells. A) RT-qPCR of IκBα in untreated and shDDX5 treated HUVEC cells normalized first to the B2MG housekeeping gene and secondly to scrambled shRNA treated cells. B) RT-qPCR of A20 in untreated and shDDX5 treated HUVEC cells first normalized to the B2MG housekeeping gene and secondly to scrambled shRNA treated cells. control: untreated HUVEC cells. shDDX5: HUVEC cells treated with shDDX5 (also called shA) lentiviral particle.

DDX5 knockdown did not have an impact on NF-κB negative feedback regulators, IκBα and A20 in primary HUVEC cells upon TNF stimulation (Figure 32).
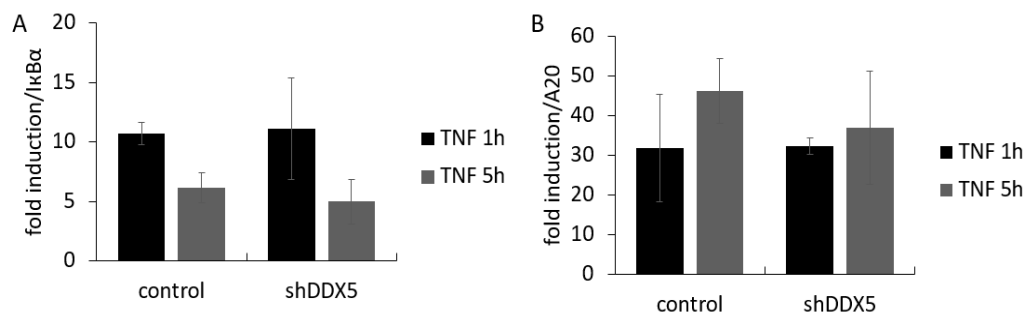
Figure 32: Analysis of TNF (10 ng/ml) stimulated cells after 1 h and 5 h stimulation in HUVEC cells treated with lentiviral particle shDDX5 (also called shA) and untreated control. A) RT-qPCR results on TNF stimulated HUVEC cells treated with lentiviral particle shA and untreated control of IκBα mRNA induction levels first normalized to the B2MG housekeeping gene and secondly to the scrambled shRNA treated cells. B) RT-qPCR on TNF stimulated HUVEC cells treated with lentiviral particle shDDX5 and untreated control of A20 mRNA induction levels first normalized to the B2MG housekeeping gene and secondly to the scrambled shRNA treated cells. Control: HUVEC cells untreated by lentiviral particle, but stimulated with TNF. shDDX5: shDDX5 (also called shA) treated HUVEC cells, TNF stimulated. TNF 1h: Cell harvested after 1h TNF stimulation. TNF 5h: Cells harvested after 5h.

4.5.5. Analysis of cell cycle related genes in DDX5ΔPfam HeLa cells

Intrigued by the different proliferation rate of DDX5ΔPfam HeLa cells F, G and I, I analyzed the mRNA levels of cell cycle dependent genes (p21 and Cyclin D1) in those cells as well as in wild type HeLa cells.

Basal levels of cell cycle associated genes' expression differed in the wild type and individual DDX5ΔPfam HeLa cells (Figure 33).
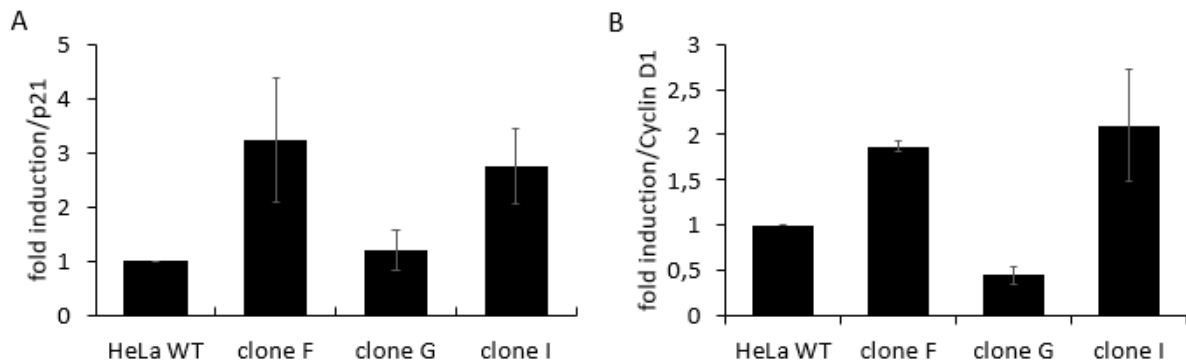
Figure 33: Analysis of cell cycle dependent genes in wild type HeLa cells and in DDX5ΔPfam HeLa cells. A) RT-qPCR results of p21 mRNA levels first normalized to the B2MG housekeeping gene and secondly to wild type HeLa cells, in wild type HeLa cells and in DDX5ΔPfam HeLa cells. B) RT-qPCR results of Cyclin D1 mRNA levels first normalized to the B2MG housekeeping gene and secondly to wild type HeLa cells, in wild type HeLa cells and in DDX5ΔPfam HeLa cells. HeLa WT: wild type HeLa cells. clone F, G, I: DDX5ΔPfam HeLa cells F, G and I.

Giving the interesting results in the distribution of cells through the cell cycle upon the TNF and etoposide treatment, mRNA levels of p21 and Cyclin D1 upon the TNF and etoposide stimulation were analyzed. Upon the TNF stimulation p21 and Cyclin D1 mRNA levels were not statistically significantly different in DDX5ΔPfam HeLa cells, in comparison with wild type cells (Figure 34; Figure 35, respectively).
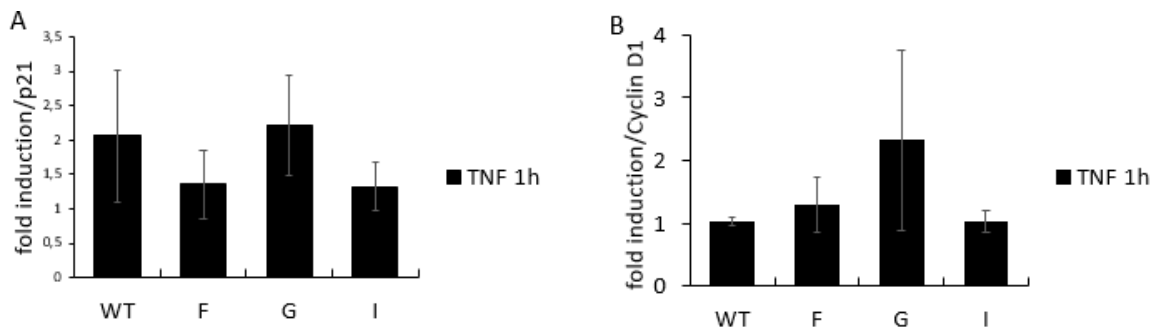
Figure 34: Analysis of mRNA induction levels of cell cycle dependent genes. Analysis were performed on wild type HeLa cells and DDX5ΔPfam HeLa cells upon TNF (10 ng/ml) stimulation, cells were harvested 1 h post-stimulation. A) RT-qPCR results of p21 mRNA levels in wild type HeLa cells and in DDX5ΔPfam HeLa cells, upon TNF stimulation first normalized to the B2MG housekeeping gene and secondly to unstimulated corresponding cells. B) RT-qPCR results of Cyclin D1 mRNA levels in wild type HeLa cells and in DDX5ΔPfam HeLa cells upon TNF stimulation first normalized to the B2MG housekeeping gene and

secondly to unstimulated corresponding cells. WT: wild type HeLa cells. F, G, I: DDX5ΔPfam HeLa cells F, G and I. TNF 1h: cells were harvested 1h post-TNF stimulation.

Since it was shown that TNF influences Cyclin A1 [42], Western blot analysis of Cyclin A1 in DDX5ΔPfam HeLa cells was performed. It showed higher basal levels of Cyclin A1 protein in DDX5ΔPfam HeLa cells in comparison with wild type cells, but also lower induction of Cyclin A1 protein in DDX5ΔPfam HeLa cells upon TNF stimulation (Figure 35).
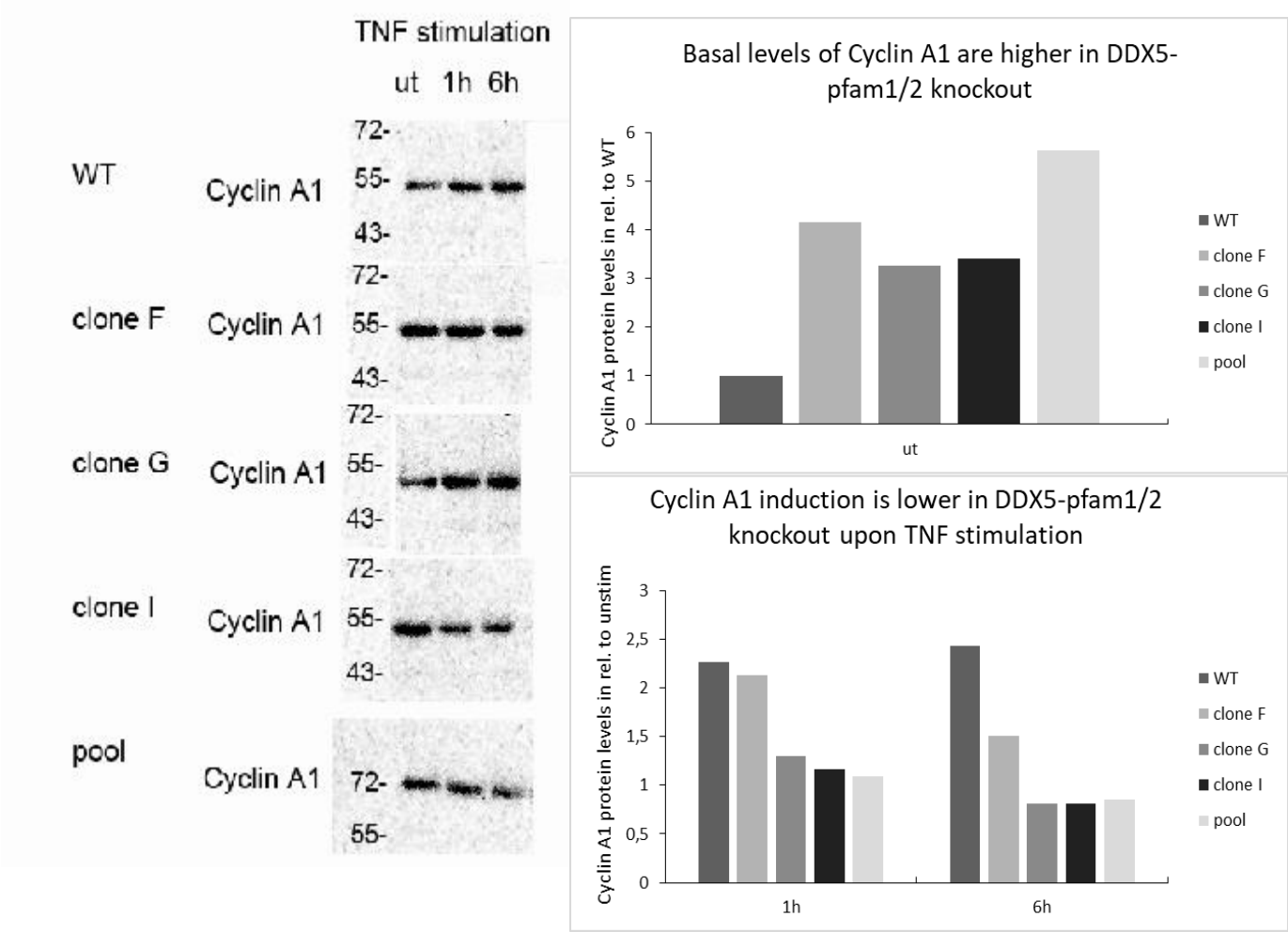
Figure 35: Western blot analysis of Cyclin A1 in wild type Hela cells and DDX5ΔPfam HeLa cells. Left: Western blot analysis of isolated proteins from wild type HeLa cells and DDX5ΔPfam HeLa whole cell lysates, probed against Cyclin A1. Right: Quantification of the Western blot performed with ImageJ-win64.exe measuring the integrated density of each band and normalizing it to the integrated density of PonceauS staining of the respected line.

Upon the etoposide stimulation, p21 mRNA levels increased, compared to the basal levels, especially in DDX5ΔPfam HeLa cells G, while Cyclin D1 mRNA levels were below basal values, even though they were higher in DDX5ΔPfam HeLa cells than the wild type HeLa cells (Figure 36).
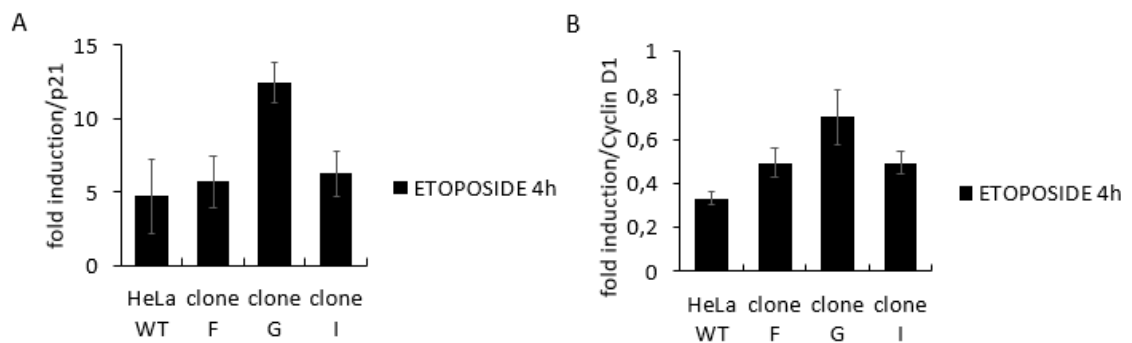
Figure 36: Analysis of mRNA induction levels of cell cycle dependent genes upon the etoposide treatment in HeLa wild type cells and DDX5ΔPfam HeLa cells. A) RT-qPCR results of p21 mRNA levels in wild type HeLa cells and in DDX5ΔPfam HeLa cells (F, G and I) upon etoposide stimulation first normalized to the B2MG housekeeping gene and secondly to unstimulated corresponding cells. B) RT-qPCR results of Cyclin D1 mRNA levels in wild type HeLa cells and in DDX5ΔPfam HeLa cells (F, G and I) upon etoposide stimulation first normalized to the B2MG housekeeping gene and secondly to unstimulated corresponding cells. WT: wild type HeLa cells. F, G, I: DDX5ΔPfam HeLa cells F, G and I. ETOPOSIDE 4h: cells were harvested 4 h post-etoposide stimulation.

To finally asses the function for which the DDX5ΔPfam HeLa cells were constructed, I looked into basal mRNA levels of NF-κB dependent genes, and saw that it differed from those of the wild type HeLa cells, as well as among the individual DDX5ΔPfam HeLa cell clones. Upon the TNF stimulation, induction levels of mRNA of the NF-κB dependent genes tend to be lower in DDX5ΔPfam HeLa cells, except in the case of IL8 in DDX5ΔPfam HeLa cells F (Figure 37).
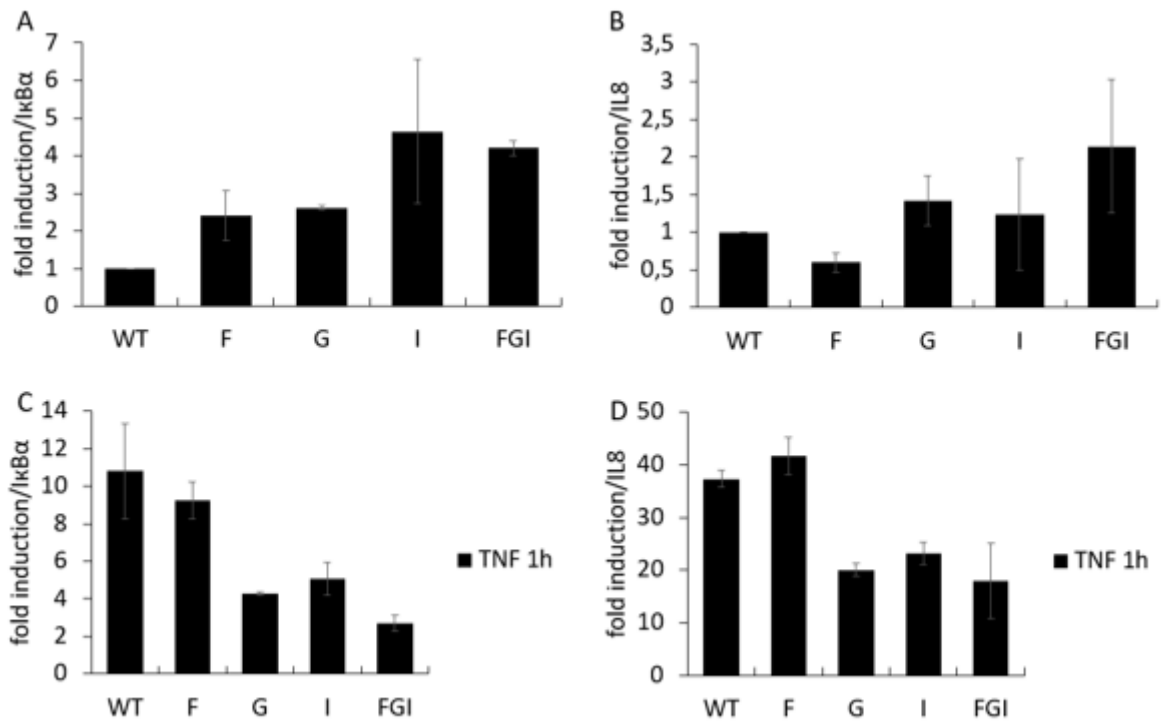
Figure 37: Analysis of mRNA induction levels of NF-κB dependent genes in wild type HeLa cells and in DDX5ΔPfam HeLa cells. A) RT-qPCR results of IκBα basal mRNA levels in wild type HeLa cells and in DDX5ΔPfam HeLa cells first normalized to the B2MG housekeeping gene and secondly to wild type HeLa cells. B) RT-qPCR results of IL8 basal mRNA levels in wild type HeLa cells and in DDX5ΔPfam HeLa cells first normalized to the B2MG housekeeping gene and secondly to wild type HeLa cells. C) RT-qPCR results of IκBα mRNA levels in wild type HeLa cells and in DDX5ΔPfam HeLa cells upon TNF stimulation first normalized to the B2MG housekeeping gene and secondly to unstimulated corresponding cells. D) RT-qPCR results of IL8 mRNA levels in wild type HeLa cells and in DDX5ΔPfam HeLa cells upon TNF stimulation first normalized to the B2MG housekeeping gene and secondly to unstimulated corresponding cells. WT: wild type HeLa cells. F, G, I: DDX5ΔPfam HeLa cells F, G and I. TNF 1h: cells were harvested 1 h post-TNF stimulation.

To see if there is a difference between DDX5ΔPfam HeLa cells and wild type HeLa cells response upon non-canonical NF-κB response, cells were stimulated with CD40L. Upon the CD40L stimulation, DDX5ΔPfam HeLa cells had higher mRNA levels of NF-κB dependent genes (Figure 38).
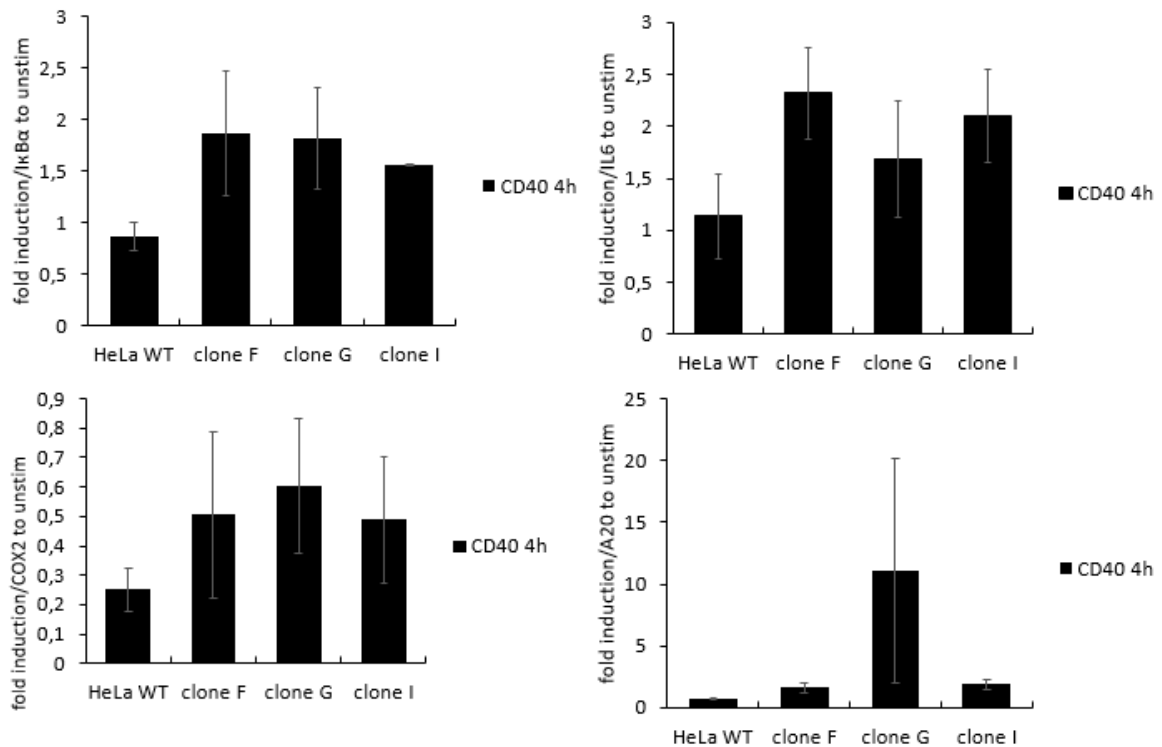
Figure 38: Induction levels of NF-κB dependent genes upon CD40L stimulation in HeLa wild type cells and DDX5ΔPfam HeLa cells. Cells were stimulated with CD40L (100 ng/ml) for 4 h and mRNA levels NF-κB dependent genes were analyzed by RT-qPCR. A) RT-qPCR results of IκBα induction mRNA levels in wild type HeLa cells and in DDX5ΔPfam HeLa cells first normalized to the B2MG housekeeping gene and secondly to unstimulated corresponding cells. B) RT-qPCR results of IL6 induction mRNA levels in wild type HeLa cells and in DDX5ΔPfam HeLa cells first normalized to the B2MG housekeeping gene and secondly to unstimulated corresponding cells C) RT-qPCR results of COX2 induction mRNA levels in wild type HeLa cells and in DDX5ΔPfam HeLa cells first normalized to the B2MG housekeeping gene and secondly to unstimulated corresponding cells. D) RT-qPCR results of A20 induction mRNA levels in wild type HeLa cells and in DDX5ΔPfam HeLa cells first normalized to the B2MG housekeeping gene and secondly to unstimulated corresponding cells.

4.5.6. IκBα kinetics analysis

In order to elucidate the NF-κB activity IκBα kinetics analysis was performed as the IκBα is a negative feedback loop mechanism in NF- κB pathway, IκBα kinetics analysis was performed. In HeLa knockdown cells it was more looked in to the lentiviral particle shD mediated knockdown cells because as shown before that construct gave the most prominent knockdown of DDX5 in HeLa cells. Basal levels of IκBα are higher in the DDX5 knockdown HeLa cells and upon induction with TNF the IκBα protein levels in HeLa knockdown cells need more time to go down (Figure 39).
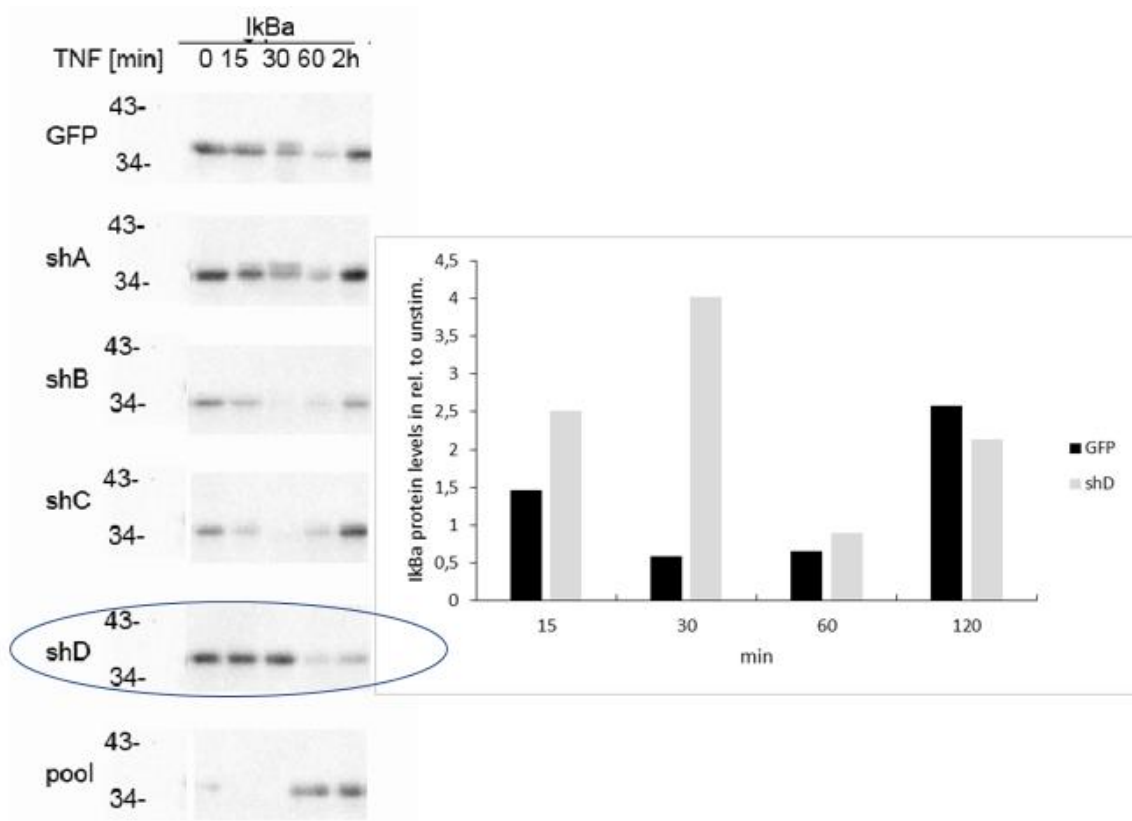
Figure 39: IκBα kinetics analysis in HeLa DDX5 knockout cells. Lentiviral particle treated cells were stimulated with TNF (10 ng/ml) and harvested 15 min, 30 min, 60 min and 2 h post-TNF stimulation, the proteins were isolated from whole cell lysate and probed with antibody against IκBα. Left: Western blot analysis of IκBα kinetics upon TNF stimulation. Right: Quantification of the Western blot performed with ImageJ-win64.exe measuring the integrated density of each band and normalizing it to the integrated density of PonceauS staining of the respected line. GFP: cells treated with scrambled shRNA. shA: cells treated with shA shRNA. shB: cells treated with shB sh RNA. shC: cells treated with shC shRNA. shD: cells treated with shD shRNA

Similar experiment was done in the DDX5ΔPfam HeLa cells for the same reason. The basal levels of the IκBα were higher in all the DDX5ΔPfam HeLa cells whit the exception of clone F. After 25 min of TNF stimulation all the IκBα protein levels were lower than the levels in wild type HeLa cells (Figure 40).
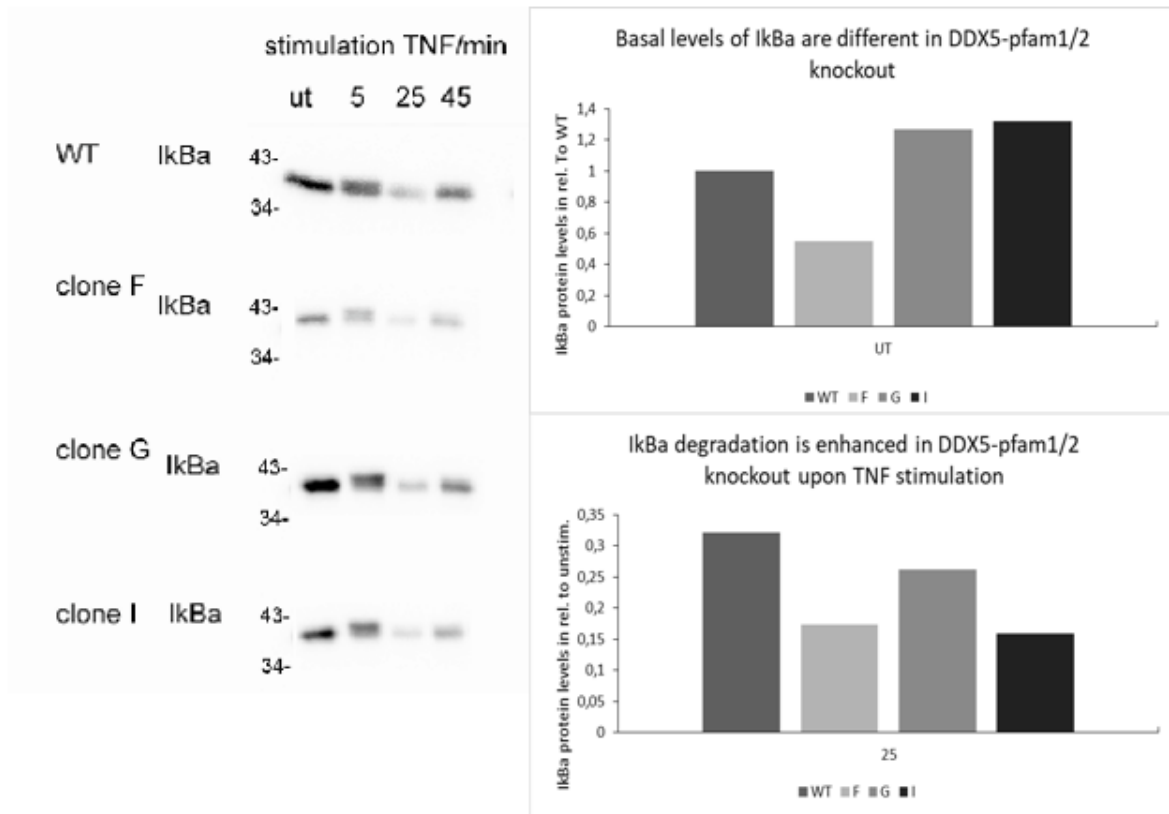
Figure 40: IκBα kinetics analysis in the wild type HeLa cells and DDX5ΔPfam HeLa cells. HeLa cells and DDX5ΔPfam HeLa cells were stimulated with TNF (10 ng/ml) and harvested 5 min, 25 min and 45 min post-TNF stimulation, the proteins were isolated from whole cell lysate and probed with antibody against IκBα. Right: Quantification of the Western blot performed with ImageJ-win64.exe measuring the integrated density of each band and normalizing it to the integrated density of PonceauS staining of the respected line. WT: wild type HeLa cells. F, G, I: DDX5ΔPfam HeLa cells (F, G and I).

5. Discussion:

It was shown before by overexpression experiments that the NF-κB pathway is influenced by DDX5, more precisely the Pfam domains of the DDX5 protein in the lab Rainer de Martin. That experiment I have confirmed by reporter gene assay in HEK293 cells. To complement those results with loss of function studies I have started with CRISPR/Cas9 editing of the HeLa cells as they are quite resilient to the stress of transfection and appropriate for culturing in higher passages. The first approach was to generate a full DDX5 knockout cells by introducing in-frame STOP codon in the first or second exon of *DDX5* gene by two component strategy. This experiment was not immediately successful and it took multiple transfections of the cells until the point of picking individual colonies was achieved. At that point it was also visible that the remaining cells after the double-selection grew at a slow rate.

Reputed DDX5 HeLa knockout cells were impaired in proliferation which lead to unsustainable culture maintenance. It was shown that DDX5 protein is lethal in *vivo*, mice embryos died on embryonal day 11.5 and displayed malformations of blood vessels [43]. The yield of generated cells was so low that there were not enough cells for the planed and developed downstream experiments for the conformation of the knockout and functional analysis. To enable knockout cells to proliferate, a rescue experiment was performed, introducing into the cells an alternative source of DDX5 expression, on a plasmid vector. It could be that the transfection of those cells was not successful. It is also possible that DDX5 in necessary for plasmid stablility as shown by Mauzurek et al [23].

DDX5 protein among other functions has an impact on the cytoskeleton organization through miRNA regulation of cofilin and profilin [44]. In this study, it was also observed that DDX5 knockout cells and wild type HeLa differed in morphology. The DDX5 knockout cells resembled in appearance to the IκBα overexpressed HeLa cells with inhibited NF-κB pathway, as they both had an elongated, flattened and more branched appearance [45].

As it was indicated in previous experiments, in the Rainer de Martin lab, that DDX5 Pfam domain was supposed to be responsible for the impact on NF-κB pathway. That was the reason I proceeded with an editing of a specific region in *DDX5* gene which could in the end give a truncated DDX5 protein lacking Pfam domains. More straight-forward approach was employed by constructing an all-in-one vector carrying Cas9 sequence as well as that coding for sgRNA. This approach also took substantial amount of trials, but in the end it was possible to culture cells and confirm the knockout.

During the culture maintenance, it was observed that the DDX5ΔPfam HeLa cells proliferated at a slower rate than the wild type HeLa cells. Through performing a proliferation assay and a cell cycle assay, it was shown that the cells have a problem in the G1/S-phase transition. The same observation in DDX5 knockdown cells was made in a significant number of studies [21, 23, 25, 43]. In the report by Kaltschmidt et al [45], the IκBα overexpressed HeLa cells were characterized by a decrease in the cell number in the S-

phase in comparesment to the control. Similar effect was observed in DDX5ΔPfam HeLa cells in. This data could indicate the connection between DDX5 Pfam domain and the NF-κB pathway. Scientists also noticed decreased basal phosphorylation of a protein with a molecular weight of 68 kDa which could be DDX5. The DDX5, upon TNF treatment, is dephosphorylated at tyrosine residues. This signaling could lead to TNF-induced proliferation inhibition and apoptosis [24].

To further investigate the role of DDX5 Pfam domain, the cell cycle differences were investigated, with TNF mediated activation of the NF-κB pathway and etoposide (inhibitor of topoisomerase II) mediated induced DNA damage in wild type HeLa cells, as well as in DDX5ΔPfam HeLa cells. In the control cells (wild type HeLa), a reduction in the S-phase was observed upon treatments with regards to the untreated cells, while in the DDX5ΔPfam HeLa cells this was not observed. Upon the TNF treatment, the S-phase is accelerated to the G2/M-phase by triggering higher expression of Cyclin A1 [42]. This phenomenon can also be seen in the data presented in this study on wild type Hela cells, while in the DDX5ΔPfam HeLa cells, which have high basal values of Cyclin A1, no further induction resulting from TNF treatment was observed. The G1- and the G2/M-phase cell percentage followed the pattern of the wild type cells upon stimulation, with the already observed increase in the G1-phase. The etoposide treatment of MCF-7 DDX5 or p21 knockdown cells led to the same result, namely failure in the G1/S checkpoint, which then allowed them to progress through S- to G2/M-phase [22]. The reason why a further decrease in S-phase in the stimulated DDX5ΔPfam HeLa cells was not seen, can also be the failure in the G1/S checkpoint allowing cells to progress to G2/M.

To further investigate the G1/S checkpoint, the p21 and Cyclin D1 mRNA levels were analyzed by RT-qPCR. In the DDX5ΔPfam HeLa cells, the basal levels of p21 mRNA were higher in regard to the wild type HeLa cells. These data were not consistent with research done by Nicol et al [22] on knockdown DDX5 cells where p21 levels were decreased. The reason for this could be that in our DDX5ΔPfam HeLa cells there was still truncated DDX5 protein present, lacking the C-terminal domain. Unfortunately, the attempts to show the size of the DDX5 protein in Western blot analysis probing it with an anti N-terminal DDX5 antibody, did not succeed due to the many unspecific bands on the blot (data not shown). The basal levels of Cyclin D1 also behaved unexpectedly, since they were higher in two clones [23]. Still, it could, be that the induction of p21 levels in the DDX5ΔPfam HeLa cells was enough to result in cell cycle arrest upon the G1/S-phase transition, which correlated with the cell cycle analysis data.

Upon the TNF stimulation, both mRNA levels of p21 and Cyclin D1 were upregulated in all the cells, in comparison to the untreated control cells, as it would be expected [46]. The induction levels of p21 were lower in the DDX5ΔPfam HeLa cells compared to the wild type HeLa cells, while the opposite effect was noticed on the Cyclin D1 mRNA induction levels. This could indicate that upon the TNF treatment, the DDX5ΔPfam HeLa cells are able to pass

the G1/S checkpoint and progress through the cell cycle, resulting in more cells in the G2/M phase compared to the wild type HeLa cells. These data were indeed observed in Clone G, but not in other clones which have, nonetheless, a higher percentage of G2/M-phase cells than the untreated cells.

The etoposide stimulated cells also behaved as expected, in the sense that the p21 mRNA induction levels were increased and Cyclin D1 mRNA levels decreased, when compared to the untreated cells [47]. In this case, the DDX5ΔPfam HeLa cells followed the trend of wild type HeLa cells, with larger induction of p21 and a smaller decrease of Cyclin D1. However, in the end they also resulted in an increase in the G2/M-phase in comparison to the untreated cells, but not as profound as upon the TNF treatment.

The DDX5ΔPfam HeLa cell cycle needs further investigation to elucidate what exactly is happening. It would be interesting to see how levels of the Cyclin dependent kinase behave, especially of those involved in the G1/S transition, as well as the processes of Rb phosphorylation and E2F transcription factor induction.

The reporter gene assay in HEK293 cells clearly showed that the DDX5 activated the NF-κB pathway through its Pfam domains, since the overexpression of the DDX5 mutant without those domains did not result in the induction of the NF-κB pathway. In glioma cells it has been shown that the DDX5 binds directly to the p50 through its N-terminal domain, and that the proliferation is also stimulated through the N-terminal [27]. In this study we saw the opposite effect, the DDX5 influenced NF-κB activity through the C-terminal domain containing Pfam domains. This effect could be seen in the HEK293 cells overexpressing DDX5 as in the overexpressing DDX5 and p65. To further elucidate how DDX5 activates NF-κB, IKK1 or IKK2 were overexpressed along with DDX5. While IKK1 increased NF-κB activation, IKK2 did not. It could be that IKK2 levels were already at their top and that further induction of NF-κB by addition of DDX5 could thus not be observed. The two kinase subunits of the IKK complex, IKK1 and IKK2 have the ability to phosphorylate the IκBα inhibitor of the NF-κB, which then releases p65 (NF-κB transcription factor) [48]. While investigating the N-terminal end of the DDX5 protein, Wang et al [27] found that in the state of DDX5 overexpression, the NF-κB p50 binds a lower level of IκB-α, allowing more p50 protein to localize in the nucleus. It could be that the Pfam domains have a similar effect on our system.

In addition, the effect of the DDX5 Pfam domain on the NF-κB pathway were investigated in CRISPR/Cas9 edited DDX5ΔPfam HeLa cells by a reporter gene assay. The basal induction was the same as in wild type HeLa cells. In the case of co-overexpression of p65 (to establish NF-κB activation) in the DDX5ΔPfam HeLa cells we saw the opposite effect than expected, NF-κB activity was lower than the basal value. It could be that the remaining truncated DDX5 protein in the DDX5ΔPfam HeLa cells was behaving as a dominant negative in relation to NF-κB activity. The DDX5 acts as a co-regulator of several highly regulated transcription factors such as ERα, MyoD, p53, Runx2 and β-catenin, and it could be that it plays a role in the nucleus, along with p65, and thus inhibits NF-κB activity in its truncated version. This

hypothesis needs further investigation through immunoprecipitation with and without nucleic acids, to confirm the relations between the p65 and DDX5 wild type protein, and enable comparison to the DDX5ΔPfam HeLa cells.

In HeLa cells with a lentivirus mediated shRNA knockdown, the construct shD, which yielded the most pronounced knockdown shown by the Western blot analysis and RT-qPCR, NF-κB dependent gene *IL8* (interleukin 8) [49], had higher basal levels of IL8 mRNA in comparison to the scrambled shRNA treated cells. On the other hand, the inducibility of IL8 by TNF was lower in comparison to the scrambled shRNA treated cells. It seemed that with the DDX5 depletion in the cells, the NF-κB had high basal activity, not being able to be induced by TNF. NF-κB is controlled by a negative feedback mechanism: it can induce transcription of its own inhibitor IκBα. It was considered what impact Pfam domains and DDX5 knockdown had upon the degradation of IκBα. In the shD treated HeLa cells, it took longer for the IκBα levels to go down than in the scrambled shRNA treated cells. It also seemed that the first response to the TNF stimulation was not for the IκBα levels to go down, as they went up, in a way, postponing the NF-κB response. The IκBα levels went up again in both cases after 2 h so the NF-κB response could be shorter in the case of lower DDX5 levels.

The DDX5 knockdown in the primary HUVEC cells did not change the basal levels of NF-κB negative feedback regulators, IκBα and A20 [48, 50], and no difference was observed between the cells upon TNF stimulation. This could be due to the fact that HUVEC are primary cells and that the DDX5 induction of NF-κB is cell specific.

In the DDX5ΔPfam HeLa cells, basal levels of IκBα and IL8 had a tendency to increase in regard to the wild type HeLa cells and tendency to decrease upon the TNF stimulation, complementing the findings on HeLa DDX5 knockdown cells. Also, the results of IκBα degradation confirmed the initial high levels of IκBα. Upon the induction with TNF the degradation of IκBα was enhanced.

In order to examine the non-canonical NF-κB pathway in the DDX5ΔPfam HeLa cells, I stimulated the cells with CD40L (upstream of non-canonical NF-κB pathway) and quantified the NF-κB dependent genes by RT-qPCR in regard to the stimulation [48, 50-52]. All of them had higher induction than in wild type HeLa cells, indicating that the DDX5 also plays a role in the non-canonical NF-κB pathway.

The p21 and CyclinD1 are both NF-κB target genes [53, 54] connecting the NF-κB to the cell proliferation and control of the cell cycle, both of which were affected in DDX5ΔPfam HeLa cells.

Taken together, CRISPR/Cas9 mediated deletion of the C-terminal domain of DDX5 resulted in reduced cell proliferation, in accordance with knockdown data published by others in a variety of cells [20, 23-25, 27]. In regard to NF-κB activation, previous data on the role of the Pfam domains were verified by reporter gene assays. The DDX5ΔPfam HeLa cells showed diminished NF-κB activation and inducibility of IL8 and IκBα upon TNF stimulation compared

to wild type HeLa cells. On the other hand, upon CD40L stimulation DDX5ΔPfam HeLa cells had higher inducibility of IL6, IκBα and A20 than the control HeLa cells. This may reflect different roles of DDX5 in the canonical and non-canonical NF-κB pathways.

6. Conclusions:

The DDX5 protein is involved in many important functions in a cell life and therefore its complete knockout impaired proliferation in HeLa cells and subsequently leds to cell death.

The DDX5 HeLa knockout cells had a different morphology compared to wild type HeLa cells.

Deletion of the DDX5 Pfam domains at the C-terminal end of the protein showed only a weaker effect on proliferation, so cultivation was possible.

The DDX5ΔPfam HeLa cells grew at a slower rate due to a delay in G1/S transition.

The DDX5 Pfam domains may differentially affect the canonical and non-canonical NF-κB pathways.

Regulation of IκBα was different in HeLa DDX5 knockdown cells in comparison with DDX5ΔPfam HeLa cells and wild type HeLa cells.

The primary HUVEC cells behaved differently from the HeLa cells upon the DDX5 knockdown.

7. Literature:

[1] Gookin, S., Min, M., Phadke, H., Chung, M., Moser, J., Miller, I., Carter, D., Spencer, S. L. (2017): A map of protein dynamics during cell-cycle progression and cell-cycle exit. PLoS biology. 15: 1-25.

[2] Niida, H., Nakanishi, M. (2006): DNA damage checkpoints in mammals. Mutagenesis. 21: 3-9.

[3] Gerondakis, S., Fulford, T. S., Messina, N. L., Grumont, R. J. (2014): NF-kappaB control of T cell development. Nature immunology. 15: 15-25.

[4] Zhang, Q., Lenardo, M. J., Baltimore, D. (2017): 30 Years of NF-kappaB: A Blossoming of Relevance to Human Pathobiology. Cell. 168: 37-57.

[5] Oeckinghaus, A., Hayden, M. S., Ghosh, S. (2011): Crosstalk in NF-kappaB signaling pathways. Nature immunology. 12: 695-708.

[6] Oeckinghaus, A., Ghosh, S. (2009): The NF-kappaB family of transcription factors and its regulation. Cold Spring Harbor perspectives in biology. 1: 1-15.

[7] Fuller-Pace, F. V. (1994): RNA helicases: modulators of RNA structure. Trends in cell biology. 4: 271-274.

[8] Iggo, R. D., Lane, D. P. (1989): Nuclear protein p68 is an RNA-dependent ATPase. The EMBO journal. 8: 1827-1831.

[9] Lane, D. P., Hoeffler, W. K. (1980): SV40 large T shares an antigenic determinant with a cellular protein of molecular weight 68,000. Nature. 288: 167-170.

[10] Schmid, S. R., Linder, P. (1992): D-E-A-D protein family of putative RNA helicases. Molecular microbiology. 6: 283-291.

[11] Liu, Z. R. (2002): p68 RNA helicase is an essential human splicing factor that acts at the U1 snRNA-5 ' splice site duplex. Molecular and cellular biology. 22: 5443-5450.

[12] Guil, S., Gattoni, R., Carrascal, M., Abian, J., Stevenin, J., Bach-Elias, M. (2003): Roles of hnRNP A1, SR proteins, and p68 helicase in c-H-ras alternative splicing regulation. Molecular and cellular biology. 23: 2927-2941.

[13] Gregory, R. I., Yan, K. P., Amuthan, G., Chendrimada, T., Doratotaj, B., Cooch, N., Shiekhattar, R. (2004): The Microprocessor complex mediates the genesis of microRNAs. Nature. 432: 235-240.

[14] Samaan, S., Tranchevent, L. C., Dardenne, E., Polay Espinoza, M., Zonta, E., Germann, S., Gratadou, L., Dutertre, M., Auboeuf, D. (2014): The Ddx5 and Ddx17 RNA helicases are cornerstones in the complex regulatory array of steroid hormone-signaling pathways. Nucleic acids research. 42: 2197-2207.

[15] Li, H., Lai, P., Jia, J., Song, Y., Xia, Q., Huang, K., He, N., Ping, W., Chen, J., Yang, Z., Li, J., Yao, M., Dong, X., Zhao, J., Hou, C., Esteban, M. A., Gao, S., Pei, D., Hutchins, A. P., Yao, H. (2017): RNA Helicase DDX5 Inhibits Reprogramming to Pluripotency by miRNA-Based Repression of RYBP and its PRC1-Dependent and -Independent Functions. Cell stem cell. 20: 462-477.

[16] Uniprot.

[17] Caretti, G., Schiltz, R. L., Dilworth, F. J., Di Padova, M., Zhao, P., Ogryzko, V., Fuller-Pace, F. V., Hoffman, E. P., Tapscott, S. J., Sartorelli, V. (2006): The RNA helicases p68/p72 and the noncoding RNA SRA are coregulators of MyoD and skeletal muscle differentiation. Developmental cell 11: 547-560.

[18] Dardenne, E., Polay Espinoza, M., Fattet, L., Germann, S., Lambert, M. P., Neil, H., Zonta, E., Mortada, H., Gratadou, L., Deygas, M., Chakrama, F. Z., Samaan, S., Desmet, F. O., Tranchevent, L. C., Dutertre, M., Rimokh, R., Bourgeois, C. F., Auboeuf, D. (2014): RNA helicases DDX5 and DDX17 dynamically orchestrate transcription, miRNA, and splicing programs in cell differentiation. Cell reports. 7: 1900-1913.

[19] Jensen, E. D., Niu, L., Caretti, G., Nicol, S. M., Teplyuk, N., Stein, G. S., Sartorelli, V., van Wijnen, A. J., Fuller-Pace, F. V., Westendorf, J. J. (2008): p68 (Ddx5) interacts with Runx2 and regulates osteoblast differentiation. Journal of cellular biochemistry. 103: 1438-1451.

[20] Du, C., Li, D. Q., Li, N., Chen, L., Li, S. S., Yang, Y., Hou, M. X., Xie, M. J., Zheng, Z. D. (2017): DDX5 promotes gastric cancer cell proliferation in vitro and in vivo through mTOR signaling pathway. Sci Rep-Uk. 7: 1-11.

[21] Kokolo, M., Bach-Elias, M. (2017): Downregulation of p68 RNA Helicase (DDX5) Activates a Survival Pathway Involving mTOR and MDM2 Signals. Folia biologica. 63: 52-59.

[22] Nicol, S. M., Bray, S. E., Black, H. D., Lorimore, S. A., Wright, E. G., Lane, D. P., Meek, D. W., Coates, P. J., Fuller-Pace, F. V. (2013): The RNA helicase p68 (DDX5) is selectively required for the induction of p53-dependent p21 expression and cell-cycle arrest after DNA damage. Oncogene. 32: 3461-3469.

[23] Mazurek, A., Luo, W. J., Krasnitz, A., Hicks, J., Powers, R. S., Stillman, B. (2012): DDX5 Regulates DNA Replication and Is Required for Cell Proliferation in a Subset of Breast Cancer Cells. Cancer Discov. 2: 812-825.

[24] Yang, L., Lin, C., Liu, Z. R. (2005): Phosphorylations of DEAD box p68 RNA helicase are associated with cancer development and cell proliferation. Molecular cancer research : MCR. 3: 355-363.

[25] Yang, L., Lin, C., Zhao, S., Wang, H., Liu, Z. R. (2007): Phosphorylation of p68 RNA helicase plays a role in platelet-derived growth factor-induced cell proliferation by up-regulating cyclin D1 and c-Myc expression. The Journal of biological chemistry. 282: 16811-16819.

[26] Fuller-Pace, F. V. (2013): The DEAD box proteins DDX5 (p68) and DDX17 (p72): Multi-tasking transcriptional regulators. Bba-Gene Regul Mech. 1829: 756-763.

[27] Wang, R., Jiao, Z., Li, R., Yue, H., Chen, L. (2012): p68 RNA helicase promotes glioma cell proliferation in vitro and in vivo via direct regulation of NF-kappaB transcription factor p50. Neuro-oncology. 14: 1116-1124.

[28] Doudna, J. A., Charpentier, E. (2014): Genome editing. The new frontier of genome engineering with CRISPR-Cas9. Science. 346: 1258096.

[29] Jinek, M., Chylinski, K., Fonfara, I., Hauer, M., Doudna, J. A., Charpentier, E. (2012): A programmable dual-RNA-guided DNA endonuclease in adaptive bacterial immunity. Science. 337: 816-821.

[30] Fonfara, I., Le Rhun, A., Chylinski, K., Makarova, K. S., Lecrivain, A. L., Bzdrenga, J., Koonin, E. V., Charpentier, E. (2014): Phylogeny of Cas9 determines functional exchangeability of dual-RNA and Cas9 among orthologous type II CRISPR-Cas systems. Nucleic acids research. 42: 2577-2590.

[31] Ran, F. A., Hsu, P. D., Wright, J., Agarwala, V., Scott, D. A., Zhang, F. (2013): Genome engineering using the CRISPR-Cas9 system. Nature protocols. 8: 2281-2308.

[32] Hsu, P. D., Lander, E. S., Zhang, F. (2014): Development and applications of CRISPR-Cas9 for genome engineering. Cell. 157: 1262-1278.

[33] Chen, C. A., Okayama, H. (1988): Calcium phosphate-mediated gene transfer: a highly efficient transfection system for stably transforming cells with plasmid DNA. Biotechniques. 6: 632-638.

[34] Baker, A., Saltik, M., Lehrmann, H., Killisch, I., Mautner, V., Lamm, G., Christofori, G., Cotten, M. (1997): Polyethylenimine (PEI) is a simple, inexpensive and effective reagent for condensing and linking plasmid DNA to adenovirus for gene delivery. Gene therapy. 4: 773-782.

[35] Birnboim, H. C., Doly, J. (1979): A rapid alkaline extraction procedure for screening recombinant plasmid DNA. Nucleic acids research. 7: 1513-1523.

[36] Kurien, B. T., Scofield, R. H. (2006): Western blotting. Methods. 38: 283-293.

[37] Lanctot, C., Meister, P. (2013): Microscopic analysis of chromatin localization and dynamics in C. elegans. Methods in molecular biology. 1042: 153-172.

[38] Qiu, P., Shandilya, H., D'Alessio, J. M., O'Connor, K., Durocher, J., Gerard, G. F. (2004): Mutation detection using Surveyor nuclease. Biotechniques. 36 702-707.

[39] Juers, D. H., Matthews, B. W., Huber, R. E. (2012): LacZ beta-galactosidase: Structure and function of an enzyme of historical and molecular biological importance. Protein Sci. 21: 1792-1807.

[40] Kim, K. H., Sederstrom, J. M. (2015): Assaying Cell Cycle Status Using Flow Cytometry. Current protocols in molecular biology. 111: 28 26 21-11.

[41] Zhang, X. H., Tee, L. Y., Wang, X. G., Huang, Q. S., Yang, S. H. (2015): Off-target Effects in CRISPR/Cas9-mediated Genome Engineering. Molecular therapy. Nucleic acids. 4: e264.

[42] Volland, S., Amtmann, E., Sauer, G. (1994): TNF accelerates the S-phase of the cell cycle in tumor cells. International journal of cancer. 56: 698-705.

[43] Fukuda, T., Yamagata, K., Fujiyama, S., Matsumoto, T., Koshida, I., Yoshimura, K., Mihara, M., Naitou, M., Endoh, H., Nakamura, T., Akimoto, C., Yamamoto, Y., Katagiri, T., Foulds, C., Takezawa, S., Kitagawa, H., Takeyama, K., O'Malley, B. W., Kato, S. (2007): DEAD-box RNA helicase subunits of the Drosha complex are required for processing of rRNA and a subset of microRNAs. Nat Cell Biol. 9: 604-611.

[44] Wang, D., Huang, J., Hu, Z. (2012): RNA helicase DDX5 regulates microRNA expression and contributes to cytoskeletal reorganization in basal breast cancer cells. Molecular & cellular proteomics : MCP. 11: 1-12.

[45] Kaltschmidt, B., Kaltschmidt, C., Hehner, S. P., Droge, W., Schmitz, M. L. (1999): Repression of NF-kappa B impairs HeLa cell proliferation by functional interference with cell cycle checkpoint regulators. Oncogene. 18: 3213-3225.

[46] Yu, C., Takeda, M., Soliven, B. (2000): Regulation of cell cycle proteins by TNF-alpha and TGF-beta in cells of oligodendroglial lineage. J Neuroimmunol. 108: 2-10.

[47] Zhang, F., Xu, L., Qu, X., Zhao, M., Jin, B., Kang, J., Liu, Y., Hu, X. (2011): Synergistic antitumor effect of beta-elemene and etoposide is mediated via induction of cell apoptosis and cell cycle arrest in non-small cell lung carcinoma cells. Molecular medicine reports. 4: 1189-1193.

[48] Mercurio, F., Zhu, H., Murray, B. W., Shevchenko, A., Bennett, B. L., Li, J., Young, D. B., Barbosa, M., Mann, M., Manning, A., Rao, A. (1997): IKK-1 and IKK-2: cytokine-activated IkappaB kinases essential for NF-kappaB activation. Science. 278: 860-866.

[49] Kunsch, C., Rosen, C. A. (1993): NF-kappa B subunit-specific regulation of the interleukin-8 promoter. Molecular and cellular biology. 13: 6137-6146.

[50] Krikos, A., Laherty, C. D., Dixit, V. M. (1992): Transcriptional activation of the tumor necrosis factor alpha-inducible zinc finger protein, A20, is mediated by kappa B elements. The Journal of biological chemistry. 267: 17971-17976.

[51] Son, Y. H., Jeong, Y. T., Lee, K. A., Choi, K. H., Kim, S. M., Rhim, B. Y., Kim, K. (2008): Roles of MAPK and NF-kappaB in interleukin-6 induction by lipopolysaccharide in vascular smooth muscle cells. Journal of cardiovascular pharmacology. 51: 71-77.

[52] Yamamoto, K., Arakawa, T., Ueda, N., Yamamoto, S. (1995): Transcriptional roles of nuclear factor kappa B and nuclear factor-interleukin-6 in the tumor necrosis factor alpha-dependent induction of cyclooxygenase-2 in MC3T3-E1 cells. The Journal of biological chemistry. 270: 31315-31320.

[53] Hinata, K., Gervin, A. M., Jennifer Zhang, Y., Khavari, P. A. (2003): Divergent gene regulation and growth effects by NF-kappa B in epithelial and mesenchymal cells of human skin. Oncogene. 22: 1955-1964.

[54] Hinz, M., Krappmann, D., Eichten, A., Heder, A., Scheidereit, C., Strauss, M. (1999): NF-kappaB function in growth control: regulation of cyclin D1 expression and G0/G1-to-S-phase transition. Molecular and cellular biology. 19: 2690-2698.

8. Supplemental materials

8.1. Sequences of sgRNA used in CRISPR/Cas9 cloning

Sequences of sgRNAs used in the experiment "Establishing a stable CRISPR/Cas9 DDX5 knockout in HeLa cells":

sgA: CGGTCTCGGTCACTCGAATA (exon 1/13)

sgB: AATCGAGGTGCACCAAAC (exon 2/13)

sgC: CTGTGCGCCTAGCCAAATCA (exon 2/13)

C-terminus targeting sg sequences:

sgRNA 1: GGTCGTTCCAGGGGTAGAGG**AGG**

8.2. Plasmid maps
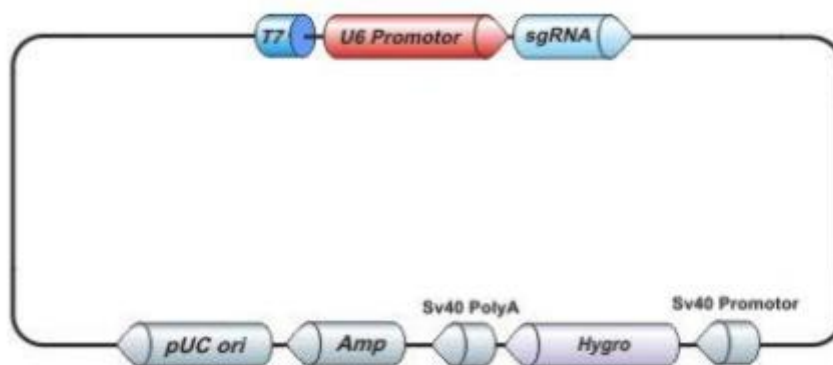
Figure 41: Map of a HCP plasmid vector used to introduce sgRNAs to the cells
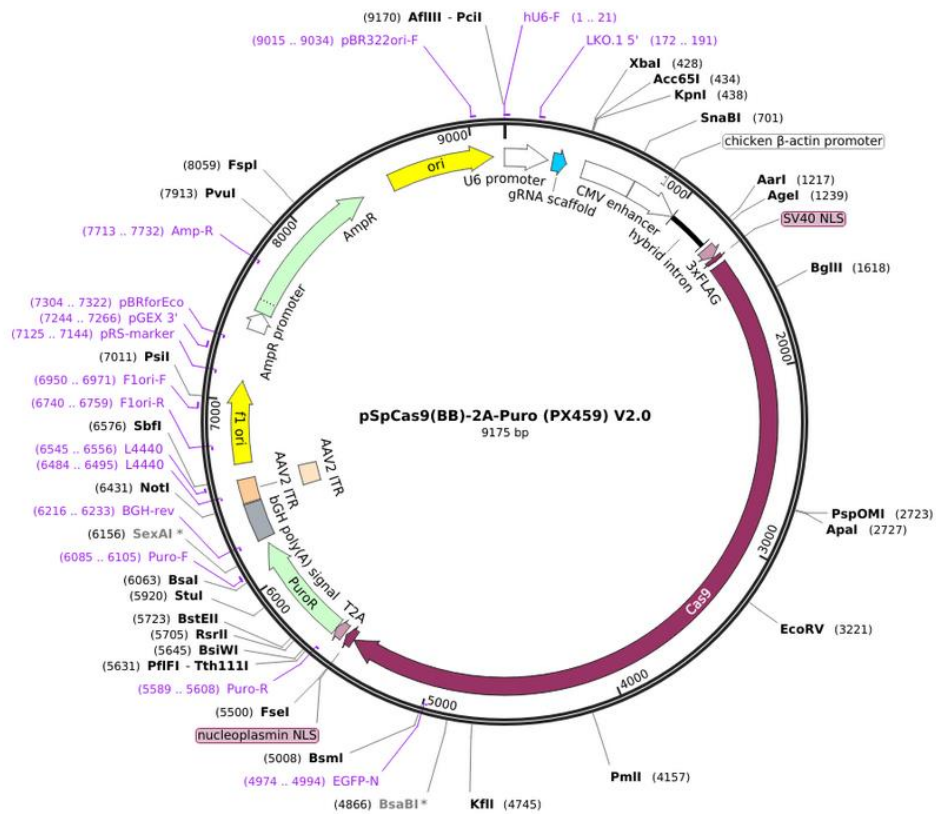
Figure 42: Map of the PX459 plasmid
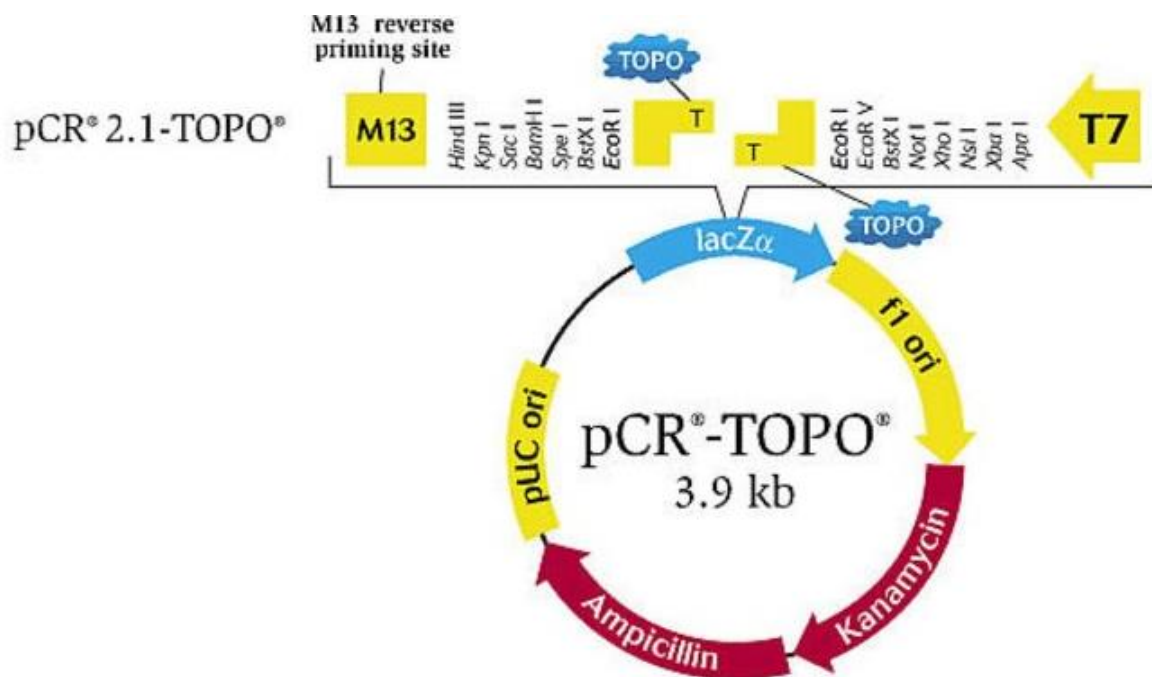
Figure 43: Map of the pCR-TOPO vector

8.3. Genomic DNA isolation buffer components

Table 14: Components of the Lysis Buffer 2x.

Reagent	Volume (ml)	Final concentration
10% SDS	1	1%
Tris pH 7.5 1 M	0.2	20 mM
EDTA 0.5 M pH 8	0.8	40 mM
NaCl 5 M	0.2	100 mM
ddH$_2$O	7.8	

8.4. Primer list

Table 15: List of all the used primers; the primers were synthesized at Microsynth.

Name	Sequence
px459_hu6 fwd	ACTATCATATCGTAAC
DDX5 check fwd	TGCTCGCAGTACCAAAACAG
DDX5 check rev	CCAAAGCTCCCATTGGTGTA
M13r	CAGGAAACAGCTATGAC
T1 fwd	AAGGAATTACTGGCCTGGAGA
T1 rev	AAGAATCCCAACCCCACACT
T2 fwd	CAGCGGACTAATTTGGGAGA
T2 rev	CGTACCAGTGTTGCAGAGGA
T3 fwd	GAGACCTGAACCTGGGATGA
T3 rev	TGGTTGCTCTCGTATACTTATTGG
Hs_DDX5_qRT-fwd	GTCATCGGTGTCCTTCCTC
Hs_DDX5_qRT-rev	GAGGTGCACCAAACCCTCG
Hs_p21_qRT-fwd	GAGCGATGGAACTTCGACTT
Hs_p21_qRT-rev	CAGGTCCACATGGTCTTCCT

Hs_CyclinD1_qRT-fwd	AACTACCTGGACCGCTTCCT
Hs_CyclinD1_qRT-rev	CCACTTGAGCTTGTTCACCA
Hs_IL8_qRT-fwd	CTCTGTGTGAAGGTGCAGTTTTG
Hs_IL8_qRT-rev	CCCAGTTTTCCTTGGGGTCC
Hs_IκBα_ qRT-fwd	CAGCAGCTCACCGAGGAC
Hs_IκBα_ qRT- rev	ACAGCCAAGTGGAGTGGAGT
Hs_A20_ qRT-fwd	CATGCATGCCACTTCTCAGT
Hs_A20_ qRT-rev	CATGGGTGTGTCTGTGGAAG
Hs_IL6_qRT-fwd	ATGAGGAGACTTGCCTGGTG
Hs_IL6_qRT-rev	CAGGGGTGGTTATTGCATCT
Hs_COX2_qRT-fwd	CTGCTCAACACCGGAATTTT
Hs_COX2_qRT-rev	GAGAAGGCTTCCCAGCTTTT
Hs_B2MG_qRT-fwd	GATGAGTATGCCTGCCGTGTG
Hs_B2MG_qRT-rev	CAATCCAAATGCGGCATCT

8.5. Sequencing results

8.5.1. Sequencing results of two plasmids px459, containing the inserted sequence for expression of sgRNA used in the experiment "Establishing a stable CRISPR/Cas9 DDX5-pfam1/2 knockout in HeLa cells" (SG1); shown in yellow is the sgRNA nucleotide sequence:
SG1_a px459_hU6fwd
TGGAAAGGACGAAACACCGGGTCGTTCCAGGGGTAGAGGGTTTTAGAGCTAGAAATAGCAAGTTAA
AATAAGGCTAGTCCGTTATCAACTTGAAAAAGTGGCACCGAGTCGGTGCTTTTTTGTTTTAGAGCTAG
AAATAGCAAGTTAAAATAAGGCTAGTCCGTTTTTAGCGCGTGCGCCAATTCTGCAGACAAATGGCTC
TAGAGGTACCCGTTACATAACTTACGGTAAATGGCCCGCCTGGCTGACCGCCCAACGACCCCCGCCC
ATTGACGTCAATAGTAACGCCAATAGGGACTTTCCATTGACGTCAATGGGTGGAGTATTTACGGTAA
ACTGCCCACTTGGCAGTACATCAAGTGTATCATATGCCAAGTACGCCCCCTATTGACGTCAATGACGG
TAAATGGCCCGCCTGGCATTGTGCCCAGTACATGACCTTATGGGACTTTCCTACTTGGCAGTACATCT
ACGTATTAGTCATCGCTATTACCATGGTCGAGGTGAGCCCCACGTTCTGCTTCACTCTCCCCATCTCCC
CCCCCTCCCCACCCCCAATTTTGTATTTATTTATTTTTTAATTATTTTGTGCAGCGATGGGGGCGGGGG
GGGGGGGGGGGNC

SG1_b px459_hU6fwd

NGGACGAAACACCG==GGTCGTTCCAGGGGTAGAGG==GTTTTAGAGCTAGAAATAGCAAGTTAAAATAA
GGCTAGTCCGTTATCAACTTGAAAAAGTGGCACCGAGTCGGTGCTTTTTTGTTTTAGAGCTAGAAATA
GCAAGTTAAAATAAGGCTAGTCCGTTTTTAGCGCGTGCGCCAATTCTGCAGACAAATGGCTCTAGAG
GTACCCGTTACATAACTTACGGTAAATGGCCCGCCTGGCTGACCGCCCAACGACCCCCGCCCATTGAC
GTCAATAGTAACGCCAATAGGGACTTTCCATTGACGTCAATGGGTGGAGTATTTACGGTAAACTGCC
CACTTGGCAGTACATCAAGTGTATCATATGCCAAGTACGCCCCCTATTGACGTCAATGACGGTAAATG
GCCCGCCTGGCATTGTGCCCAGTACATGACCTTATGGGACTTTCCTACTTGGCAGTACATCTACGTAT
TAGTCATCGCTATTACCATGGTCGAGGTGAGCCCCACGTTCTGCTTCACTCTCCCCATCTCCCCCCCCT
CCCCACCCCCAATTTTGTATTTATTTATTTTTTAATTATTTTGTGCAGCGATGGGGGCGGGGGGGGGG
GGGGKGNN

8.5.2. Sequencing results of the pCR-TOPO vector with inserted PCR product which includes target sites from the DDX5-pfam1/2 knockouts: F, G and I

F1 M13r

TCCACTAGTAACGGCCGCCAGTGTGCTGGAATTCGCCCTTCCAAAGCTCCCATTGGTGTAATTTGCAG
CACTGTAAACACCATTCTGAGTTTTTGCCCCAAAATCTCTTTTAAGCAGGCTAGAGTAACCTCTGTCAT
AATTTTCCCTGTCTCTAAAGGTATTAAATCCACCCCTTTTGCCCGCAGAGTATCTGTCCCGACGGTCAT
CCTTCATGCCTCCTCCTACCCCTGGAACGACCTGTCAAGAAACAATTGCAAATTGATCAATTATGTCT
ATGACACAAATCATTGTGGACAGAAAGAAACAGATCTATTCATGGTAGGCGTGAAATGTTTTTACAA
TTTTTCAGCTTAAGTTTTCACATTCAAGGTTTTACTCACCCTCCAATACCATTTAAATGGATTTGTAGAC
AACGATGTGACTCGTAACTACCAACATTTCCTATCAGTCATCCTTACCTGAACCTCTGTCTTCGACCAA
CTGAAGCAACTTGGGATTAATTGCTTGATTAGCTTCACGAAGCACAGAGATAAGGTCGCTCACTTGC
TTTATGTTATTAGGTGTAAAGAAAGTGTATGCTGTGCCTGTTTTGGTACTGCGAGCAAAGGGCGAAT
TCTGCAGATATCCATCACACTGGCGGCCGCTCGAGCATGCATCTAGAGGGCCCAATTCGCCCTATAG
TGAGTCGTATTACAATTCACTGGCCGTCGTTTTACAACGTCGTGACTGGGAAAACCCTGGCGTTACCC
AACTTAATCGCCTTGCAGCACATCCCCCTTTCGCCAGCTGGCGTAATAGCGAAGAGGCCCGCACCGA
TCGCCCTTCCCAACAGTTGCGCAGCCTGAATGGCGAATGGACGCGCCCTGTAGCGGCGCATTAAGCG
CGGCGGGTGTGGTGGTTACGCGCAGCGTGACCGCTACACTTGCCAGCGCCCTAGCGCCCGCTCCTTT
CGCTTTCTTCCCTTCCTTTCTCGCCACGTTCGCCGGCTTTCCCCGTCAAGCTCTAAATCGGGGGCTCCC
TTTAGGGTTCCGATTTAGTGCTTTACGGCACCTCGACCCCAAAAAACTTGATTAAGGTGATGGTTCAC
GTARTGGGGCCATCNCC

F2 M13r

CCACTAGTAACGGCCGCCAGTGTGCTGGAATTCGCCCTTCCAAAGCTCCCATTGGTGTAATTTGCAGC
ACTGTAAACACCATTCTGAGTTTTTGCCCCAAAATCTCTTTTAAGCAGGCTAGAGTAACCTCTGTCATA
ATTTTCCCTGTCTCTAAAGGTATTAAATCCACCCCTTTTGCCCGCAGAGTATCTGTCCCGACGGTCATC
CTTCATGCCCCCTACCCCTGGAACGACCTGTCAAGAAACAATTGCAAATTGATCAATTATGTCTATG
ACACAAATCATTGTGGACAGAAAGAAACAGATCTATTCATGGTAGGCGTGAAATGTTTTTACAATTTT
TCAGCTTAAGTTTTCACATTCAAGGTTTTACTCACCCTCCAATACCATTTAAATGGATTTGTAGACAAC
GATGTGACTCGTAACTACCAACATTTCCTATCAGTCATCCTTACCTGAACCTCTGTCTTCGACCAACTG
AAGCAACTTGGGATTAATTGCTTGATTAGCTTCACGAAGCACAGAGATAAGGTCGCCCACTTGCTTTA

TGTTATTAGGTGTAAAGAAAGTGTATGCTGTGCCTGTTTTGGTACTGCGAGCAAAGGGCGAATTCTG
CAGATATCCATCACACTGGCGGCCGCTCGAGCATGCATCTAGAGGGCCCAATTCGCCCTATAGTGAG
TCGTATTACAATTCACTGGCCGTCGTTTTACAACGTCGTGACTGGGAAAACCCTGGCGTTACCCAACT
TAATCGCCTTGCAGCACATCCCCCTTTCGCCAGCTGGCGTAATAGCGAAGAGGCCCGCACCGATCGC
CCTTCCCAACAGTTGCGCAGCCTGAATGGCGAATGGACGCGCCCTGTAGCGGCGCATTAAGCGCGG
CGGGTGTGGTGGTTACGCGCAGCGTGACCGCTACACTTGCCAGCGCCCTAGCGCCCGCTCCTTTCGC
TTTCTTCCCTTCCTTTCTCGCCACGTTCGCCGGCTTTCCCCGTCAAGCTCTAAATCGGGGGCTCCCTTTA
GGGTTCCGATTTAGTGCTTTACGGCACCTCGACCCCAAAAAACTTGATTAGGGTGATGGTTC

F3 M13r
GCTCGGATCCACTAGTAACGGCCGCCAGTGTGCTGGAATTCGCCCTTCCAAAGCTCCCATTGGTGTA
ATTTGCAGCACTGTAAACACCATTCTGAGTTTTTGCCCCAAAATCTCTTTTAAGCAGGCTAGAGTAAC
CTCTGTCATAATTTTCCCTGTCTCTAAAGGTATTAAATCCACCCCTTTTGCCCGCAGAGTATCTGTCCC
GACGGTCATCCTTCATGCCCCCTACCCCTGGAACGACCTGTCAAGAAACAATTGCAAATTGATCAAT
TATGTCTATGACACAAATCATTGTGGACAGAAAGAAACAGATCTATTCATGGCAGGCGTGAAATGTT
TTTACAATTTTTCAGCTTAAGTTTTCACATTCAAGGTTTTACTCACCCTCCAATACCATTTAAATGGATT
TGTAGACAACGATGTGACTCGTAACTACCAACATTTCCTATCAGTCATCCTTACCTGAACCTCTGTCTT
CGACCAACTGAAGCAACTTGGGATTAATTGCTTGATTAGCTTCACGAAGCACAGAGATAAGGTCGCT
CACTTGCTTTATGTTATTAGGTGTAAAGAAAGTGTATGCTGTGCCTGTTTTGGTACTGCGAGCAAAGG
GCGAATTCTGCAGATATCCATCACACTGGCGGCCGCTCGAGCATGCATCTAGAGGGCCCAATTCGCC
CTATAGTGAGTCGTATTACAATTCACTGGCCGTCGTTTTACAACGTCGTGACTGGGAAAACCCTGGCG
TTACCCAACTTAATCGCCTTGCAGCACATCCCCCTTTCGCCAGCTGGCGTAATAGCGAAGAGGCCCGC
ACCGATCGCCCTTCCCAACAGTTGCGCAGCCTGAATGGCGAATGGACGCGCCCTGTAGCGGCGCATT
AAGCGCGGCGGGTGTGGTGGTTACGCGCAGCGTGACCGCTACACTTGCCAGCGCCCTAGCGCCCGC
TCCTTTCGCTTTCTTCCCTTCCTTTCTCGCCACGTTCGCCGGCTTTCCCCGTCAAGCTCTAAATCGGGGG
CTCCCTTTAGGGTTCCGATTTAGTGCTTTACGGCACCTCGACCCCAAAAAACTTGATTAGGGTGATGG
TTCACGTARTGGGCCATCGCCCTGAAAAACGGTTTTTCGCCCTTTGACGTTGGAGTCCACGTTCTTTA
AAAATGGACTNTNGGTTCCAAACTGGAACAAACATCNAACCCTATCNCGGYCTATTTCTTTTGATTTA
TAAGGGGATTTTGCCCAATTTCGGCCTATTGGGTTAAAAA

F4 M13r
CCACTAGTAACGGCCGCCAGTGTGCTGGAATTCGCCCTTCCAAAGCTCCCATTGGTGTAATTTGCAGC
ACTGTAAACACCATTCTGAGTTTTTGCCCCAAAATCTCCTTTAAGCAGGCTAGAGTAACCTCTGTCATA
ATTTTCCCTGTCTCTAAAGGTATTAAATCCACCCCTTTTGCCCGCAGAGTATCTGTCCCGACGGTCATC
CTTCATGCCCCCTACCCCTGGAACGACCTGTCAAGAAACAATTGCAAATTGATCAATTATGTCTATG
ACACAAATCATTGTGGACAGAAAGAAACAGATCTATTCATGGTAGGCGTGAAATGTTTTTACAATTTT
TCAGCTTAAGTTTTCACATTCAAGGTTTTACTCACCCTCCAATACCATTTAAATGGATTTGTAGACAAC
GATGTGACTCGTAACTACCAACATTTCCTATCAGTCATCCTTACCTGAACCTCTGTCTTCGACCAACTG
AAGCAACTTGGGATTAATTGCTTGATTAGCTTCACGAAGCACAGAGATAAGGTCGCTCACTTGCTTTA
TGTTATTAGGTGTAAAGAAAGTGTATGCTGTGCCTGTTTTGGTACTGCGAGCAAAGGGCGAATTCTG
CAGATATCCATCACACTGGCGGCCGCTCGAGCATGCATCTAGAGGGCCCAATTCGCCCTATAGTGAG
TCGTATTACAATTCACTGGCCGTCGTTTTACAACGTCGTGACTGGGAAAACCCTGGCGTTACCCAACT

TAATCGCCTTGCAGCACATCCCCCTTTCGCCAGCTGGCGTAATAGCGAAGAGGCCCGCACCGATCGC
CCTTCCCAACAGTTGCGCAGCCTGAATGGCGAATGGACGCGCCCTGTAGCGGCGCATTAAGCGCGG
CGGGTGTGGTGGTTACGCGCAGCGTGACCGCTACACTTGCCAGCGCCCTAGCGCCCGCTCCTTTCGC
TTTCTTCCCTTCCTTTCTCGCCACGTTCGCCGGCTTTCCCCGTCAAGCTCTAAATCGGGGGCTCCCTTTA
GGGTTCCGATTTAGTGCTTTACGGCACCTCGACCCCAAAAAACTTGATTAGGGTGATGGTTCACGTAR
TGGGGCCATCGCCCTGAAAA

G 2 M13r
CTAGTAACGGCCGCCAGTGTGCTGGAATTCGCCCTTCCAAAGCTCCCATTGGTGTAATTTGCAGCACT
GTAAACACCATTCTGAGTTTTTGCCCCAAAATCTCTTTTAAGCAGGCTAGAGTAACCTCTGTCATAATT
TTCCCTGTCTCTAAAGGTATTAAATCCACCCCTTTTGCCCGCAGAGCATCTGTCCCGACGGTCATCCTT
CATGCCTCCTCCTACCCCTGGAACGACCTGTCAAGAAAACAATTGCAAATTGATCAATTATGTCTATG
ACACAAATCATTGTGGACAGAAAGAAACAGATCTATTCATGGTAGGCGTGAAATGTTTTTACAATTTT
TCAGCTTAAGTTTTCACATTCAAGGTTTTACTCACCCTCCAATACCATTTAAATGGATTTGTAGACAAC
GATGTGACTCGTAACTACCAACATTTCCTATCAGTCATCCTTACCTGAACCTCTGTCTTCGACCAACTG
AAGCAACTTGGGATTAATTGCTTGATTAGCTTCACGAAGCACAGAGATAAGGTCGCTCACTTGCTTTA
TGTTATTAGGTGTAAAGAAAGTGTATGCTGTGCCTGTTTTGGTACTGCGAGCAAAGGGCGAATTCTG
CAGATATCCATCACACTGGCGGCCGCTCGAGCATGCATCTAGAGGGCCCAATTCGCCCTATAGTGAG
TCGTATTACAATTCACTGGCCGTCGTTTTACAACGTCGTGACTGGGAAAACCCTGGCGTTACCCAACT
TAATCGCCTTGCAGCACATCCCCCTTTCGCCAGCTGGCGTAATAGCGAAGAGGCCCGCACCGATCGC
CCTTCCCAACAGTTGCGCAGCCTGAATGGCGAATGGACGCGCCCTGTAGCGGCGCATTAAGCGCGG
CGGGTGTGGTGGTTACGCGCAGCGTGACCGCTACACTTGCCAGCGCCCTAGCGCCCGCTCCTTTCGC
TTTCTTCCCTTCCTTTCTCGCCACGTTCGCCGGCTTTCCCCGTCAAGCTCTAAATCGGGGGCTCCCTTTA
GGGTTCCGATTTAGTGCTTTACGGCACCTCGACCCCAAAAAACTTGATTAAGGGTGATGGTTCACGT
AGTGGGGCCATCGCCCTGAAAAAACGGTTTTTCNGCCCTTTGACGTTGGANTCCACGTTCTTTAA

G 3 M13r
CGGATCCACTAGTAACGGCCGCCAGTGTGCTGGAATTCGCCCTTCCAAAGCTCCCATTGGTGTAATTT
GCAGCACTGTAAACACCATTCTGAGTTTTTGCCCCAAAATCTCTTTTAAGCAGGCTAGAGTAACCTCT
GTCATAATTTTCCCTGTCTCTAAAGGTATTAAATCCACCCCTTTTGCCCGCAGAGTATCTGTCCCGACG
GTCATCCTTCATGCCTCCTGGAACGACCTGTCAAGAAAACAATTGCAAATTGATCAATTATGTCTATG
ACACAAATCATTGTGGACAGAAAGAAACAGATCTATTCATGGTAGGCGTGAAATGTTTTTACAATTTT
TCAGCTTAAGTTTTCACATTCAAGGTTTTACTCACCCTCCAATACCATTTAAATGGATTTGTAGACAAC
GATGTGACTCGTAACTACCAACATTTCCTATCAGTCATCCTTACCTGAACCTCTGTCTTCGACCAACTG
AAGCAACTTGGGATTAATTGCTTGATTAGCTTCACGAAGCACAGAGATAAGGTCGCTCACTTGCTTTA
TGTTATTAGGTGTAAAGAAAGTGTATGCTGTGCCTGTTTTGGTACTGCGAGCAAAGGGCGAATTCTG
CAGATATCCATCACACTGGCGGCCGCTCGAGCATGCATCTAGAGGGCCCAATTCGCCCTATAGTGAG
TCGTATTACAATTCACTGGCCGTCGTTTTACAACGTCGTGACTGGGAAAACCCTGGCGTTACCCAACT
TAATCGCCTTGCAGCACATCCCCCTTTCGCCAGCTGGCGTAATAGCGAAGAGGCCCGCACCGATCGC
CCTTCCCAACAGTTGCGCAGCCTGAATGGCGAATGGACGCGCCCTGTAGCGGCGCATTAAGCGCGG
CGGGTGTGGTGGTTACGCGCAGCGTGACCGCTACACTTGCCAGCGCCCTAGCGCCCGCTCCTTTCGC
TTTCTTCCCTTCCTTTCTCGCCACGTTCGCCGGCTTTCCCCGTCAAGCTCTAAATCGGGGGCTCCCTTTA

GGGTTCCGATTTAGTGCTTTACGGCACCTCGACCCCAAAAAACTTGATTAGGGTGATGGTTCACGTA
GTGGGCCATCGCCCTGATAAACGGTTTTTCGCCCTTTGACGTTGGA

I 1 M13r

CCACTAGTAACGGCCGCCAGTGTGCTGGAATTCGCCCTTTGCTCGCAGTACCAAAACAGGCACAGCA
TACACTTTCTTTACACCTAATAACATAAAGCAAGTGAGCGACCTTATCTCTGTGCTTCGTGAAGCTAGT
CAAGCAATTAATCCCAAGTTGCTTCAGTTGGTCGAAGACAGAGGTTCAGGTAAGGATGACTGATAGG
AAATGTTGGTAGTTACGAGTCACATCGTTGTCTACAAATCCATTTAAATGGTATTGGAGGGTGAGTA
AAACCTTGAATGTGAAAACTTAAGCTGAAAAATTGTAAAAACATTTCACGCCTACCATGAATAGATCT
GTTTCTTTCTGTCCACAATGATTTGTGTCATAGACATAATTGATCAATTTGCAATTGTTTTCTTGACAG
GTCGTTCCAGGGGTAAGGAGGCATGAAGGATGACCGTCGGGACAGATACTCTGCGGGCAAAAGGG
GTGGATTTAATACCTTTAGAGACAGGGAAAATTATGACAGAGGTTACTCTAGCCTGCTTAAAAGAGA
TTTTGGGGCAAAAACTCAGAATGGTGTTTACAGTGCTGCAAATTACACCAATGGGAGCTTTGGAAGG
GCGAATTCTGCAGATATCCATCACACTGGCGGCCGCTCGAGCATGCATCTAGAGGGCCCAATTCGCC
CTATAGTGAGTCGTATTACAATTCACTGGCCGTCGTTTTACAACGTCGTGACTGGGAAAACCCTGGCG
TTACCCAACTTAATCGCCTTGCAGCACATCCCCCTTTCGCCAGCTGGCGTAATAGCGAAGAGGCCCGC
ACCGATCGCCCTTCCCAACAGTTGCGCAGCCTGAATGGCGAATGGACGCGCCCTGTAGCGGCGCATT
AAGCGCGGCGGGTGTGGTGGTTACGCGCAGCGTGACCGCTACACTTGCCAGCGCCCTAGCGCCCGC
TCCTTTCGCTTTCTTCCCTTCCTTTCTCGCCACGTTCGCCGGCTTTCCCCGTCAAGCTCTAAATCGGGGG
CTCCCTTTAGGGTTCCGATTTAGTGCTTTACGGCACCTCGACCCCAAAAAACTTGATTAGGGTGATGG
TTCACGTARTGGGCCATCGCCCTGAAAAAACGGTTTTTCGCCCTTTGACGTTGGA

I2 M13r

TCCACTAGTAACGGCCGCCAGTGTGCTGGAATTCGCCCTTATTCCGATAGAAGGGCGAATTCTGCAG
ATATCCATCACACTGGCGGCCGCTCGAGCATGCATCTAGAGGGCCCAATTCGCCCTATAGTGAGTCG
TATTACAATTCACTGGCCGTCGTTTTACAACGTCGTGACTGGGAAAACCCTGGCGTTACCCAACTTAA
TCGCCTTGCAGCACATCCCCCTTTCGCCAGCTGGCGTAATAGCGAAGAGGCCCGCACCGATCGCCCTT
CCCAACAGTTGCGCAGCCTGAATGGCGAATGGACGCGCCCTGTAGCGGCGCATTAAGCGCGGCGGG
TGTGGTGGTTACGCGCAGCGTGACCGCTACACTTGCCAGCGCCCTAGCGCCCGCTCCTTTCGCTTTCT
TCCCTTCCTTTCTCGCCACGTTCGCCGGCTTTCCCCGTCAAGCTCTAAATCGGGGGCTCCCTTTAGGGT
TCCGATTTAGTGCTTTACGGCACCTCGACCCCAAAAAACTTGATTAGGGTGATGGTTCACGTAGTGG
GCCATCGCCCTGATAGACGGTTTTTCGCCCTTTGACGTTGGAGTCCACGTTCTTTAATAGTGGACTCTT
GTTCCAAACTGGAACAACACTCAACCCTATCTCGGTCTATTCTTTTGATTTATAAGGGATTTTGCCGAT
TTCGGCCTATTGGTTAAAAAATGAGCTGATTTAACAAAAATTTAACGCGAATTTTAACAAAATTCAGG
GCGCAAGGGCTGCTAAAGGAAGCGGAACACGTAGAAAGCCAGTCCGCAGAAACGGTGCTGACCCC
GGATGAATGTCAGCTACTGGGCTATCTGGACAAGGGAAAACGCAAGCGCAAAGAGAAAGCAGGTA
GCTTGCAGTGGGCTTACATGGCGATAGCTAGACTGGGCGGTTTTATGGACAGCAAGCGAACCGGAA
TTGCCAGCTGGGGCGCCCTCTGGTAAGGTTGGGAAGCCCTGCAAAGTAAACTGGATGGCTTTCTTGC
CGCCAAGGATCTGATGGCGCAGGGGATCAAGATCTGATCAAGAGACAGGATGAGGATCGTTTCGCA
TGATTGAACAAAATGGATTGCRCGCAGGTTCYCCGGCCGCTTGGGTGGAA

I3 M13r
CTCGGATCCACTAGTAACGGCCGCCAGTGTGCTGGAATTCGCCCTTTGCTCGCAGTACCAAAACAGG
CACAGCATACACTTTCTTTACACCTAATAACATAGAGCAAGTGAGCGACCTTATCTCTGTGCTTCGTG
AAGCTAATCAAGCAATTAATCCCAAGTTGCTTCAGTTGGTCGAAGACAGAGGTTCAGGTAAGGATGA
CTGATAGGAAATGTTGGTAGTTACGAGTCACATCGTTGTCTACAAATCCATTTAAATGGTATTGGAG
GGTGAGTAAAACCTTGAATGTGAAAACTTAAGCTGAAAAATTGTAAAAACATTTCACGCCTACCACG
AATAGATCTGTTTCTTTCTGTCCACAATGATTTGTGTCATAGACATAATTGATCAATTTGCAATTGTTTT
CTTGACAGGTCGTTCCAGGGGTAGGAGGCATGAAGGATGACCGTCGGGACAGATACTCTGCGGGCA
AAAGGGGTGGATTTAATACCTTTAGAGACAGGGAAAATTATGACAGAGGTTACTCTAGCCTGCTTAA
AAGAGATTTTGGGGCAAAAACTCAGAATGGTGTTTACAGTGCTGCAAATTACACCAATGGGAGCTTT
GGAAGGGCGAATTCTGCAGATATCCATCACACTGGCGGCCGCTCGAGCATGCATCTAGAGGGCCCA
ATTCGCCCTATAGTGAGTCGTATTACAATTCACTGGCCGTCGTTTTACAACGTCGTGACTGGGAAAAC
CCTGGCGTTACCCAACTTAATCGCCTTGCAGCACATCCCCCTTTCGCCAGCTGGCGTAATAGCGAAGA
GGCCCGCACCGATCGCCCTTCCCAACAGTTGCGCAGCCTGAATGGCGAATGGACGCGCCCTGTAGCG
GCGCATTAAGCGCGGCGGGTGTGGTGGTTACRGCAGCGTGACCGCTACACTTGCCMGCGCCCYAA
CGCCCGCTCCTTTYGCTTTCTTCCCTTCCTTTCTCGCCACGTTCGCCGGYTTTCCCCGTCAAGCTCTAAA
TCGGGGGCTCCCTTTAGGGTTCCGATTTANTGCTTTACGGCACCTCCACCCCAAAAAACTTGATTAAG
GGGGATGGTTCACRTAANGGGGCCATCCCCCC

8.5.3. Sequencing results of top three off-targets, both forward and reverse sequences
T1: off-target1, T2: off-target2, T3: off-target3

T1: Homo sapiens SHC SH2-domain binding protein 1 pseudogene (LOC100420587), non-coding RNA. (from RefSeq NR_110759); GATCTTTCCTGGGGTAGAGGGAG

T1 rev clone F
ATCCTTCTTTGTTCCGTCTCTGCCTTATTCTAAACCAGCTCCTCCCATCAGCGCCGCTCCTTGTGTGTTT
CCAAGTCTCTCCAGGCCAGTAATTCCT

T1 fwd clone F
GGGAGGAGCTGGTTTAGAATAAGGCAGAGACGGAACAAAGAAGGATCTTTCCTGGGGTAGAGGGA
GGGTGGTGGGAGGACAATGGGGAG

Correct nucleotides upstream and downstream of the target site: -43; +23

T1 rev clone G
AAGATCCTTCTTTGTTCCGTCTCTGCCTTATTCTAAACCAGCTCCTCCCATCAGCGCCGCTCCTTGTGTG
TTTCCAAGTCTCTCCAGGCCAGTAATTCCTA

T1 fwd clone G

ATGGGAGGAGCTGGTTTAGAATAAGGCAGAGACGGAACAAAGAAGGATCTTTCCTGGGGTAGAGG
GAGGGTGGTGGGAGGACAATGGGGAGTGTGGGGNTGNGNNNCA

Correct nucleotides upstream and downstream of the target site: -97; +31

T1 rev clone I
GAAGATCCTTCTTTGTTCCGTCTCTGCCTTATTCTAAACCAGCTCCWCCCATCAGCGCCGCTCCTTGTG
TGTTTCCAAGTCTCTCCAGGCCAGTAATTCCTA

T1 fwd clone I
TGGGAGGAGCTGGTTTAGAATAAGGCAGAGACGGAACAAAGAAGGATCTTTCCTGGGGTAGAGGG
AGGGTGGTGGGAGGACAATGGGGCG

Correct nucleotides upstream and downstream of the target site: -103; +24

T2: H3K27Ac Mark (Often Found Near Regulatory Elements) on 7 cell lines from ENCODE;
AGTTGTTCCATGGGTAGAGGGAG

T2 rev clone F
CTAATTCCTTTTCATCCCCTCCTCCCTCTACCCATGGAACAACTGACAAGCTGAATAGCTTATGGGGGT
GAGTTGATCAGTAGGAGTGAGTGAAGAAGGCTAAGGCAGACAATTCTCCCAAATTAGTCCGCTGAG
AC

T2 fwd clone F
TNCTCCTACTGATCAACTCACCCCCATAAGCTATTCAGCTTGTCAGTTGTTCCATGGGTAGAGGGAGG
AGGGGATGAAAAGGAATTAGGATATGCTTCTCCCTTTCACTTAATACCTAGCATCCTCNGCAACACTG
GTACGA

Correct nucleotides upstream and downstream of the target site: -93; +55

T2 rev clone G
AATTCCTTTTCATCCCCTCCTCCCTCTACCCATGGAACAACTGACAAGCTGAATAGCTTATGGGGGTG
AGTTGATCAGTAGGAGTGAGTGAAGAAGGCTAAGGCAGACAATTCTCCCAAATTAGTCCGCTGATTT

T2 fwd clone G
ACTGATCAACTCACCCCCATAAGCTATTCAGCTTGTCAGTTGTTCCATGGGTAGAGGGAGGAGGGGA
TGAAAAGGAATTAGGATATGCTTCTCCCTTTCACTTAATACCTAGCATCCTCTGCAACACTGGTACGA
CTA

Correct nucleotides upstream and downstream of the target site: -94; +78

T2 rev clone I
CCTAATTCCTTTTCATCCCCTCCTCCCTCTACCCATGGAACAACTGACAAGCTGAATAGCTTATGGGGG
TGAGTTGATCAGTAGGAGTGAGTGAAGAAGGCTAAGGCAGACAATTCTCCCAAATTAGTCCGCTGA
CCT

T2 fwd clone I
CACCCCCATAAGCTATTCAGCTTGTCAGTTGTTCCATGGGTAGAGGGAGGAGGGGATGAAAAGGAA
TTAGGATATGCTTCTCCCTTTCACTTAATACCTAGCATCCTCTGCAACACTGGTACA

Correct nucleotides upstream and downstream of the target site: -93; +74

T3: Homo sapiens RNA binding motif protein 17 (RBM17), transcript variant 1, mRNA. (from RefSeq NM_032905), intron 4/11; TGAAGTTGCAGGGGTAGAGGGGG

T3 rev clone F
ACTTTTCATACTTTTATCTACTTTAGTCTTTTACCAGTTATGCTTCCTACCCCCTCTACCCCTGCAACTTC
ATAGTTGATTGTGACAGGATTTGGATATCTTCTGGTCAAGAGGAAGTCATCCCAGGTTCAGGTCTCC

T3 fwd clone F
CAATCAACTATGAAGTTGCAGGGGTAGAGGGGGTAGGAAGCATAACTGGTAAAAGACTAAAGTAG
ATAAAAGTATGAAAAGTGAGAAAAATTCAAGAGATAAATTGAACCAATAAGTATACGAGAGCAACC
AANTC

Correct nucleotides upstream and downstream of the target site: -66; +99

T3 rev clone G
CTNCTTTTNTACTTTTATCTACTTTAGTCTTTTACCAGTTATGCTTCCTACCCCCTCTACCCCTGCAACTT
CATAGTTGATTGTGACAGGATTTGGATATCTTCTGGTCAAGAGGAAGTCATCCCAGGTTCAGGTCTC
AGTC

T3 fwd clone G
ACAATCAACTATGAAGTTGCAGGGGTAGAGGGGGTAGGAAGCATAACTGGTAAAAGACTAAAGTA
GATAAAAGTATGAAAAGTGAGAAAAATTCAAGAGATAAATTGAACCAATAAGTATACGAGAGCAAC
CATN

Correct nucleotides upstream and downstream of the target site: -69; +99

T3 rev clone I
CTTTTNTACTTTTATCTACTTTAGTCTTTTACCAGTTATGCTTCCTACCCCCTCTACCCCTGCAACTTCAT
AGTTGATTGTGACAGGATTTGGATATCTTCTGGTCAAGAGGAAGTCATCCCAGGTTCAGGTCTCAATT

T3 fwd clone I
ATCAACTATGAAGTTGCAGGGGTAGAGGGGGTAGGAAGCATAACTGGTAAAAGACTAAAGTAGAT
AAAAGTATGAAAAGTGAGAAAAATTCAAGAGATAAATTGAACCAATAAGTATACGAGAGCAACCAA
NTNG

Correct nucleotides upstream and downstream of the target site: - 70; +100

8.6. Human shRNA lentiviral particles (4, 29mer target-specific shRNA, 1 scramble control) for generating a DDX5 knockdown in HeLa and primary HUVEC cells
DDX5 targeting:

shA (also shDDX5 in text): AAACTCAGAATGGTGTTTACAGTGCTGCA (OriGene Technologies, TL313515V)

shB: CAAGTGAGCGACCTTATCTCTGTGCTTCG (OriGene Technologies, TL313515V)

shC: TCCTCAGAGGATTATATTCATCGAATTGG (OriGene Technologies, TL313515V)

shD: CATCGAATTGGAAGAACTGCTCGCAGTAC (OriGene Technologies, TL313515V)

Control (in text GFP or scrambled shRNA): Lenti shRNA scramble control particles (OriGene Technologies, TR30021V)

8.7. Reagent components of Reaction and Injection mix used for Reporter gene assay

Table 16: Components of Reaction mix.

Reagent	Volume (ml)
Gly-Gly 25 mM, pH 7.8	9
ATP 20 mM, pH 7.5 (Sigma-Aldrich)	1
MgSO$_4$ 1 M (Sigma-Aldrich)	0.1

Table 17: Components of Injection mix.

Reagent	Volume (ml)
Gly-Gly 25 mM, pH 7.8	4
Luciferine 1 mM (Sigma-Aldrich)	1

8.8. Reagent components of buffers used in Western blot analysis

Table 18: Reagent composition of Solution A used for generating separation gels.

Reagent	Amount
Tris	181.5 g
Sodium Dodecylsulfat	4 g
Hydrochlorid acid	Adjust the pH to 8.8
H$_2$O	Up to 1 L

Table 19: Reagent composition of Solution Ast used for generating stacking gels.

Reagent	Amount
Tris	60 g
Phenolred	400 mg
Sodium Dodecylsulfat	4 g
Hydrochlorid acid	Adjust the pH to 6.8
H_2O	Up to 1 L

Table 20: Reagent composition for preparing 10 X Running Buffer for SDS PAGE.

Reagent	Amount
Tris	30 g
Glycine	144 g
Sodium Dodecylsulfat	10 g
H_2O	Up to 1 L

Table 21: Reagent composition for preparing TBS.

Reagent	Final concentration
Tris	50 mM
Sodium Chloride	150 mM
Hydrochlorid acid	Adjust the pH to 7.4
H_2O	To the required volume

Table 22: Reagent composition for 1 X Towbin Buffer.

Reagent	Final concentration
Tris (Roth)	0.025 M
Glycine	0.192 M
MeOH	20%
Hydrochlorid acid	Adjust the pH to 8.3
H_2O	For the final volume of 1 L

Table 23: Reagent composition and concentration of stock solution used for preparing home-made ECL substrate.

Reagent	Final concentration
Tris (pH 8.5)	100 mM
Luminol (Sigma-Aldrich) 1g in 22.5 ml DMSO	250 mM
Paracoumaric acid (Sigma-Aldrich) 0.5 g in 33.8 ml DMSO	90 mM
Hydrogen Peroxide (Sigma-Aldrich)	5.4 mM
Preparing 5 ml ECL substrate	5 ml Tris
	22 µl PCA
	50 µl Luminol
	7 µl H_2O

8.9. Plasmid list

Table 24: Plasmid list.

Plasmid name	Description
pmaxGFP (Amax)	GFP expression plasmid
PX459 (Feng Zhang lab)	Cas9 expression plasmid
HCP plasmid (GeneCopoeia)	sgRNA delivery plasmid (sgRNA constructs: sgA, sgB or sgC)
pCR-TOPO vector (Invitrogen)	TOPO cloning vector
pcDNA3 plasmid (Invitrogen)	empty-vector
5xNF-κB-luc (Stratagene)	NF-κB reporter plasmid
UBT-ß-gal (Rainer de Martin´s lab)	ubiquitin-driven ß-galactosidase expression plasmid
N-terminal flag-tagged DDX5 pcDNA3 (Rainer de Martin´s lab)	DDX5 expression plasmid
B1-pfam in pcDNA3 (Rainer de Martin´s lab)	DDX5 truncated mutant lacking Pfam domain expression plasmid
HA-p65- in pcDNA3 (Manolis Pasparakis lab)	p65 expression plasmid
HA-IKK1 in pcDNA3 (Manolis Pasparakis lab)	IKK1 expression plasmid
myc-IKK2 (Johannes Schmid lab)	IKK2 expression plasmid

8.10. Components of commercial kits used in this study

Table 25: Components of Monarch® Plasmid Miniprep Kit (New England BioLabs$_{inc}$).

Buffer	Components
Resuspension Buffer (B1)	Tris-based resuspension buffer
Lysis Buffer (B2)	Sodium hydroxide and SDS-based lysis buffer
Neutralization Buffer (B3)	Guanidine hydrochloride-based neutralization buffer, containing RNAse
Plasmid Wash Buffer 1	Guanidine/isopropanol-based wash buffer
Plasmid Wash Buffer 2	Ethanol-based wash buffer
DNA Elution Buffer	10 mM Tris, 0.1 mM EDTA, pH 8.5 elution buffer

Table 26: Components of QIAGEN Plasmid Midi Kit (Quiagen).

Buffer	Components
Buffer P1 – Resuspension Buffer	50 mM Tris-Cl, pH 8.0, 10 mM EDTA, 100 µg/mL RNase A
Buffer P2 – Lysis Buffer	200 mM NaOH, 1% SDS
Buffer P3 – Neutralization Buffer	3.0 M potassium acetate, pH 5.5
Buffer QC – Wash Buffer	1.0 M NaCl, 50 mM MOPS, pH 7.0, 15% isopropanol
Buffer QBT - Equilibrium Buffer	750 mM NaCl, 50 mM MOPS, pH 7.0, 15% isopropanol, 0.15% Triton X-100
Buffer QF – Elution Buffer	1.25 M NaCl, 50 mM Tris-Cl, pH 8.5, 15% isopropanol

Table 27: Components of GFX™ PCR DNA and a Gel Band Purification Kit (GE Healthcare).

Buffer	Step	Comments
Capture buffer type 3	Denaturation/solubilization	Proteins are denatured. For gel band
GFX column	Capture	The sample is passed through the GFX column to capture the DNA onto the glass fiber matrix
Wash buffer type 1	Washing/ Drying	Matrix-bound DNA is washed with an ethanolic buffer to remove salts and other contaminants. This step also dries the matrix prior to elution.
Elution buffer type 4	Elution of DNA	10 mM Tris-HCl, pH 8.0
Elution buffer type 6	Elution of DNA	sterile nuclease free water

Table 28: Components of PeqGold Total RNA Isolation Kit (Peqlab).

Buffer	Components
Wash Buffer I	30% EtOH, 30% guanidine thiocyanate
Wash Buffer II	80% EtOH
Lysis Buffer	4 M guanidine thiocyanate, 2% Sarkosyl, 50 mM Tris, pH 7.6, 10 mM EDTA, 1% β-mercaptoethanol

SANDRA POSTIĆ
Mag.oecol.et prot.nat.

Date of birth: 13.2.1991.
Nationality: Croatian

EDUCATION

MEDICAL UNIVERSITY OF VIENNA Vienna, Austria 2017 – 2018	**GRADUATION THESIS** Science project: Role of the RNA-helicase DDX5 in the NF-kB signaling pathway Group of Reiner de Martin; Department of Vascular Biology and Thrombosis Research
UNIVERSITY OF VIENNA Vienna, Austria 2016 – 2017	**ERASMUS EXCHANGE PROGRAM** Molecular biology exchange student
UNIVERSITY OF ZAGREB Zagreb, Croatia 2015-present	**MASTER IN MOLECULAR BIOLOGY** Faculty of science
UNIVERSITY OF ZAGREB Zagreb, Croatia 2012-2015	**MASTER IN ECOLOGY AND ENVIRONMENTAL PROTECTION** Morphology, systematics and distribution of species of the subgenus *Eucarabus* (Coleoptera, Carabidae) in Croatia Faculty of science
UNIVERSITY OF ZAGREB Zagreb, Croatia 2009-2012	**BACHELOR IN BIOLOGY** Free radicals and antioxidants in normal physiological functions and human diseases Faculty of science